Investigating Strategies to Enhance Microbial Production of and Tolerance Towards Aromatic Biochemicals

by

Michael Machas

A Dissertation Presented in Partial Fulfillment
of the Requirements for the Degree
Doctor of Philosophy

Approved July 2019 by the
Graduate Supervisor Committee:

David R. Nielsen, Chair
Karmella Haynes
Xuan Wang
Brent Nannenga
Arul Varman

ARIZONA STATE UNIVERSITY

August 2019

ABSTRACT

Aromatic compounds have traditionally been generated via petroleum feedstocks and have wide ranging applications in a variety of fields such as cosmetics, food, plastics, and pharmaceuticals. Substantial improvements have been made to sustainably produce many aromatic chemicals from renewable sources utilizing microbes as bio-factories. By assembling and optimizing native and non-native pathways to produce natural and non-natural bioproducts, the diversity of biochemical aromatics which can be produced is constantly being improved upon. One such compound, 2-Phenylethanol (2PE), is a key molecule used in the fragrance and food industries, as well as a potential biofuel. Here, a novel, non-natural pathway was engineered in *Escherichia coli* and subsequently evaluated. Following strain and bioprocess optimization, accumulation of inhibitory acetate byproduct was reduced and 2PE titers approached 2 g/L – a ~2-fold increase over previously implemented pathways in *E. coli.* Furthermore, a recently developed mechanism to allow *E. coli* to consume xylose and glucose, two ubiquitous and industrially relevant microbial feedstocks, simultaneously was implemented and systematically evaluated for its effects on L-phenylalanine (Phe; a precursor to many microbially-derived aromatics such as 2PE) production. Ultimately, by incorporating this mutation into a Phe overproducing strain of *E. coli*, improvements in overall Phe titers, yields and sugar consumption in glucose-xylose mixed feeds could be obtained. While upstream efforts to improve precursor availability are necessary to ultimately reach economically-viable production, the effect of end-product toxicity on production metrics for many aromatics is severe. By utilizing a transcriptional profiling technique (i.e., RNA sequencing), key insights into the mechanisms behind styrene-induced toxicity in *E. coli* and the cellular response systems that are activated to maintain cell viability were obtained. By investigating variances in the transcriptional response between styrene-producing cells and cells where styrene was added exogenously, better understanding on how mechanisms such as the phage shock, heat-shock and membrane-altering responses react in different scenarios. Ultimately, these efforts to diversify the collection of microbially-produced aromatics, improve intracellular precursor pools and further the understanding of cellular response to toxic aromatic compounds, give insight into methods for improved future metabolic engineering endeavors.

AKNOWLEDGMENTS

I would firstly like thank my advisor, David Nielsen (and Maeve!), for being the greatest mentor in the world. His support and guidance were unmatched, and I could not have asked for a better PhD advisor. Without his patience (so much patience!), approachability and leadership, this would have been a much less rewarding experience and I am extremely appreciative. Thank you to my committee, Drs. Karmella Haynes, Xuan Wang, Brent Nannenga, Arul Varman, for taking time out of their busy schedule to provide guidance and insight and be a big part of my academic journey. A very special thank you to Mr. Fred Pena for his expertise and skillset – his knowledge regarding engineering equipment and processes and willingness to always provide me with assistance has been vital to my success here at ASU. I would like to thank all of the graduate students and lab members at ASU who I have had the pleasure of working with during my time here and who have always been willing to lend a helping hand, talk through problems and make the lab experience so worthwhile: Andrew Flores, Zach Dookeran, Rodrigo Martinez, Cody Kamoku, Sydney Parrish, Anirudh Vasudevan, Daniel Herschel, Yifei Xu, John Hagstrom, Lizbeth Nieves and Drs. Brian Thompson, Kyle Staggs, Gavin Kurgan, Christopher Jones, Yuji Aso, Bohan Shan, Matt Christensen, Karthik Pushpavanam, Stefan Tekel and many others. A big thank you to all the undergraduate and high school students who I was able to work and made the lab a little more exciting every day: Jordan Hines, Zeynap Ayla, Kaleigh Johnson, Christopher Gregson, Min Su Park, Jimmy Xu, Chantal Navrital, Adit Sakthi, Gavin Steeber, Brian Wynne, Alyssa Shapiro and Aidan Schneider.

I would like to thank all my roommates and friends that I have had during my graduate school career – without them, I would have never made it: Dr. Zoran Bundalo, Dr. Jared Schoepf, Tim Duarte, Amelia Bourke, Marwan Osman, Jamie Balesteri, Jay Rubenstein, Dr. Jeff Johannesmeyer, Kristen Riske, Justin Jordan, Isaac Sitter, Greg Mirza, Ryan Jordan, Dr. Chad Campbell, Gabrielle Porti, Erica Engelschall, Taylor Barker, Frankie Kennedy, Dr. Eric Stevens, Jordan Cunningham, Quan Truong, Ben Pohle, Josh Topel, David Reinkensmeyer, Dr. Tarek Kaakani and Dr. Adam Odeh.

I would especially like to acknowledge and thank Daryl and Christine Burton and the entire Burton family for supporting me and my research adventure for the past two years through ARCS Foundation (Phoenix Chapter). They have been so encouraging and excited about the research that I have done, and I am grateful that I have been able to develop this relationship with such an amazing and supportive family.

I have the greatest girlfriend of all time (Lindsay!) and I can't believe she put up with me going to lab pretty much every day, leaving her to take care of our crazy dog and spending more time with my bacteria babies than her. I appreciate everything that she does for me and I'm so lucky that she was willing to take this journey with me. Thanks to her parents, Linda and Brian, brother, Zach, and whole extended family for treating me like a member of the family. Also, extra special shout-out to Serena and Boomer! Thanks to my dog, Mia, for teaching me what patience really means but always being there with a big tail wag when I have a bad day.

Without my parents, Jim and Stephanie, I would not be here, and I am forever grateful for everything they have given me. They are the best parents that anyone could ever ask for and I am so lucky to have them. Thanks to my sister, Melina, for growing up with me and constantly supporting me and always being my friend even when I am particularly annoying. I am also extremely grateful to my extended family – grandparents, aunts, uncles, cousins, godparents, and everyone in my Greek family – for providing me with an amazing and loving support system.

TABLE OF CONTENTS

Page

CHAPTER Page

CHAPTER Page

LIST OF TABLES

Table Page

LIST OF FIGURES

Figure Page

Figure Page

CHAPTER 1. EMERGING TOOLS, ENABLING TECHNOLOGIES, AND FUTURE OPPORTUNITIES FOR THE BIOPRODUCTION OF AROMATIC CHEMICALS

Abstract

Aromatic compounds, which are traditionally derived from petroleum feedstocks, represent a diverse class of molecules with a wide range of industrial and commercial applications. Significant progress has been made to alternatively and sustainably produce many aromatics from renewable substrates using microbial biocatalysts. While the construction of both natural and non-natural pathways has expanded the number and diversity of aromatic bioproducts, pathway modularization in both single- and multi-strain systems continues to support the enhancement of key production metrics towards economically-viable levels. While product toxicity persists as a key challenge limiting the production of many aromatics, various successful strategies have been demonstrated towards improving tolerance, including via membrane and efflux pump engineering as well as by exploiting alternative production hosts. Finally, as a further step towards sustainable and economical aromatic bioproduction, non-model substrates including lignin-derived compounds continue to emerge as viable feedstocks. This chapter highlights recent and notable achievements related to such efforts while offering future outlooks towards engineering microbial cell factories for aromatic production.

This chapter contains sections from the published work below:

Machas, M., Kurgan, G., Jha, A.K., Flores, A., Schneider, A., Coyle, S., Varman, A., Wang, X., Nielsen, D.R. Emerging Tools, Enabling Technologies, and Future Opportunities for the Bioproduction of Aromatic Chemicals. *J Chem Technol Biotechnol* 2018, doi: 10.1002/jctb.5762.

1.1 Introduction

Aromatic chemicals represent a diverse and important class of conventional petrochemicals with a wide range of commercial and industrial applications. It has been estimated that about 40% (by mass) of bulk petrochemicals contain aromatic functionality (i.e., one or more substituted benzene rings) [1], serving, for example, as monomers for synthesizing highly durable and thermostable polymers and coatings, building blocks for active pharmaceutical ingredients, and even fuel additives. In recent years, significant and growing interest has emerged in the development of alternative, microbial production routes for aromatic chemicals from renewable, biomass-derived substrates. Such efforts have been aided by advancements in metabolic engineering, protein engineering, and systems and synthetic biology [2,3], which continue to guide both rational and combinatorial approaches towards efficient biocatalyst development. As a result, the *de novo* biosynthesis of a diversity of different aromatic chemicals is now a reality, with applications that, like their petroleum-derived counterparts, include bulk chemicals and plastics, specialty chemicals, flavors and fragrances, and pharmaceuticals and nutraceuticals (**Figure 1.1**).

Several notable reviews have reported on recent and important progress made towards the microbial biosynthesis of aromatic chemicals [4-9], predominantly focusing on key developments in both host and pathway engineering that have enabled the high-level biosynthesis of a growing list of aromatic products. In particular, these reviews comprehensively summarize the diversity of different aromatic biochemicals that have been produced to date, as well as comparing different carbon sources, host strains/organisms, culture conditions and important metabolic engineering strategies employed; illustrating key progress made with respect to engineering microbial production of both naturally occurring (i.e., amino acids) and novel aromatic biochemicals. Accordingly, with the goal of complementing rather than duplicating these existing works, the objective of this chapter is more specifically to highlight the role of emerging tools and enabling technologies as applied to this end, while also identifying potential avenues for future advancements in this area. As will be discussed, this includes the use of modular engineering strategies for improving biosynthetic function, tolerance engineering to increase strain robustness,

and alternative biomass feedstocks to improve economic viability and sustainability. Finally, while the primary focus will be related to the bioproduction of molecules with aromatic functionality, select products derived from aromatic biosynthesis (e.g., *cis,cis*-muconic acid) will also be highlighted as illustrative examples, where appropriate.

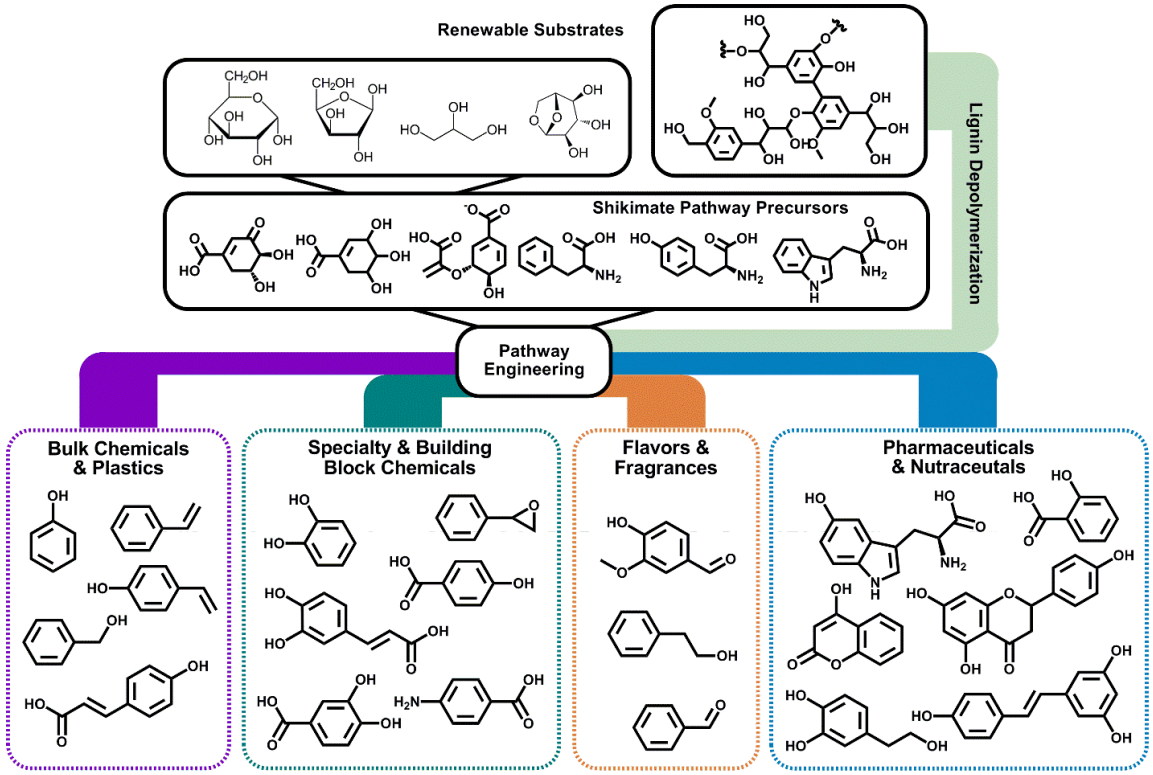

Figure 1.1 Bioproduction of Aromatic Chemicals from Renewable Substrates.

Metabolic and pathway engineering strategies have enabled the de novo microbial production of an array of aromatic biochemicals with a range of possible end uses. In addition to glucose, other biomass-derived sugars, lignin, and lignin-derived monomers have been investigated as renewable substrates to this end.

1.2 Modular Engineering Strategies for Optimizing Pathway Flux and Function

Microbial production of aromatic chemicals has largely been enabled via pathway engineering, generally consisting of either: *a)* the functional reconstruction of naturally-occurring but non-native (often plant) pathways, or *b)* the bottom-up construction of novel pathways comprised of individual enzymes derived from a diversity of heterologous sources. Recent examples include the successful engineering of microbes capable of the *de novo* production of, in the first case,

flavonoids (usually consisting of two phenyl groups and a heterocyclic ring) [10,11], stilbenes (ethylene moiety with two phenyl groups) [12,13], and coumarins (containing a 1,2-benzopyrone backbone) [14,15], and, in the second case, numerous aromatic aldehydes, alcohols, and acids [16-21], styrenics [22-25], and phenolics [26-33]. In most cases, these heterologous pathways stem from natively produced aromatic chemicals such as the aromatic amino acids (i.e., L-phenylalanine, L-tyrosine, and L-tryptophan) or their precursors (e.g., chorismate; derived from the shikimate pathway). Irrespective of the target, both approaches require the synchronous function of multiple enzymatic 'steps', each with net activities precisely tuned so as to balance metabolite flux and avoid formation of undesirable bottlenecks. For a multi-step pathway, achieving this outcome often requires the construction and screening of a large number of unique pathway variants. As has been demonstrated for the case of other, non-aromatic biochemicals [34-36], the identification of optimal pathway configurations can often be facilitated through modularization of the biosynthesis scheme. Two main approaches have been explored to this end, including the engineering of: *i)* modular pathways, and *ii)* modular cells.

1.2.1 Engineering Modular Aromatic Biosynthesis Pathways

Modular pathway engineering involves compartmentalizing a multi-step pathway into discrete modules in order to facilitate the combinatorial screening of relevant expression parameters for the collective purpose of achieving optimal expression levels and maximal pathway flux. Juminaga et al., for example, successfully implemented such an approach towards the efficient production of tyrosine in *Escherichia coli* [37]. Specifically, the entire tyrosine biosynthesis pathway – from erythrose-4-phosphate (E4P) and phosphoenolpyruvate (PEP) to tyrosine – was decomposed into two modules: *i)* the 'shikimate module' (comprised of *aroG**, *aroB*, *aroD*, and *ydiB*, along with *ppsA* and *tktA*), and *ii)* the 'tyrosine module' (comprised of *aroK*, *aroA*, *aroC*, *tyrA**, and *tyrB*), split at the intermediate shikimate (* indicates a gene encoding a feedback-resistant mutant). In the final design, constructs were systematically optimized with respect to each of the plasmid copy number, promoter strength, gene codon usage, and the relative placement of genes in each operon, ultimately leading to the production of >2 g/L tyrosine at 80% of the theoretical yield.

Analogous strategies have also been adopted to enhance microbial production of naringenin which, like other flavonoids, displays important human health benefits (e.g., anti-cancer, anti-oxidant), and is naturally produced in plants from endogenous malonyl-CoA and phenylpropanoid precursors [38]. Wu et al., for example, constructed a naringenin biosynthesis pathway in *E. coli* comprised of three modules expressing: 1) tyrosine ammonia lyase and 4-coumaroyl-CoA ligase, 2) chalcone synthase and chalcone isomerase, and 3) malonate synthetase and malonate carrier protein [39]. In this case, by simultaneously varying both plasmid copy number and promoter strength across all three modules, final naringenin titers were improved by almost 3-fold, reaching up to 100 mg/L. These efforts built upon the important preceding works of Santos et al. who also demonstrated a modular approach towards flux balancing of the naringenin pathway, in their case by varying the enzyme sources and tuning expression levels [40]. More recently, modular pathway engineering has also been extended to aid production of aromatic bulk chemicals, including styrene [25], for example.

In addition to aiding the systematic and simultaneous optimization of multiple expression parameters for a single pathway/product, modular pathway engineering strategies can also be used to facilitate targeting of additional products of interest. In particular, from common intermediates, different modules can be combined to create multiple pathways. Chorismate, for example, is a versatile endogenous intermediate with the potential to be converted to various aromatic end products. Following extensive host engineering to enhance endogenous chorismate production, Noda and co-workers introduced seven unique downstream pathway modules to produce seven unique chorismate-derived products, including salicylate, phenol, 3-hydroxybenzoate, and *cis,cis*-muconic acid, among others [41]. This approach was further exploited by Shen et al., in this case to convert chorismate to either salicyl alcohol (precursor to the anti-inflammatory, salicin) or gentisyl alcohol (an antioxidant and antibiotic); both through salicylate as a common intermediate [42].

1.3 Metabolic Control Strategies for Enhancing Aromatic Bioproduction

Various different metabolic control strategies have recently emerged as powerful tools for use in scenarios where classical gene knockouts are incompatible. This includes not only enabling individual growth essential genes to be targeted for tunable downregulation, but also, as such

methods are typically amenable to multiplexing, parallel targeting of multiple distinct processes with minimal strain engineering required. To date, the most promising strategies involve the use of: *i)* antisense RNAs (asRNAs), *ii)* synthetic small RNAs (sRNAs), *iii)* clustered regularly interspaced short palindromic repeats interference (CRISPRi), and *iv)* conditional gene expression using synthetic circuits.

1.3.1 Application and Potential of asRNA and Synthetic sRNAs for Aromatic Bioproduction

Both asRNA and synthetic sRNAs can be designed to target specific mRNA sequences, binding to transcripts and, as a result, inhibiting translation. sRNA, however, offers potential benefits such as improved silencing efficiency and longer half-lives due to association with and stabilization by an RNA chaperone [43]. Na et al., were among the first to report on the utility of synthetic sRNAs for biochemical production, doing so to enhance tyrosine biosynthesis. Specifically, by constructing sRNAs to simultaneously inhibit production of both TyrR and CsrA in *E. coli*, final tyrosine titers reaching 2 g/L were realized [44]. The same system was later utilized as a platform for phenol bioproduction, with final titers of 1.69 g/L reported for fed-batch cultures following introduction of tyrosine-phenol lyase (TPL) [45]. On the other hand, naringenin production in *E. coli*, for example, has been enhanced via the use of asRNA. Specifically, using anti-*fabB*/*fabF* asRNAs targeting various positions in the 5'-UTR to tune the level of down-regulation and balance malonyl-CoA flux between fatty acid biosynthesis and flavonoid production, final naringenin titers were increased by 431% [46]. Later, Yang et al. also utilized asRNAs to target not only *fabB* and *fabF* but also *fabD* and *fabH* as a strategy to similarly enhance malonyl-CoA availability and improve naringenin production, as well as that of 4-hydroxycoumarin and resveratrol (note: both *fabB* and *fabD* are growth essential) [47].

1.3.2 Application and Potential of CRISPRi for Aromatic Bioproduction

Similar to asRNA- and synthetic sRNA-based approaches, CRISPRi enables targeting of desired genes for tunable down-regulation, in this case via the design and introduction of custom single guide RNAs (sgRNAs) which associate with a catalytically-inactive version of *Streptococcus pyogenes* Cas9 (dCas9) to inhibit transcription [48,49]. Notable examples employing CRISPRi to

enhance aromatic bioproduction are again seen with respect to flavonoids. In a series of studies by Wu et al., for example, CRISPRi was employed to preserve malonyl-CoA availability in *E. coli* by targeting both *fabB* and *fabF*, along with several other less intuitive targets (e.g., *fumC*, *sucC*, *adhE*, *eno*) in a multiplexed manner. As a result, production of naringenin was improved 7.4-fold [50] and that of pinocembrin was improved 9.8-fold [51]. Similar strategies have since also been used to support pinosylvin production in *E. coli* [52] and naringenin production in *S. cerevisiae* [53]. Meanwhile, in addition to *S. pyogenes* dCas9, the use of alternative CRISPR systems have also been employed. For instance, Cress et al. recently reported on the development of CRISPathBrick, which instead utilizes Type II-A CRISPR arrays to rapidly assemble multiplexed modules for gene repression [54]. Validation of this alternative system was achieved by demonstrating improved production of naringenin.

1.3.3 Application and Potential of Synthetic Gene Circuits for Aromatic Bioproduction

Shikimate is a valuable precursor for the synthesis of oseltamivir phosphate (i.e., Tamiflu®) and other high-value pharmaceuticals [55]. However, it is also a key intermediate of the shikimate pathway and thus is a precursor to several growth essential compounds (e.g., aromatic amino acids). As deletion of genes immediately downstream of shikimate cannot be accomplished without generating multiple auxotrophies, these genes (i.e., encoding shikimate kinase) are ideal targets for emerging metabolic control strategies [56]. Gu et al., for example, developed a synthetic gene circuit to function as a switch for controlling expression of *aroK* (encoding the main shikimate kinase in *E. coli*) [57]. In this case, the native *aroK* promoter was replaced with $P_L$tetO1 and *tetR* expression was controlled by P_{BAD}, thus allowing arabinose addition to tunably down-regulate *aroK* expression at desired times and levels. As a result, the culture could be controlled through initial growth and subsequent production phases, enabling production of 13.15 g/L shikimate from glucose in fed-batch culture.

One shortcoming experienced by at least the majority of the above examples is the need to add an exogenous inducer molecule which in turn increases overall costs. This requirement has been circumvented by others, for example, by instead incorporating quorum sensing (QS) to control

induction of the synthetic gene circuit. By modulating the efficacy of QS circuits, gene expression profiles can be altered to respond in a tunable manner to increasing cell densities, making them suitable for use in different applications. In a recent demonstration, Williams et al. engineered a synthetic QS circuit in *S. cerevisiae* to improve the production of 4-hydroxybenzoate [58]. Here, the QS circuit was coupled to various RNA interference (RNAi) [59] modules to down-regulate key genes responsible for consuming phosphoenolpyruvate (*CDC19*, *PYK2*) and chorismate (*ARO7*), thereby enhancing chorismate availability and resulting in a 37-fold increase in 4-hydroxybenzoate titer.

1.4 Biosensor-Based Approaches for Improving Aromatic Chemical Production

Microbes have evolved various mechanisms for sensing and responding to extracellular and intracellular chemical changes, including through the use of numerous small molecule-responsive transcription factors and their cognate promoters [60]. When linked to an appropriate readout (e.g., fluorescent reporter or antibiotic resistance gene), such a machinery can be used to construct *in vivo* biosensors useful for detecting and responding to the intracellular presence of various products [61] (or intermediates [62,63]) of interest, typically with high selectivity and sensitivity, as well as in a dose-dependent manner [64] (**Figure 1.2**).

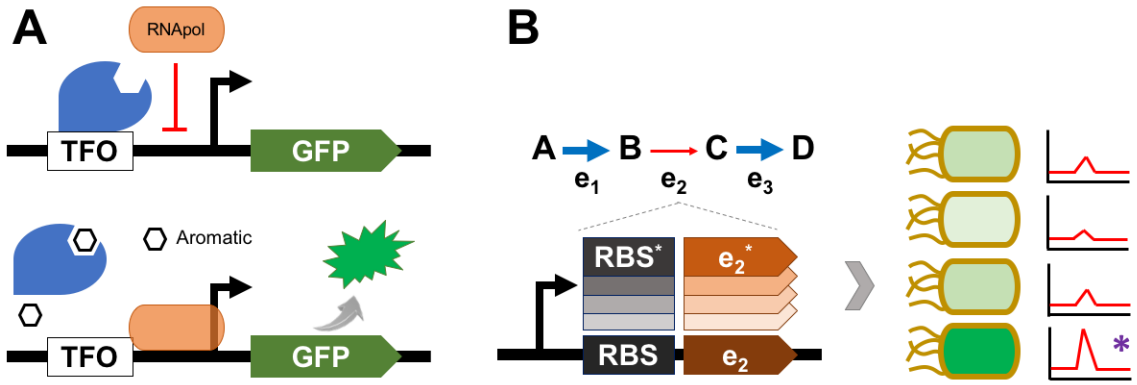

Figure 1.2 Biosensors Facilitate Optimization of Aromatic Bioproduction.

(A) An aromatic biosensor can be constructed by using an aromatic-responsive transcriptional regulator that, in the absence of an aromatic, binds to its cognate transcription factor operator (TFO), blocking RNA polymerase (RNApol) and thus expression of a suitable reporter (e.g., GFP). In the presence of a recognized aromatic, transcriptional repression is released and reporter expression is "turned on". (B) Such biosensors can be used to facilitate library screening (e.g., RBS and/or enzyme) allowing, for example, flux bottlenecks to be overcome. In the example shown, the most effective combination of RBS and enzyme (e2) variants will produce the most product 'D' which, once detected by the biosensor, will yield the highest output signal.

1.4.1 Development of Aromatic-Responsive Biosensors

To date, a diversity of naturally-evolved transcriptional regulators have been identified to control gene expression in response to the presence of various aromatic compounds of interest. These regulators are largely derived from soil bacteria where they serve to control the expression of aromatic degradation pathways [65-67] and tolerance mechanisms [68,69]. A comprehensive review by Diaz and Prieto summarizes the characterized function of a wide range of aromatic-responsive regulators, including aromatic effectors that are also bioproduct targets of interest (e.g., phenol, salicylate, benzoate, and styrene) [66]. More recently, Xue et al. further probed the response of four such previously identified regulators (NahR, XylS, HbpR, and DmpR) towards a panel of 20 unique aromatic compounds, also including select bioproducts (e.g., phenol, catechol, and 2-phenylacetate) [70], whereas others have since also been reported in the literature (e.g., QsuR for chorismate [71] and MarR for salicylate [72]). Taken together, these examples provide a glimpse of the spectrum of aromatic chemicals that can currently be detected using just naturally-evolved, transcriptional regulators. In addition to transcription factor-based biosensors, meanwhile,

regulatory RNA-based riboswitches have also been developed as small molecule-inducible gene expression activators [73,74], and hold similar potential with respect to detecting and responding to aromatic biochemicals. Although the diversity of aromatic effectors reported thus far is limited, promising results with tryptophan [74], dopamine and 2,4-dinitrotoluene [75], for example, bode well for the future potential of such devices.

1.4.2 Improving Aromatic Bioproduction Using in vivo Biosensors as Screening Tools

Once developed and optimized, *in vivo* biosensors can be used to facilitate the engineering/evolution of strains with improved bioproduction phenotypes via the use of high-throughput screening [76] (**Figure 1.2**). For example, by utilizing *E. coli*'s native TyrR (a transcriptional repressor that controls expression of multiple genes in the shikimate pathway), to sense elevated phenylalanine levels and drive *yfp* expression from its cognate *tyrP* promoter, a screening platform was developed to improve phenylalanine biosynthesis [77]. The same platform was further employed to sequentially screen both a ribosome binding site (RBS) library (expressing *aroD*, a known bottleneck in the shikimate pathway [78]) and a whole cell random mutagenesis library (generated by atmospheric and room-temperature plasma), together leading to the isolation of strains capable of ~290% greater phenylalanine production (9.29 g/L vs. 3.21 g/L). Other successful examples have also been reported outside of *E. coli*. For example, a shikimate biosensor was recently developed in *Corynebacterium glutamicum* using the native transcriptional regulator ShiR for shikimate and GFP as reporter and used to screen an RBS library for optimal precursor supply. Using FACS to facilitate selection, a 2.4-fold improvement in final titer was ultimately attained [79].

Finally, in addition to reporters offering externally detectable feedback (e.g., GFP), genes conferring a fitness advantage can alternatively be expressed to enable cell screening under selective conditions. Raman et al., employed such an approach utilizing a TtgR-TolC "sensor-selector" to screen targeted genome-wide mutagenesis libraries (generated by multiplexed automated genome engineering, MAGE [80]) to improve naringenin production in *E. coli* by 36-fold [81]. Chou and Keasling, meanwhile, recently reported a novel strain evolution platform wherein TyrR regulated the

expression of a mutator protein encoded by *mutD5* via a modified *aroF* promoter. This scheme enabled higher *mutD5* expression and thus higher mutation rates in strains producing low levels of tyrosine, and the *mutD5* expression reduced as tyrosine levels rose [82]. This 'feedback-regulated evolution of phenotype' (FREP) method enabled the isolation of an evolved strain capable of 5-fold increased tyrosine titers.

1.5 Future Outlooks

Aromatic biochemicals remain as attractive bioproduction targets due to their broad utility in chemical, pharmaceutical and food industries, as well as, in some cases, their high commercial value and difficulties associated with their chemical synthesis [9]. Accordingly, pathway engineering efforts are expected to continue in this area, including with respect to both the reconstitution of naturally-occurring routes and *de novo* construction of novel ones. In both cases, these efforts will continue to be fueled by both the discovery and engineering of unique enzyme chemistries. Recently, for example, Beller and co-workers applied a metagenomics and metaproteomics approach towards the discovery of a novel phenylacetate decarboxylase (encoded by *phdB*) [83]. Isolated from anoxic lake sediments, PhdB (a glycyl radical enzyme) is responsible for the biosynthesis of toluene, an aromatic bulk chemical and potential fuel additive, from phenylacetate. Additional product diversity is also possible via the interfacing of enzymatic and non-enzymatic processes. For example, Wallace and Balskus recently reported on the coupling of styrene production by *E. coli* with an *in situ* cyclopropanation reaction (catalyzied by iron(III) phthalocyanine in biocompatible micelles) to demonstrate production of non-natural phenyl cyclopropanes from glucose [84].

Once pathways are developed, strains must then be optimized to achieve meaningful production metrics. As efficient strain optimization demands more rapid design-build-test cycles, emerging tools supporting more precise metabolic control will play an increasingly important role by supporting facile implementation for rapid hypothesis testing and multiplexing for high-throughput screening. Meanwhile, , new approaches relying upon, for example, genome-wide sgRNA libraries[85-88] for CRISPRi applications will surely continue to accelerate the strain optimization

process. Furthermore, new insights gained by studying naturally-occurring microbial and fungal consortia will support the discovery of novel products of interest as well as new strategies for engineering co-cultures using 'modular' cells [89]. Such efforts will likely find future applications for aromatic bioproduction, in particular for the biosynthesis of high-value natural products whose synthesis relies upon complex and difficult to optimize pathways. As a result of these and other collective efforts, the list of aromatic compounds that can be produced as renewable bioproducts will undoubtedly continue to grow.

As aromatic toxicity remains a persistent challenge, the further development of strategies for increasing strain robustness will be important to achieving competitive product titers and yields. This will no doubt include, for example, the prospecting for as well as engineering of efficient aromatic efflux pumps. Meanwhile, as known trade-offs exist with respect to the overexpression of membrane transporters, for which an optimal balance between function and burden has been reported [90], more sophisticated control strategies for transporter expression in response to aromatic production levels might play a key role towards circumventing this caveat [91,92]. Such prospective applications, meanwhile, also further highlight the importance of developing aromatic biosensors and their potential utility for allowing cells to autonomously respond to their changing production environment. Further identification and engineering of alternative hosts with greater inherent aromatic tolerance will also be important to addressing product toxicity. Several bacteria with enhanced tolerance to other membrane disruptive compounds have already been identified, for example, including species of *Clostridium* [93], *Lactobacillus* [94], *Zymomonas* [93,95], and *Deinococcus* [96]. Although, to the best of our knowledge, these have not yet been investigated as potential hosts for aromatic bioproduction, they and others might indeed prove useful to this end.

Finally, in addition to expanding biochemical diversity and improving production metrics, the utilization of alternative feedstocks remains as an alluring prospect due to the potential for lower costs and, in some cases, higher theoretical yields. Important to this outcome is the exploitation of non-model organisms that can naturally depolymerize and metabolize lignin to directly produce high value aromatic products. Key to this will be further understanding of the involved pathways

and their regulation, as well as the continued identification and elimination of associated pathway bottlenecks [97,98]. Thus, further discovery of non-conventional microbes and development of genetic tools for their subsequent engineering will be critical to achieving this goal.

1.6 Conclusions

Through extensive metabolic engineering efforts, microbial bioproduction of a multitude of aromatic products is currently possible and will only continue to grow. Progress to this end continues to be enabled by the development of versatile synthetic and systems biology tools, as well as the discovery of novel biomolecules, phenotypes, and strains. Though much work surely remains, continued efforts in this area will undoubtedly lead to the commercialization of bio-based aromatic products, in some cases supplanting their conventional, petroleum-derived predecessors.

CHAPTER 2. EXPANDING UPON STYRENE BIOSYNTEHSIS TO ENGINEER A NOVEL ROUTE TO 2-PHENYLETHANOL

Abstract

2-Phenylethanol (2PE) is a key molecule used in the fragrance and food industries, as well as a potential biofuel. In contrast to its extraction from plant biomass and/or more common chemical synthesis, microbial 2PE production has been demonstrated via both native and heterologous expression of the yeast Ehrlich pathway. Here, a novel alternative to this established pathway was systematically engineered in *Escherichia coli* and evaluated as a more robust and efficient route. This novel pathway was constructed via the modular extension of a previously-engineered styrene biosynthesis pathway, proceeding from endogenous L-phenylalanine in five steps and involving four heterologous enzymes. This 'styrene-derived' pathway boasts a ~10-fold greater thermodynamic driving force than the Ehrlich pathway, and enables reduced accumulation of acetate byproduct. When directly compared using a host strain engineered for L-phenylalanine over-production, preservation of phosphoenolpyruvate, and reduced formation of byproduct 2-phenylacetic acid, final 2PE titers via the styrene-derived and Ehrlich pathways reached 1817 and 1164 mg/L, respectively, at yields of 60.6 and 38.8 mg/g. Following optimization of induction timing and initial glucose loading, 2PE titers by the styrene-derived pathway approached as high as 2 g/L – a ~2-fold increase over prior reports for 2PE production by *E. coli* employing the Ehrlich pathway.

This chapter contains work published in:

Machas, M.S., McKenna, R., Nielsen, D.R. Expanding Upon Styrene Biosynthesis to Engineer a Novel Route to 2-Phenylethanol *Biotechnol J* 2017 (12)10. doi: 10.1002/biot.201700310.

2.1 Introduction

With its 'rose-like' aroma, 2-phenylethanol (2PE) is an important molecule in the flavor and fragrance industries [16,99]. More specifically, 2PE is used in the production of various foods and beverages and, most notably, remains the most used fragrance compound in the cosmetics and perfume industries [100]. Meanwhile, in addition to its traditional usage as a specialty chemical, 2PE has also garnered recent interest as a potential biofuel molecule due to its low volatility, high energy density and non-hygroscopic properties [101], or alternatively as a fuel additive helpful for preventing knocking as a result of its high octane number and reduced gas-phase reactivity [102,103]. Altogether, annual global demand for 2PE exceeds 10,000 tons [99], with a market size expected to reach $700 million by 2019 [104]. Traditional 2PE production methods involve its extraction from the essential oils of many flowering plant species – most notably, rose oil, which contains up to 60% 2PE [105]. Although extraction is still practiced to obtain the natural product, this process is expensive and poorly scalable, and thus the bulk of 2PE production instead presently occurs via its chemical synthesis from petrochemical feedstocks. Though cheaper, 2PE production in such a manner is both non-renewable and unsustainable, and furthermore employs carcinogenic precursors (i.e., benzene [99]) as feedstocks; undesirable from a 'green chemistry' perspective and a feature that imposes usage restrictions, especially in flavor/fragrance applications [105].

In light of the above limitations, microbiological production of 2PE via a variety of synthesis routes has recently been explored as a more sustainable alternative. A natural fermentation product of several yeast strains (albeit typically at only trace levels), 2PE is in large part responsible for the 'floral' aromas present in many fermented foods and beverages [106,107]. In yeast, 2PE is produced via the Ehrlich pathway [108,109]; a two-step pathway stemming from phenylpyruvate, an intermediate of the shikimic acid (SA) pathway and direct precursor to L-phenylalanine (Phe). First, phenylpyruvate decarboxylase (PPDC) serves to convert phenylpyruvate to 2-phenylacetaldehyde which is subsequently reduced to 2PE by an alcohol dehydrogenase (**Figure 2.1**). In *S. cerevisiae*, for example, Aro10p, a thiamine pyrophosphate-dependent enzyme, catalyzes the first step [110] whereas reduction of 2-phenylacetaldehyde to 2PE occurs by the aid of one or more native

dehydrogenases (including *ADH1-5*) [111]. Achieving high levels of 2PE via their native Ehrlich pathway, however, typically requires select yeast strains (e.g., *S. cerevisiae* [111,112], *Kluyveromyces marxianus* [113]) to be cultured under nitrogen limited conditions while supplementing the medium with excess exogenous Phe [105,112] (note: Phe transaminase (e.g., ARO9 in *S. cerevisiae* [114]) converts Phe and 2-ketoglutarate to phenylpyruvate and L-glutamate, the latter being degraded to provide nitrogen for growth). However, as Phe is a relatively expensive feedstock with limited scalability, 2PE production directly from renewable biomass sugars could represent a more promising approach.

To date, microbial 2PE production from glucose has focused predominantly on expanded applications of the Ehrlich pathway, most commonly via its functional reconstruction in other, heterologous microbes. For example, Atsumi *et al.* first reported the functional reconstruction of the Ehrlich pathway in *E. coli* (comprised of *kivd* from *Lactococcus lactis* and *ADH2* from *S. cerevisiae*), demonstrating production of 57.3 mg/L 2PE from 36 g/L glucose (a yield of 1.59 mg/g) using a wild-type background [101]. Kang *et al.* later also reconstructed the Ehrlich pathway in *E. coli* (in this case instead using *kdc* and *ADH1* from *Pichia pastoris* and *S. cerevisiae*, respectively) and, following deregulation of metabolite flux through the SA pathway, reported 2PE titers as high as 285 mg/L [115]. Finally, expressing the Ehrlich pathway composed instead of *ipdC* from *Azospirillum brasilense* and *yahK* from *E. coli* in a Phe over-producing host, Koma *et al.* engineered *E. coli* for direct 2PE production from glucose at titers reaching 940.6 mg/L and a yield of 94.06 mg/g [16]. To the best of our knowledge, this output represents the highest 2PE production from glucose by engineered *E. coli* reported to date.

For several years, our research has focused on the engineering of non-natural pathways for the renewable production of various bulk and specialty aromatic chemicals [19,32,116], including a recent series of studies demonstrating: i) engineering of a novel pathway for styrene biosynthesis from glucose (**Figure 2.1**; from Phe, comprised of *PAL2* from *Arabidopsis thaliana* and *FDC1* from *S. cerevisiae*) [117], and ii) subsequent extension of the styrene pathway to *(S)*-styrene oxide (i.e., by additional co-expression of *styAB* from *Pseudomonas putida* S12, encoding styrene

monooxygenase (SMO)) [118]. Common to numerous *Pseudomonas* sp., SMO serves as the first step in one of the principle aerobic styrene degradation pathways [119]. Following SMO, styrene oxide isomerase (SOI; encoded by *styC* in *P. putida* S12, for example) is subsequently responsible for converting *(S)*-styrene oxide to 2-phenylacetaldehyde before further catabolism then takes place. Recognizing, however, that 2-phenylacetaldehyde also serves as precursor to 2PE (as in the Ehrlich pathway), as further illustrated in **Figure 2.1**, it was postulated that a novel, 'styrene-derived' pathway could also be engineered for *de novo* 2PE production from glucose. Accordingly, this non-natural pathway, which couples styrene biosynthesis with its subsequent, partial aerobic degradation, was systematically engineered and comparatively evaluated as an alternative to the established Ehrlich pathway.

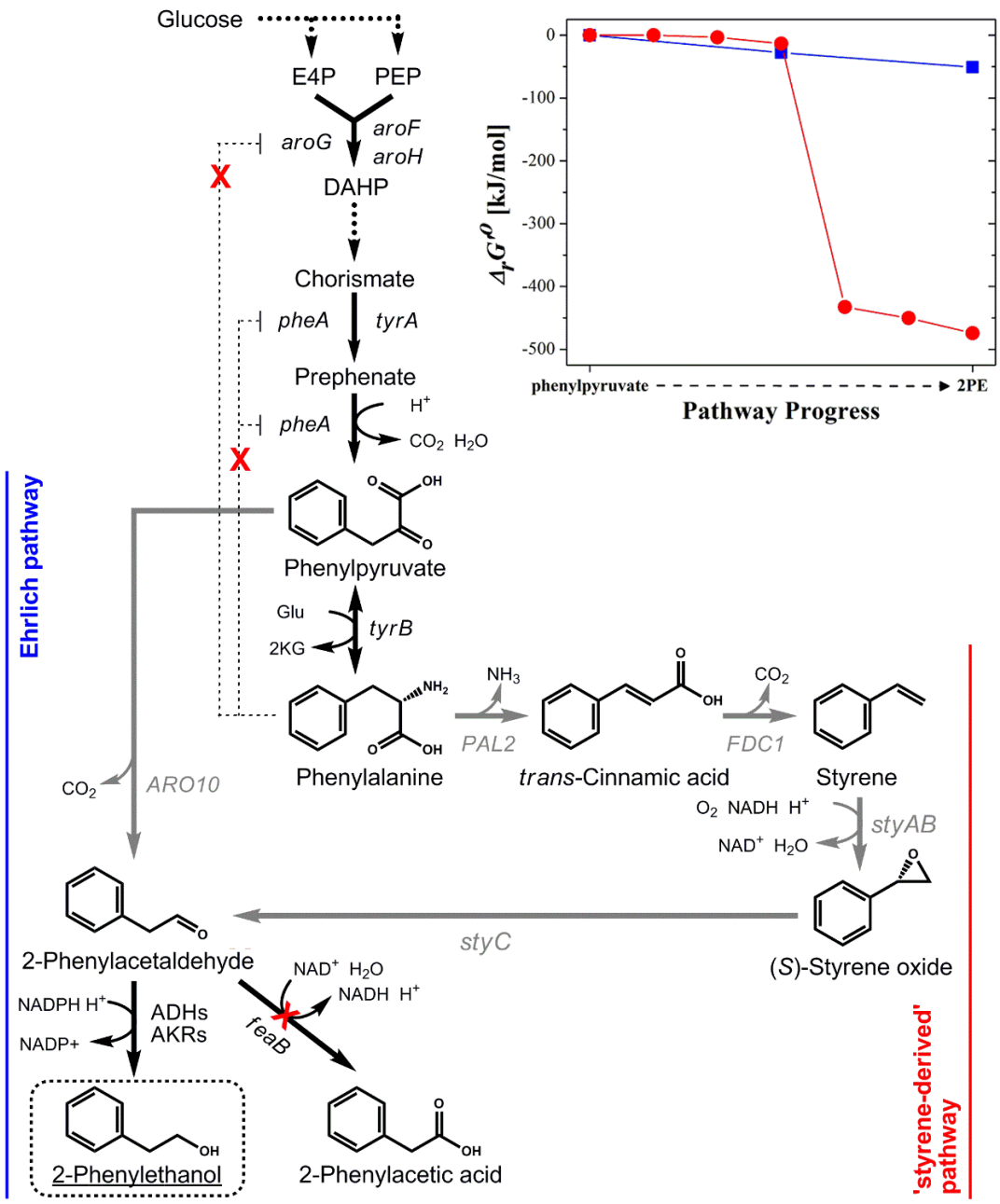

Figure 2.1 2-Phenylethanol Bioproduction Routes in *E. coli*.

Comparing 2PE biosynthesis via the established Ehrlich and proposed styrene-derived pathways. Endogenous pathway steps shown with black arrows whereas heterologous steps are shown in gray. In the case of aroG and pheA, 'X' indicates alleviation of allosteric inhibition caused by Phe due to the presence of feedback resistant mutants of these genes in E. coli NST74. In the case of feaB, 'X' indicates its chromosomal deletion. Inset: Comparing the change in Gibbs free energy due to reaction ($\Delta_r G'°$) with progress through each of the two pathways (Ehrlich pathway, blue squares; styrene-derived pathway, red circles) from phenylpyruvate to 2PE.

2.2 Materials and Methods

2.2.1 Microorganisms

All strains used in this study are listed in **Table 2.1**. *E. coli* NEB 10-beta was obtained from New England Biolabs (NEB; Ipswich, MA) and was used for cloning and the propagation of all plasmids. *E. coli* NST74 (ATCC 31884), a feedback resistant mutant of *E. coli* which overproduces Phe [120], and *P. putida* S12 (ATCC 700801), which served as the genetic source of s*tyABC*, were both purchased from the American Type Culture Collection (ATCC; Manassas, VA). *S. cerevisiae W303*, which served as the genetic source of *ARO10*, was a kind gift from Prof. Kristala Prather (MIT). *E. coli* strains JW1380-1, JW1843-2, JW1666-3, and JW2410-1 were obtained from the Coli Genetic Stock Center (CGSC; New Haven, CT) and served as the genetic source for the *feaB::FRT-kan^R-FRT*, *pykA::FRT-kan^R-FRT*, *pykF::FRT-kan^R-FRT*, and *crr::FRT-kan^R-FRT* deletion cassettes, respectively, along with wild-type *E. coli* BW25113. Chromosomal in-frame gene deletions in *E. coli* and subsequent *kan^R* marker removal were accomplished via a method modified from that of Datsenko and Wanner [121], as previously described [32].

Table 2.1 Strains, Plasmids, and Pathways Constructed and/or Used for 2PE Production.

Strains	Description	Source
E. coli NST74	*aroH367, tyrR366, tna-2, lacY5, aroF394(fbr), malT384, pheA101(fbr),pheO352, aroG397(fbr)*	ATCC 31884
E. coli BW25113	*Δ(araD-araB)567, ΔlacZ4787::rrnB-3, λ$^-$, rph-1, Δ(rhaD-rhaB)568, hsdR514*	CGSC
E. coli NEB-10 beta	*araD139 Δ(ara,leu)7697 fhuA lacX74 galK16 galE15 mcrA f80d(lacZΔM15)recA1 relA1 endA1 nupG rpsL rph spoT1Δ(mrr-hsdRMS-mcrBC)*	NEB
S. cerevisiae W303	Source of *ARO10*, *FDC1*	Prather Lab, MIT
P. putida S12	Source of *styABC*	ATCC 700801
E. coli NST74 *ΔfeaB*	*ΔfeaB* mutation in *E. coli* NST74	This study
E. coli NST74 *ΔfeaB Δcrr*	*Δcrr* mutation in *E. coli* NST74 *ΔfeaB*	This study

E. coli NST74 *ΔfeaB Δcrr ΔpykA*	*ΔpykA* mutation in *E. coli* NST74 *ΔfeaB Δcrr*	This study
E. coli NST74 *ΔfeaB Δcrr ΔpykF*	*ΔpykF* mutation in *E. coli* NST74 *ΔfeaB Δcrr*	This study
E. coli NST74 *ΔfeaB Δcrr ΔpykA ΔpykF*	*ΔpykF* mutation in *E. coli* NST74 *ΔfeaB Δcrr ΔpykA*	This study

Plasmids	Features and/or Construction	Source
pTrcColaK	ColA ori, *lacI^q, Kan^r, P_{Trc}*	[118]
pBbA5a	p15A ori, *lacI, Amp^r*, P_{lacUV5}; derived from pY3	[37]
pCP20	FLP, ts-rep, [cI857](lambda)(ts), Amp^r	CGSC
pKD46	repA101(ts) and R101 ori, Amp^r, *araC, araBp*	CGSC
pTpal-fdc	*PAL2* from *A. thaliana* and *FDC1* of *S. cerevisiae* inserted into the *NcoI* and *XbaI* and *SbfI* and *HindIII* sites of pTrc99A	[118]
pY-PAL2FDC1	*PAL2-FDC1* operon from pTpal-fdc inserted into the *BglII* and *XhoI* sites of pY3	This study
pTrcColaK-styC	*styC* from *P. putida* S12 inserted into the *PstI* and *HindIII* sites of pTrcColaK	This study
pTrcColaK-styABC	*styABC* from *P. putida* S12 inserted into the *XbaI* and *HindIII* sites of pTrcColaK	This study
pY-ARO10	*ARO10* from *S. cerevisiae* inserted into the *BglII* and *XhoI* sites of pY3	This study

Pathway	Composed of plasmids	Source
Ehrlich	pY-ARO10	This study
Styrene-derived	pY-PAL2FDC1, pTrcColaK-styABC	This study

2.2.2 Plasmid Construction

All plasmids constructed and used in this study are listed in **Table 2.1**. Plasmid pY3 (Addgene plasmid #50606), originally derived from pBbA5a, was a gift from Prof. Jay Keasling (UC-Berkeley).

Custom DNA oligonucleotides were synthesized by Integrated DNA Technologies (Coralville, IA). Genomic DNA (gDNA) was prepared from cell cultures using the ZR Fungal/Bacterial DNA MiniPrep (Zymo Research, Irvine, CA) according to vendor protocols. All genes were PCR amplified with Q5 High-Fidelity DNA Polymerase (NEB) using standard protocols. Amplified linear DNA fragments were purified using the Zymo Research DNA Clean & Concentrator Kit (Zymo Research) according to manufacturer protocols. Once purified, DNA fragments were then digested with appropriate restriction endonuclease enzymes at 37°C for > 6 h (NEB). Digested fragments were gel purified using the Zymoclean Gel DNA Recovery Kit (Zymo Research, Irvine, CA) and ligated at room temperature for >1 h using T4 DNA ligase (NEB). Ligation reactions were transformed into chemically-competent *E. coli* NEB 10-beta (NEB) and selected by plating on Luria-Bertani (LB) solid agar containing appropriate antibiotics. Transformant pools were subsequently screened by colony PCR and restriction digest mapping.

2.2.3 Assaying SOI Activity in Whole Resting Cells

SOI activity was assayed in whole resting cells engineered to express *styC* from *P. putida* S12. More specifically, *E. coli* BW25113 was first transformed with either pTrcColaK-styC or pTrcColaK (as control). Seed cultures were prepared by growing individual colonies from LB-agar plates in 3 mL of LB for ~12 h at 32°C. Seed cultures were used to inoculate 50 mL of LB broth supplemented with 35 mg/L kanamycin in a 250 mL shake flask. Flasks were cultured at 32°C with shaking for ~8 h, at which time they were induced by addition of isopropyl β-D-1-thiogalactopyranoside (IPTG) at a final concentration of 0.2 mM. Following induction, cultures were incubated at 32°C overnight, after which cells were then harvested by centrifugation at 3,000 x *g*. The cell pellet was washed twice with pH 7.4 phosphate buffered saline (PBS) solution, and resuspended in 50 mL pH 7.4 PBS solution to a final cell density determined as an optical density at 600 nm (OD_{600}) of ~4. For the assay, a series of resting cell suspensions, each with a total volume of 50 mL in a 250 mL shake flask, were prepared at final cell densities of OD_{600} ~0.01, 0.03, and 0.07 (i.e., by resuspending an appropriate volume of the above stock suspension) in fresh pH 7.4 PBS solution supplemented with *(S)*-styrene oxide at an initial concentration of 1300 mg/L. Over the course of 6.5 h, flasks

were incubated at 32°C with shaking at 200 RPM while samples (each 0.5 mL) were periodically taken for HPLC analysis to determine concentrations of residual *(S)*-styrene oxide and produced 2-phenylacetaldehyde, as described below.

2.2.4 Assaying 2PE Toxicity

The effects of 2PE on *E. coli* growth rate and yield was determined by monitoring the impacts of its exogenous addition at increasing final concentrations on growing cultures. Approximately 1 ml of an *E. coli* NST74 seed culture was used to inoculate 50 ml of LB broth in a 250 mL shake flask. When cultures reached OD_{600} ~0.6, 2PE was added to the flasks at an array of final concentrations ranging from 0 to 2 g/L. Culturing then resumed for an additional 6 h with periodic monitoring of OD_{600}.

2.2.5 Production of 2PE from Glucose by Engineered E. coli

Seed cultures were grown in 3 mL LB broth supplemented with appropriate antibiotics at 32°C for 12 – 16 h. Next, 0.5 mL of seed culture was used to inoculate 50 mL (in 250 mL shake flasks) of pH 6.8 MM1 – a phosphate-limited minimal media adapted from McKenna and Nielsen [117], with the following recipe (in g/L): glucose (20), $MgSO_4 \cdot 7H_2O$ (0.5), $(NH_4)_2SO_4$ (4.0), MOPS (24.7), KH_2PO_4 (0.3), and K_2HPO_4 (1.0), as well as 1 mL/L of a trace mineral solution containing (in g/L): Thiamine HCl (0.101), $MnCl_2 \cdot 4H_2O$ (1.584), $ZnSO_4 \cdot 7H_2O$ (0.288), $CoCl_2 \cdot 6H_2O$ (0.714), $CuSO_4$ (0.1596), H_3BO_3 (2.48), $(NH_4)_6Mo_7O_{24} \cdot 4H_2O$ (0.370), and $FeCl_3$ (0.050). Once inoculated, cultures were grown at 32°C while shaking at 200 RPM until reaching an OD_{600} of 0.8 (~8 h), at which time they were induced by addition of IPTG at a final concentration of 0.2 mM. Following induction, strains were cultured for a total of 72 h (unless otherwise stated), during which time samples were periodically withdrawn for cell growth and metabolite analysis. Meanwhile, intermittently throughout each culture, pH was increased back to its initial value by adding a minimal volume (typically ~0.2-0.4 mL) of 0.4 g/L K_2HPO_4 solution.

2.2.6 Analytical Methods

Cell growth was measured as OD_{600} using a UV/Vis spectrophotometer (Beckman Coulter DU800, Brea, CA). Culture samples were centrifuged at 11,000 x *g* for 4 min to pellet cells, after which 0.25 mL of the resulting supernatant was then transferred to a glass HPLC vial containing an equal volume of 1 N HCl before being sealed with a Teflon-lined cap. Analysis of all aromatic metabolites was performed via high performance liquid chromatography (HPLC; Agilent 1100 series HPLC, Santa Clara, CA) using a diode array (UV/Vis) detector. Separation was achieved on a reverse-phase 5µm Hypersil Gold C18 column (4.6 mm x 100 mm; Thermo Fisher, USA) operated at 45°C using mobile phase consisting of water with 0.1% formic acid (A) and methanol (B), flowing at a constant rate of 0.75 mL/min according to the following gradient: 5% B at 0 min, 5% to 80% B from 0 to 10.67 min, 80% B from 10.67 to 13.33 min, 80% to 5% B from 13.33 to 18.67 min, and 5% B from 18.67 to 20 min. The eluent was monitored using a diode array detector (DAD) set at 215 nm for detection of Phe, trans-cinnamic acid, styrene and (*S*)-styrene oxide, and 258 nm for detection of 2-phenylacetaldehyde, 2-phenylacetic acid, and 2PE. Glucose and acetate analysis, meanwhile, was performed using the same HPLC system equipped with a refractive index detector (RID) and an Aminex HPX-87H column (BioRad, Hercules, CA) operated at 35°C. The column was eluted using 5 mM H_2SO_4 as the mobile phase at a constant flow rate of 0.55 mL/min for 20 min. External calibrations were prepared and used to quantify each species of interest.

2.2.7 Thermodynamic Analysis

To compare relative pathway energetics, net changes in Gibbs free energy due to reaction, $\Delta_r G'°$, were determined for each reaction using the eQuilibrator online tool [122], at a reference state of 25°C, pH 7, and ionic strength of 0.1 M.

2.3 Results

2.3.1 Comparative Assessment of Alternative 2PE Pathways

As seen in **Figure 2.1**, both the proposed, styrene-derived and established, Ehrlich pathways stem from precursors in the SA pathway, namely Phe and phenylpyruvate, respectively. As such, both

pathways share the same theoretical yield, estimated as 0.36 g/g on glucose (with functional PTS, based on estimates derived from Varma et al. [123]). Moreover, both pathways converge at 2-phenylacetaldehyde before its reduction to 2PE, as has been reported to readily occur via one or more native, NADPH-dependent alcohol dehydrogenases (ADHs; e.g., *yqhD*, *yahK*, *yjgB*) and/or aldo-keto reductases (AKRs; e.g., *dkgA*, *dkgB*, *yeaE*) [17,124]. However, between the last common precursor (i.e., phenylpyruvate) and 2PE, the two pathways differ greatly and in several important ways. For instance, unlike the Ehrlich pathway, which employs only one foreign enzyme, the styrene-derived pathway is instead composed of four heterologous steps. However, despite its length, the thermodynamic driving force associated with the styrene-derived pathway is nearly 10-fold greater than that of the Ehrlich pathway. More specifically, when compared from phenylpyruvate to 2PE, the net change in Gibbs free energy of reaction ($\Delta_r G'^{\circ}$) for the Ehrlich pathway is -50.9 kJ/mol compared to -474.4 kJ/mol for the styrene-derived pathway (**Figure 2.1** inset); the bulk of the difference being due to the highly favorable conversion of styrene to (*S*)-styrene oxide via styrene monooxygenase (NADH-dependent, encoded by *styAB*), which contributes -419.4 kJ/mol (or 88%) to the total $\Delta_r G'^{\circ}$ of the pathway [122]. As a consequence, however, the styrene-derived pathway consumes twice as many reducing equivalents (1 NADH and 1 NADPH per molecule of 2PE produced) than the Ehrlich pathway (only 1 NADPH). Accordingly, whereas similarities certainly exist, both 2PE pathways appear to possess their own unique and inherent merits and limitations, the likes of which were next experimentally investigated.

2.3.2 Engineering 2PE Pathways

Construction of the styrene-derived 2PE pathway began from a previously-engineered *(S)*-styrene oxide pathway, comprised of *PAL2* from *A. thaliana, FDC1* from *S. cerevisiae*, and *styAB* from *P. putida* S12 [118]. To convert (*S*)-styrene oxide to 2-phenylacetaldehyde, however, it was first necessary to identify a suitable gene encoding SOI activity. Of particular interest was *styC* from *P. putida* S12 [125] which, together with *styAB*, functions as part of its native styrene degradation pathway [126,127]. Following the cloning and subsequent expression of *styC* in *E. coli* BW25113 pTrcColaK-styC, a whole resting cell assay was performed wherein, as seen in **Figure 2.2**,

recombinant SOI activity was demonstrated via the conversion of exogenous (*S*)-styrene oxide to 2-phenylacetaldehyde (note: control experiments using *E. coli* BW25113 pTrcColaK showed no conversion of (*S*)-styrene oxide; data not shown). Initially, the assay was performed at a high cell density (i.e., OD_{600} ~4; representing that of a typical culture), however, under such conditions 100% conversion was achieved in <10 min at stoichiometric yield (data not shown). To slow the net reaction rate and allow for improved monitoring, the experiment was repeated at lower cell densities; specifically, OD_{600} of 0.01, 0.03, and 0.07. In this case, increasing cell density expectedly resulted in faster rates of (*S*)-styrene oxide consumption and 2-phenylacetaldehyde production, with the former reaching as high as 5.6 g/L-h. For comparison, when previously assayed under analogous conditions, styAB-expressing *E. coli* resting cells produced (S)-styrene oxide from exogenous styrene at rates reaching only as high as ~0.1 g/L-h; albeit at much higher cell densities (OD_{600} ~1). Consequently, it was expected that recombinant StyC activity would be sufficiently high so as to avoid a potential flux bottleneck at this step.

Based on this result, *styC* was cloned for expression as part of the full, styrene-derived pathway, in this case as part of the natural *styABC* operon (encoding both SMO and SOI) and expressed via a P_{trc} promoter in plasmid pTrcColaK-styABC. Plasmid pY-PAL2FDC1 was constructed by cloning a previously assembled operon composed of *PAL2* from *A. thaliana* and *FDC1* from *S. cerevisiae* from pTpal-fdc [118] behind the P_{lacUV5} promoter of pBbA5a [37]. In the case of the Ehrlich pathway, meanwhile, PPDC plays a key role as the first committed pathway step. Previously, Atsumi *et al.* evaluated 5 different PPDC isozymes (namely those encoded by *ARO10*, *PDC6* and *THI3* from *S. cervisiae*, *kivd* from *L. lactis*, and *pdc* from *C. acetobutylicum*) in *E. coli*, ultimately finding Aro10p to support the greatest 2PE production from glucose [101]. Accordingly, *ARO10* was fused to a P_{lacUV5} promoter in pBbA5a, resulting in pY-ARO10.

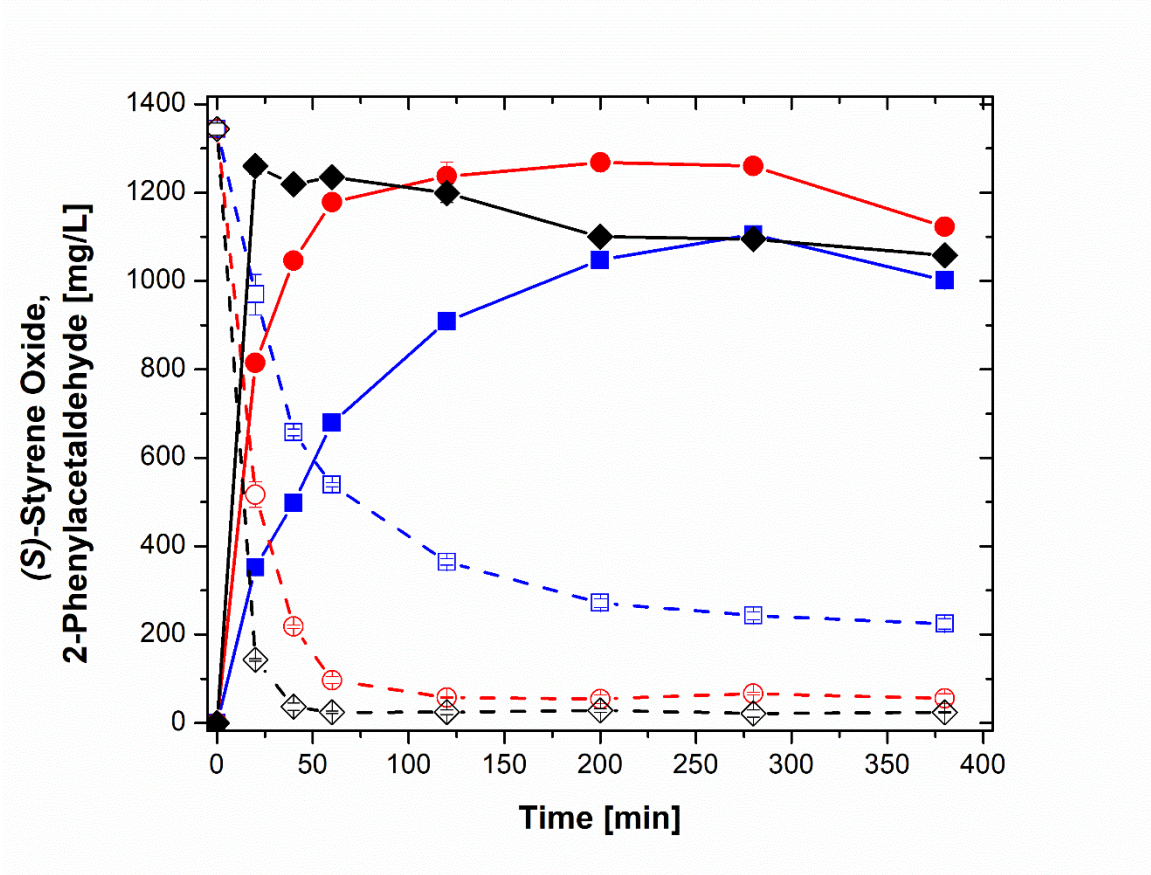

Figure 2.2 Resting Cell Assay of StyC activity in *E. coli* for Conversion of (S)-Styrene Oxide.

Screening styrene oxide isomerase enzyme activity using E. coli BW25113 pColaK-styC whole resting cells. Conversion of (S)-styrene oxide (open shapes, dotted line) to 2-phenylacetaldehyde (solid shapes, solid line) by StyC using three different cell densities (OD_{600} ~ 0.01, 0.03, and 0.07 are blue squares, red circles, and black diamonds, respectively). Error bars reported at one standard deviation from triplicates experiments.

2.3.3 Demonstrating and Comparing 2PE Production via Alternative Pathways

The Ehrlich and styrene-derived pathways were both constructed as described in **Table 2.1** and first introduced and expressed in *E. coli* NST74 (a previously-engineered, Phe-overproducing strain [120]), with the resulting strains producing 158 ± 12 and 182 ± 4 mg/L of 2PE, respectively. However, in addition to 2PE, both strains also co-produced 2-phenylacetic acid as a major byproduct, whose final titers reached 352 ± 12 and 503 ± 21 mg/L, respectively. In *E. coli*, 2-phenylacetaldehyde is converted to 2-phenylacetic acid via a native, NAD^+-dependent 2-phenylacetaldehyde dehydrogenase, encoded by *feaB* (**Figure 2.1**) [128]. In this case, the ~1.5-fold greater 2-phenylacetic acid production accompanying the styrene-derived pathway was likely due to its

aforementioned increased redox requirement, which would be partially balanced via oxidation of 2-phenylacetaldehyde to 2-phenylacetic acid (regenerating 1 NADH; **Figure 2.1**). To eliminate undesirable accumulation of 2-phenylacetic acid, *feaB* was next deleted from NST74. When introduced and expressed in NST74 Δ*feaB*, 2-phenylacetic acid production was no longer detected for either the Ehrlich or styrene-derived pathway and, after 72 h, 2PE titers now reached 552 ± 14 and 643 ± 29 mg/L, respectively; in both cases at similar glucose yields (35.1 ± 0.5 and 37.7 ± 1.2 mg/g, or 9.7 and 10.5% of the theoretical maximum).

To assess if 2PE production in these initial strains was perhaps limited by end-product inhibition, a growth challenge study was performed to characterize the response of *E. coli* growth to the addition of exogenous 2PE at a range of increasing final concentrations (**Figure 2.3**). While growth rate and yield were reduced in the presence of as little as 1 g/L 2PE, severe growth inhibition did not occur until reaching about 2 g/L 2PE. This compares well with prior reports wherein 2PE was reported to inhibit *E. coli* at levels of ~1 g/L [115], and suggests that, at least in these initial strains, 2PE production by either pathway was likely not yet limited by end-product inhibition.

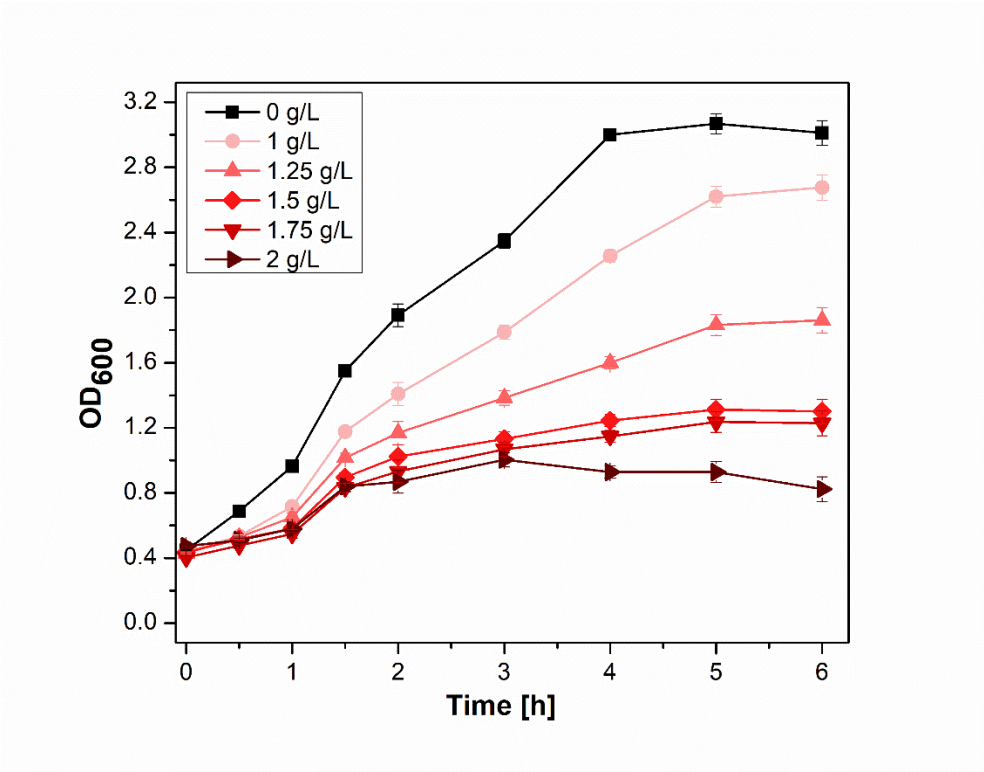

Figure 2.3 Toxicity assay of 2PE on *E. coli* NST74.

Growth response of E. coli NST74 following exogenous 2PE addition at final concentrations of 0 g/L (control; squares), 1 g/L (circles), 1.25 g/L (upright triangles), 1.5 g/L (diamonds), 1.75 g/L (inverted triangles) and 2 g/L (right triangles). Error bars reported at one standard deviation from triplicate experiments.

2.3.4 Host Strain Engineering to Increase Precursor Availability

Robust 2PE production by either pathway depends on ample production of SA pathway precursors (**Figure 2.1**), which in turn is known to benefit from increased availability of phosphoenolpyruvate (PEP). Noda et al. previously reported deletion of both *pykF* and *pykA* (encoding pyruvate kinase isozymes I and II, respectively, which convert PEP to pyruvate, producing ATP) as an effective strategy for both promoting PEP availability while reducing acetate yield (by as much as 4.5-fold), in their case also enhancing the production of various chorismate-derived aromatic products [129]. Meanwhile, it has been further demonstrated that PEP availability can be improved via the partial inactivation of the glucose-specific phosphotransferase system (PTS; which facilitates glucose uptake via its phosphorylation at the expense of PEP), as can be achieved by deleting *crr* (encoding IIA^{Glc}) [130]. This mutation also further benefits the culture by reducing rates of glucose uptake which,

in turn, also decreases overflow metabolism and the associated production of unwanted (and potentially inhibitory) acetate [130,131]. Accordingly, NST74 Δ*feaB* was further engineered to systematically introduce Δ*pykA*, Δ*pykF*, and Δ*crr* mutations, upon which the resulting strains were tested for their relative ability to support 2PE production via the two pathways. The resulting 2PE titers are compared in **Figure 2.4**, along with the relative effects of the same mutations on Phe production by each host strain (i.e., in the absence of either pathway) for comparison. As can be seen, compared to the above results using NST74 Δ*feaB* as host, deletion of *crr* had a significant effect on 2PE production by both the Ehrlich and styrene-derived pathways, improving final titers by 77% and 67%, respectively. Deletion of *crr* also resulted in expected reductions in acetate accumulation, in each case by 45-60%. Meanwhile, the additional, combined deletion of *pykA* and *pykF* led to even further improvements in 2PE production by both the Ehrlich and styrene-derived pathways, reaching 1163 ± 3 and 1468 ± 47 mg/L (or 9.52 ± 0.02 and 12.02 ± 0.38 mM), respectively, after 72 h (increases of 19% and 37% relative to using NST74 Δ*feaB* Δ*crr* as host). Interestingly, as is most prominent in the case of the styrene-derived pathway, individual deletion of just *pykA* or *pykF* alone gave little or no improvement, suggesting that full inactivation of pyruvate kinase activity was necessary to realize the beneficial effects of this strategy. That said, analogous experiments in the absence of the pathway (i.e., for Phe production) suggest the Δ*pykA* mutation to perhaps be most important (**Figure 2.4**); a surprising observation given that PykF has been reported to provide the dominant pyruvate kinase activity during aerobic growth on glucose [132]. For comparison, in the absence of either pathway, NST74 Δ*feaB* Δ*crr* Δ*pykA* Δ*pykF* produced a total of 2076 ± 19 mg/L (12.57 ± 0.11 mM) Phe. Accordingly, and assuming constant flux through the SA pathway in each case, this suggests that the styrene-derived pathway was more efficient than the Ehrlich pathway (96 vs. 76%) at assimilating and ultimately converting their corresponding endogenous precursor to 2PE.

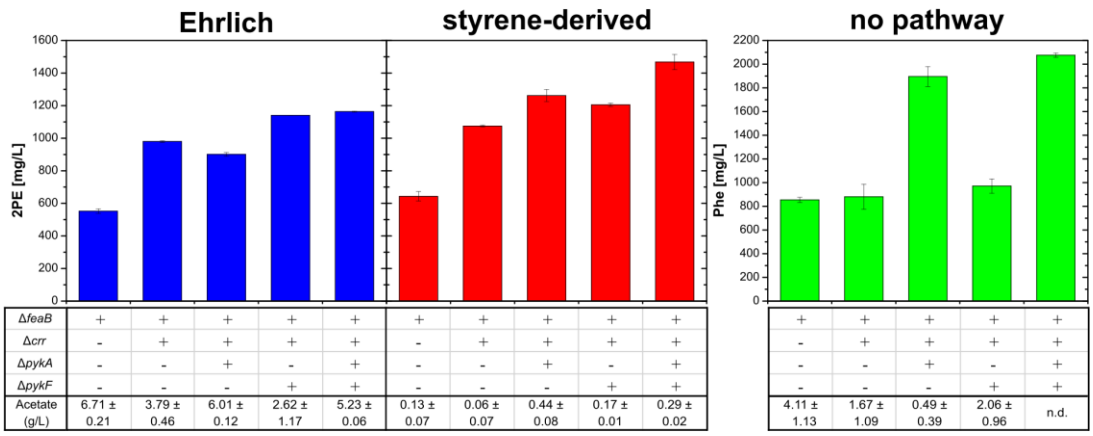

Figure 2.4 2PE Titers for the Ehrlich and Styrene-derived Pathways with Gene Deletions.

Final titers of 2PE after 72 h of culturing for the Ehrlich (blue) and styrene-derived (red) pathways in E. coli NST74 strains harboring various deletions of genes feaB, crr, pykA and pykF (left and center, respectively). Right: Final Phe titers by the same host strain in the absence of either pathway (green). Final acetate concentrations are also shown (n.d. indicates not detected). Error bars reported at one standard deviation from triplicate experiments.

Interestingly, acetate production via the styrene-derived pathway was minimal regardless of which host background was used and, in all cases, was 14- to 71-fold lower than when expressing the Ehrlich pathway. Most strikingly, although in the absence of either pathway acetate accumulation was undetected with NST74 Δ*feaB* Δ*crr* Δ*pykA* Δ*pykF*, upon introduction of the Ehrlich pathway, acetate levels rose back up to 5.23 ± 0.06 g/L (compared to just 0.29 ± 0.02 g/L with the styrene-derived pathway). Given this substantial difference, it was hypothesized that acetate production could perhaps be occurring as a result of Aro10p promiscuity. Decarboxylation of pyruvate, for example, yields acetaldehyde which, in turn, could be oxidized to acetate via *E. coli*'s $NADP^+$-dependent aldehyde dehydrogenase (encoded by *aldB*) [133]. To provide an initial assessment of this proposed phenomena, control cultures were prepared of *E. coli* BW25113 pY-ARO10 grown in the absence or presence of 6 g/L exogenously-supplied sodium pyruvate. After 48 h, accumulated acetate levels were 3.8-fold higher following sodium pyruvate addition (5.41 vs. 1.41 g/L; **Table 2.2**). While more detailed characterizations are needed, these findings certainly support the proposed, *ARO10*-associated mechanism of increased acetate accumulation.

Table 2.2 Acetate Accumulation in Wild-Type *E. coli* Expressing *ARO10* with Pyruvate Feeding.

Acetate accumulation in cultures of E. coli BW25113 pY-ARO10 grown in pH 6.8 MM1 minimal media supplemented with sodium pyruvate at a total concentration of 0 or 6 g/L (note: sodium pyruvate was added to the culture at a final concentration of 2 g/L at each of 8, 18 and 27 h, resulting in 6 g/L total).

Hours after inoculation [h]	0 g/L sodium pyruvate fed	6 g/L sodium pyruvate fed
	Acetate [g/L]	
18	0.09	0.54
27	0.49	0.95
48	1.41	5.41

2.3.5 Optimizing Culture Conditions to Further Improve 2PE Production

Induction timing and initial substrate concentration were next optimized to further improve 2PE production. In the first case, the timing of IPTG-induced expression of the Ehrlich and styrene-derived pathways in NST74 Δ*feaB* Δ*crr* Δ*pykA* Δ*pykF* was investigated at six different points (from inoculation to late exponential phase), the results of which are compared in **Figure 2.5**. In both cases, induction at inoculation gave the greatest final 2PE titers, suggesting greater net flux through each pathway was realized when each was given maximal time to compete for endogenous precursors (consistent with observations of reduced biomass production at earlier inductions; **Figure 2.5**). In contrast, when induced too late (i.e., at 19 h or beyond), neither pathway effectively competed for its requisite precursor, which instead was then assimilated into additional biomass and/or accumulated Phe. In the case of the Ehrlich pathway, net acetate accumulation followed a similar pattern to that of 2PE production (**Figures 2.5 and 2.6**, respectively), with less build-up occurring for later inductions (note: final acetate and 2PE levels were 66% and 71% lower, respectively, when cultures were induced after 29 h versus at inoculation). This observation further supports the above hypothesis that significant acetate byproduct formation is perhaps occurring due to Aro10p promiscuity.

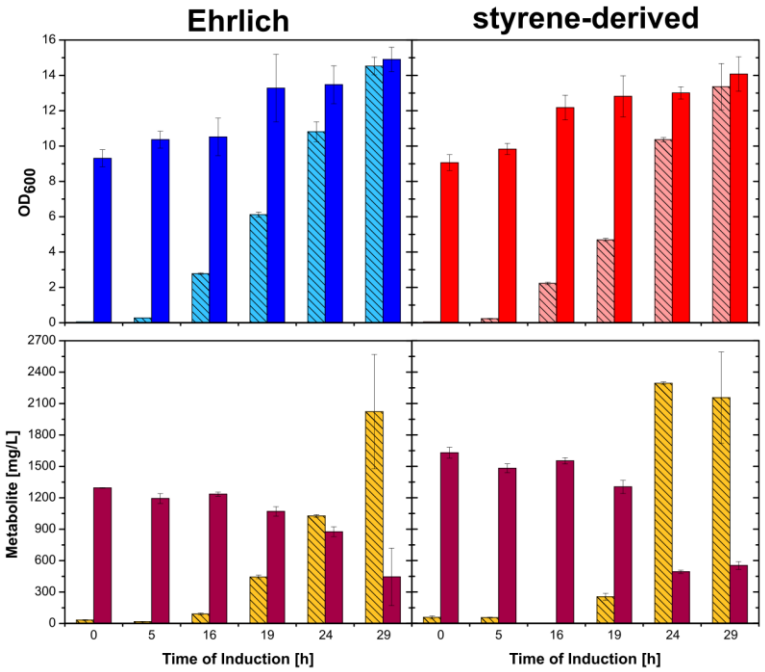

Figure 2.5 Effect of Induction Timing on 2PE Production.

Effect of induction timing on production of 2PE and Phe as well as growth after 72 h by both pathways when expressed in E. coli NST74 ΔfeaB Δcrr ΔpykA ΔpykF. Upper panels: final OD600 (solid, dark blue/red) and OD600 at time of induction for the Ehrlich (striped, light blue) and styrene-derived (striped, light red) pathways. Lower panels: Final concentrations of 2PE (solid, maroon) and Phe (striped, gold). Error bars reported at one standard deviation from duplicate experiments.

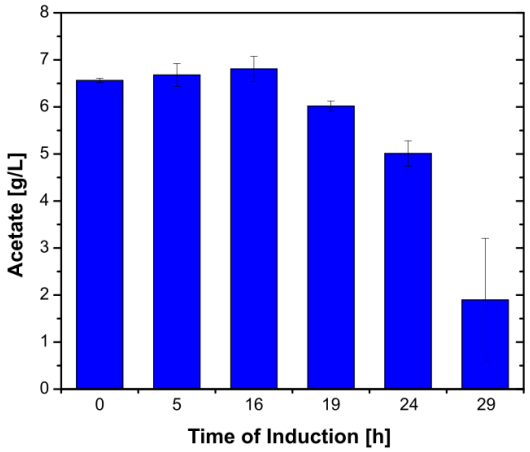

Figure 2.6 Accumulation of Acetate in *E. coli* Cells Producing 2PE via the Ehrlich Pathway.

Acetate accumulation after 72 h by E. coli NST74 ΔfeaB Δcrr ΔpykA ΔpykF expressing the Ehrlich pathway, as a function of induction timing. Error bars reported at one standard deviation from duplicate experiments.

All of the above 2PE production studies were performed by initially supplying each culture with 20 g/L glucose which, in all cases, was fully consumed within 72 h (data not shown). As this suggests a possible substrate limitation, a series of batch experiments were next performed wherein increasing amounts of initial glucose (5 to 50 g/L) were instead supplied, in all cases using the best-performing host strain (i.e., NST74 Δ*feaB* Δ*crr* Δ*pykA* Δ*pykF*) and optimal induction timing (i.e., at inoculation). **Figure 2.7** compares glucose consumption, along with 2PE yield and final titers for both pathways. In all cases, glucose is fully consumed when initially supplied at 5 to 30 g/L, with higher initial glucose levels expectedly resulting in increased 2PE titers. At higher initial glucose concentrations (i.e., 40 and 50 g/L), however, clear differences emerge with respect to the two pathways. Though also declining (perhaps due to a nutrient limitation or onset of substrate inhibition), greater conversion at higher glucose loadings and, as a result, increased 2PE titers and yields remain possible via the styrene-derived pathway. Ultimately, when supplied with 50 g/L glucose, 2PE titers via the styrene-derived pathway reached their maximum level of 1941 ± 13 mg/L at a yield of 60.5 ± 0.3 mg/g (16.8% of theoretical); a final 2PE titer ~2-fold greater than the highest value reported to date for *E. coli* expressing the Ehrlich pathway.

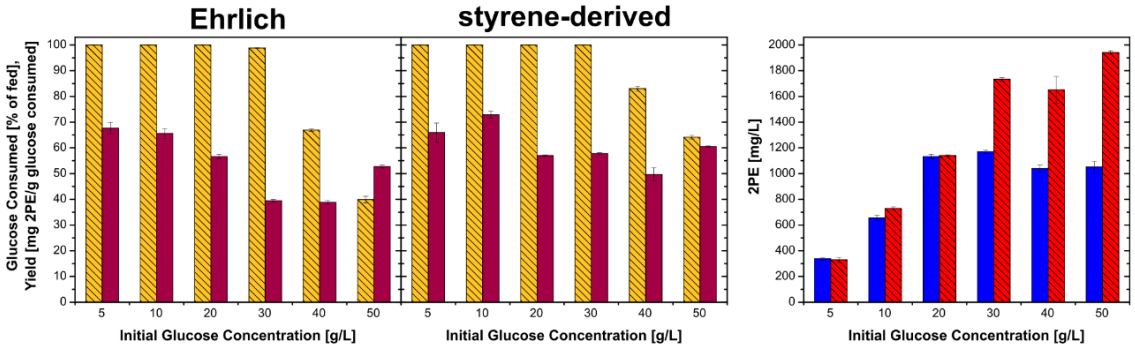

Figure 2.7 Effect of Initial Glucose Concentration on Production of 2PE.

Various initial concentrations of glucose (ranging from 5 to 50 g/L) for 2PE production of E. coli NST74 ΔfeaB Δcrr ΔpykA ΔpykF induced at inoculation. Glucose consumed as a percentage of glucose fed (striped, gold) and mass yield of 2PE from glucose (solid, maroon) after 96 h of culturing for the Ehrlich and styrene-derived pathways (left and center, respectively). Right: 2PE titers for the Ehrlich (solid, blue) and styrene-derived (striped, red) pathways at the 96 h mark are shown for various concentrations of initial glucose. Error bars reported at one standard deviation from triplicate experiments.

A series of batch cultures were lastly performed to investigate the dynamics of 2PE production via both pathways, in each case utilizing NST74 Δ*feaB* Δ*crr* Δ*pykA* Δ*pykF* as host while supplying 30 g/L glucose (to ensure full utilization) and performing induction at inoculation. **Figure 2.8** compares glucose consumption, 2PE and acetate production, and biomass accumulation in each case. Initially, rates of sugar consumption as well as 2PE and biomass production were slower for the styrene-derived pathway. Notably, for instance, while expressing the Ehrlich pathway, average volumetric rates of glucose consumption and 2PE production during the first 24 h were 401 ± 9 and 28.1 ± 2.3 mg/L-h, respectively, compared to just 230 ± 30 and 15.6 ± 0.6 mg/L-h for the styrene-derived pathway. However, by ~36 h, 2PE production by the Ehrlich pathway (which occurred coincidently with cell growth) levels off, whereas production continues for an additional ~30 h via the styrene-derived pathway (during which time cell growth had already entered the stationary phase). Ultimately, after 87 h, final 2PE titers reached 1817 ± 15 and 1164 ± 85 mg/L for the styrene-derived and Ehrlich pathways, respectively, at yields of 60.6 ± 0.5 and 38.8 ± 2.8 mg/g. It should also be noted that by 36 h, acetate accumulation in cultures expressing the Ehrlich pathway approached 2 g/L while still remaining below 0.5 g/L for the styrene-derived pathway, suggesting that the ability of the styrene-derived pathway to maintain longer periods of productivity and greater

net 2PE production may be due in part to its ability to minimize inhibitory byproduct accumulation. Notably, and in contrast to the results of **Figure 2.4**, by 87 h, acetate levels still accumulated to appreciable levels (3.32 g/L, or a net increase of ~3 g/L) for strains expressing the styrene-derived pathway. However, it was further noted that a similar net increase in acetate production (2.2 g/L) was also realized for strains expressing the Ehrlich pathway when supplied with 30 vs. 20 g/L glucose (**Table 2.3**). These behaviors suggest that, in spite of the introduced Δ*crr* Δ*pykA* Δ*pykF* mutations, increased acetate production might still be occurring due to overflow metabolism [134].

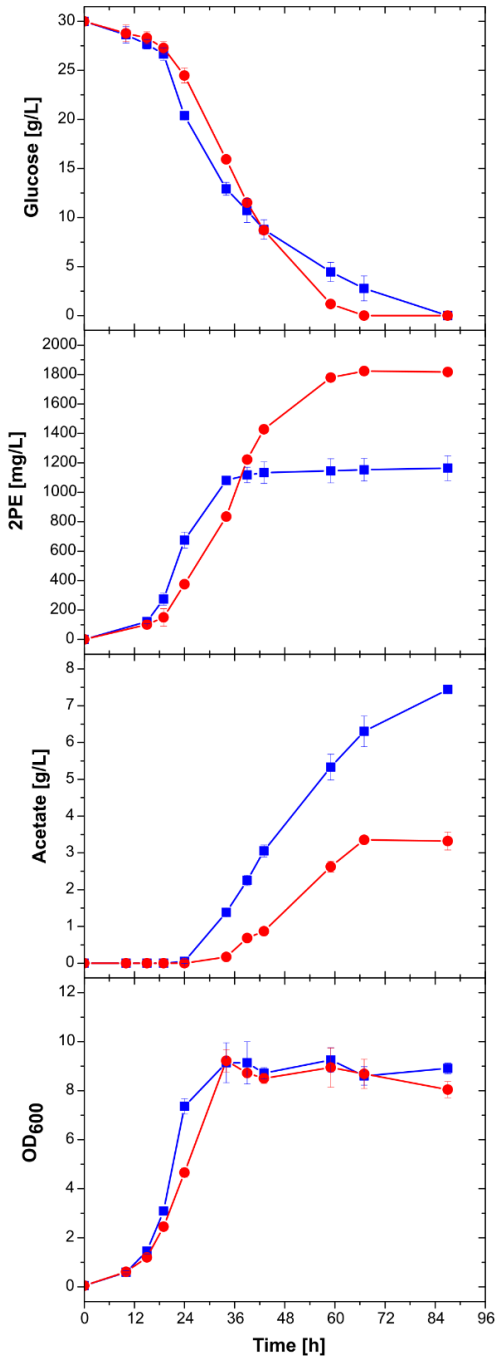

Figure 2.8 Time Course of 2PE, Cell Biomass, and Acetate Production and Glucose Consumption for the Ehrlich and Styrene-derived Pathways.

Time course analysis of 2PE production and relevant culture metrics over 87 h for the Ehrlich (blue squares) and styrene-derived (red circles) pathways in E. coli NST74 ΔfeaB Δcrr ΔpykA ΔpykF supplied with 30 g/L glucose and induced at inoculation. First: glucose consumption. Second: 2PE production. Third: Acetate production. Fourth: Cell growth as represented by OD_{600}. Error bars reported at one standard deviation from triplicate experiments.

Table 2.3 2PE Production Metrics for the Ehrlich and Styrene-derived Pathways.

Relevant culture performance and 2PE production metrics for both the Ehrlich and styrene-derived pathways at 72 h when supplied with an initial glucose concentration of either 20 or 30 g/L. Both pathways were expressed in E. coli NST74 ΔfeaB Δcrr ΔpykA ΔpykF. These data have been compiled for comparison from the results of ***Figure 2.4*** *(for 20 g/L glucose) and* ***Figure 2.8*** *(for 30 g/L glucose).*

	20 g/L glucose		30 g/L glucose	
	Ehrlich	**Styrene-derived**	**Ehrlich**	**Styrene-derived**
2PE [mg/L]	1163 ± 3	1468 ± 47	1164 ± 85	1817 ± 15
Acetate [g/L]	5.23 ± 0.06	0.29 ± 0.02	7.44 ± 0.11	3.32 ± 0.24
OD_{600}	7.63 ± 0.85	13.04 ± 2.57	8.91 ± 0.22	8.04 ± 0.33
Glucose Yield [mg 2PE/g glucose]	58.1 ± 0.2	73.4 ± 2.3	38.8 ± 2.8	60.6 ± 0.5

2.4 Discussion

Through the continued, modular extension of a previously-engineered styrene biosynthesis pathway, a novel route to 2PE has been engineered as a robust and efficient alternative to the established, Ehrlich pathway. Ultimately, for example, when compared under otherwise analogous conditions (**Figure 2.8**), 2PE titers and yields were about 56% greater via the styrene-derived versus Ehrlich pathway, with final titers capable of approaching ~2 g/L with additional glucose supplementation. As characterized via both *in silico* analyses and experimental studies, relative to the Ehrlich pathway, the styrene-derived 2PE pathway was found to possess its own unique and notable advantages, as well as certain caveats. For example, as has been previously characterized with respect to (*S*)-styrene oxide production (also produced via styrene, as in **Figure 2.1**) [118], the highly favorable SMO reaction (which is largely responsible for the ~10-fold greater thermodynamic driving force of the styrene-derived pathway), serves to effectively 'pull' more precursor (i.e., Phe) into the pathway. This phenomenon is further supported in the case of 2PE production, noting that conversion of endogenous precursors via the styrene-derived pathway was

96% versus just 76% by the Ehrlich pathway. Additionally, and in contrast to the Ehrlich pathway, which branches off from native metabolism (i.e., at phenylpyruvate), the styrene-derived pathway instead extends from a terminal pathway metabolite (i.e., Phe; **Figure 2.1**). In this way, the styrene-derived pathway also importantly avoids introducing a competitive 'branch point'. In the Ehrlich pathway, as PPDC (e.g., Aro10p, K_m = 100 µM [135]) must directly compete against native Phe aminotransferase (i.e., TyrB, K_m = 12 µM [136]) for available phenylpyruvate, kinetic limitations can in turn reduce the flux of metabolites that enter the pathway at its first committed step. While deletion of *tyrB* can eliminate such competition, preserving phenylpyruvate for the Ehrlich pathway, such a mutation significantly impairs both Phe and Tyr biosynthesis, thereby necessitating their supplementation or the use of rich media which increases costs and reduces scalability. Meanwhile, however, construction of the styrene-derived pathway requires the simultaneous expression of four heterologous genes. Though perhaps not apparent under the conditions examined here, this could ultimately lead to reduced host fitness and decreased production metrics as a result of increased metabolic burden.

One of the most significant differences between employing the two 2PE pathways concerns not the product, but rather a byproduct, namely acetate. As evidenced by the results of **Figure 2.4**, even when using a host background virtually deficient in acetate accumulation (i.e., NST74 Δ*feaB* Δ*crr* Δ*pykA* Δ*pykF*), significant acetate production reemerged upon introduction of the Ehrlich pathway, reaching final concentrations as high as 5.23 ± 0.06 g/L (in experiments with 20 g/L glucose). Previous studies have found that acetate concentrations above 1 g/L can deter biomass and protein production, reduce protein stability, and lower pH, causing cell lysis [137]. Accordingly, and regardless of the specific mechanism, the ability to significantly reduce acetate byproduct accumulation when employing the styrene-derived pathway is postulated as a significant reason for the ability of this pathway to support superior 2PE production metrics. Though still warranting further investigation, acetate byproduct accumulation when expressing the Ehrlich pathway is thought to be a result of Aro10p promiscuity. Although prior reports suggest that, at least with respect to its native expression in *S. cerevisiae*, Aro10p displays minimal activity on pyruvate (with *in vitro* assays reporting k_{cat}/K_m = 200 and 0.035 $mM^{-1} \cdot s^{-1}$ for phenylpyruvate and pyruvate,

respectively [135]), here, experimental evidence might suggest otherwise, at least with respect to its recombinant, *in vivo* function in *E. coli*.

With final 2PE titers via the styrene-derived pathway ultimately approaching ~2 g/L (at high glucose loading), and in contrast to preliminary cultures, said output now approaches the toxicity limit of 2PE. As the mode of aromatic toxicity against bacteria has most commonly been reported to be associated with their accumulation within and disruption of the cytoplasmic membrane [138], a similar phenomenon was also anticipated here. In fact, with a toxicity threshold determined as ~2 g/L, the present observations of 2PE toxicity agree well with previously-reported model used to predict the toxicity of various aromatic bioproducts (e.g., styrene, (*S*)-styrene oxide, and various phenolics) based on estimates of the membrane-water partitioning coefficient ($K_{M/W}$) [118]. Accordingly, future improvements in 2PE production will likely necessitate strategies designed to increase inherent tolerance to 2PE or to circumvent its toxic effects (e.g., via its *in situ* removal). It was recently reported that tolerance to and thus production of styrene, for example, could be improved via rigidification of *E. coli*'s cytoplamsmic membrane, in this case by increasing the proportion of *trans* unsaturated fatty acids (as achieved by expressing heterologous *cis-trans* isomerase, encoded by *cti* from *P. aeruginosa*) [139]. Meanwhile, various strategies for *in situ* 2PE removal have also been investigated, including, for example, via its extraction in a biphasic ionic liquid system which gave 3- to 5-fold increases in 2PE production by *S. cerevisiae* [140]. Other approaches, meanwhile, including pervaporation [141] and solid-phase extraction (i.e., using hydrophobic resins) [142] have shown as high as 10-fold improvements in 2PE production.

Finally, whereas the styrene-derived pathway for 2PE production represents a novel alternative to the Ehrlich pathway, two additional routes to 2PE have also recently been reported. In one case, for example, phenylacetaldehyde synthase (PAAS) from *Rosa hybrid* was expressed in *E. coli* to convert Phe to 2-phenylacetaldehyde, which was then subsequently reduced to 2PE. Although this route could, in theory, be expressed in a Phe over-producing host to enable 2PE production directly from glucose, applications to date have been limited just to 2PE production via biotransformation of exogenous Phe (with up to 0.39 g/L 2PE produced in this manner) [143]. That

said, however, while this pathway has the advantage of only requiring one heterologous step, PAAS is a pyridoxal 5'-phosphate (PLP) dependent enzyme and its expression in *E. coli* would thus necessitate external cofactor addition or introduction of a PLP production pathway. A second alternative 2PE production pathway was also recently discovered in tomato. In this case, Phe decarboxylase first converts Phe to phenylethylamine which is then further converted to 2-phenylacetaldehyde via an ammonia-lyase [100]. To our knowledge, this pathway has not yet been expressed in microbes for the purposes of 2PE production, but could provide yet another alternative route for 2PE biosynthesis.

CHAPTER 3. BIOPROCESSING AND GENETIC ALTERATIONS TO IMPROVE PRODUCTION OF L-PHENYLALANINE UTILIZING XYLOSE AND GLUCOSE FEEDSTOCKS

Abstract

A significant and persistent challenge faced by most microbial biocatalysts reamins the ability to convert multiple feedstocks (e.g., different sugars) into a single product in a resourceful manner. Glucose and xylose, for example, are produced from lignocellulosic biomass and represent the most abundant carbon sources in nature. Unfortunately, however, the metabolism of many microbes (including *E. coli*), is subject to carbon catabolite repression (CCR) - a natural regulatory mechanism that precludes their ability to utilize more than one sugar at a time. Recently, it was discovered that (R121C, P363S) mutations in XylR (xylose regulator) released glucose-induced CCR of xylose utilization under anaerobic conditions, allowing strains expressing the mutated *xylR* to efficiently and simultaneously co-utilize glucose and xylose. Here, the efficacy of this strategy was investigated for the first time under aerobic conditions in E. coli, and as a proof-of-concept, used to demonstrate enhanced production of phenylalanine from glucose-xylose mixtures. Additionally, the versatility of aromatic amino acids such as phenylalanine to be enzymatically transformed into industrially relevant and value-added compounds makes the demonstration of glucose and xylose co-utilization of great applicability to potentially improve production metrics of many aromatic compounds. Ultimately, by implementing XylR* into NST74, a L-phenylalanine overproducing strain, along with other mutations known to affect sugar assimilation rates/mechanisms (i.e., *Δcrr*) and enhanced intracellular pools of a key precursor (i.e., *ΔpykAF*, which promotes phosphoenolpyruvate, PEP), 3509 ± 465 mg/L L-phenylalanine was produced from a 2% (w/v) sugar mixture containing 67% glucose and 33% xylose. Overall, the approach shows promise to improve the production of other aromatic chemicals from biomass-derived sugars mixtures.

3.1 Introduction

Lignocellulose derived from plant biomass represents a potentially vital renewable resource to serve as substrates for microbially-catalyzed conversion to valuable chemicals and fuels [144]. While the predominant sugar utilized for the demonstration of bioproduction in *E. coli* is glucose, there is a need and desire to consume other sugars as well. As many challenges remain in terms of breaking down and converting lignocelluose into usable substrates for *E. coli* [145], extensive effort has been put into engineering microbes to efficiently utilize these substrates for the production of value-added chemicals. Glucose (via cellulose) makes up the plurality of biomass in lignocellulose (30-40% by weight) but other sugars are present as well, including xylose (the predominant portion of hemicellulose) [146]. Therefore, upon improvement of lignocellulose-degrading technology one goal for improving bioproduction is the utilization of all basal components of plant biomass, most predominantly glucose and xylose.

However, in *E. coli*, a major impediment exists to the co-utilization of both glucose and xylose – namely, carbon catabolite repression (CCR). CCR is a phenomenon that exists in bacteria that causes cells to consume sugars in a sequential basis with the sugar that leads to the fastest growth rates usually being consumed first and the many regulatory mechanisms controlling CCR has been reviewed [147]. As *E. coli* growth on xylose is usually slow and inefficient relative to glucose [148], *E. coli* cultures fed with a feedstock containing both sugars will not consume xylose until all glucose is depleted [149]. Although CCR is important for evolutionary and survival purposes, it can often limit production metrics in bioproduction scenarios. Several strategies have been utilized to overcome this phenomenon. One early example demonstrates the utilization of microbial co-cultures to consume both glucose and xylose concurrently. Here, two *E. coli* strains were engineered – one with mutation of genes necessary to consume glucose (i.e., *glk*, *ptsG*, *manZ*) and one with a mutation in *xylA*, which is necessary to consume xylose [150]. When cultured together, one strain was able to consume glucose while the other simultaneously consumed xylose, leading to improved sugar consumption rates. Another example of overcoming CCR via co-cultures is in the production of *cis,cis*-muconic acid (MA). Here, one strain of *E. coli* was able to only consume xylose for the

purpose of producing the MA intermediate DHS, while a second strain utilized only glucose and could import and convert DHS into MA [151]. This allowed for elimination of CCR in MA production with improvements in titers up to 4.7 g/L with yields as high as 0.35 g/g-total sugar.

While the utilization of co-cultures is useful to overcome CCR, it necessitates the need to multiple strains and careful balancing of the two in culture. Therefore, effort has been put into genetic engineering methods to overcome CCR between xylose and glucose. Previously, the production of the shikimic acid pathway-derived compound 4-hydroxymandelic acid (via 4-hydroxyphenylpyruvic acid and the expression of *shmaS* from *Amycolatopsis orientalis*) utilizing a co-sugar mixture of glucose and xylose has been demonstrated in *E. coli* [152]. The deletion of *ptsG* led to a reduction of CCR between the two sugars and further mutations in *pykAF*, *pheA, aspC, tyrB* and *tyrR* allowed for titers reaching 15.8 g/L of 4-hydroxymandelic acid in a fed-batch setting. The deletion of *ptsG* also allows for improvements in PEP availability and ultimately flux through the aromatic amino acid synthesis pathway via inactivation of the PTS system (converts PEP to pyruvate for the import and phosphorylation of glucose) [153]. Ultimately, after examining various ratios of glucose-xylose mixtures, researchers determined that the maximum titers were achieved at a 50-50% (by mass) ratio of glucose and xylose.

One such mutation to reduce the effects of CCR is in the gene *xylR* in *E. coli*, which was identified by Sievert et al. via adaptive laboratory evolution [154]. XylR (the production of *xylR*) is a xylose-specific activator which induces expression of xylose-utilizing genes in *E. coli* upon the presence of xylose [155]. Sievert et al. found that introducing mutations into native *xylR* (R121C and P363S) (henceforth referred to as *xylR**) led to activation of xylose-utilizing genes (i.e., *xylA* and *xylB*, which encode for a xylose isomerase and xylose dehydrogenase, respectively, and *xylFGH* which encode for a xylose ABC transporter) even in the presence of glucose and allowed for improvements in xylose consumption rates. When implemented in a D-lactate producer, 94% of sugars in a 50-50% (by mass) mixture of glucose and xylose mixture were utilized when cultured anaerobically and D-lactate titers increased by 50% [154]. While *xylR** implementation in *E. coli* allowing for improved rates of utilization of xylose has previously been demonstrated in anaerobic

fermentations for lactate and ethanol production [154,156], to the best of my knowledge, this mutation has not been utilized for aerobic culturing purposes.

3.2 Materials and Methods

3.2.1 Microorganisms

E. coli NST74 (ATCC 31884), a feedback resistant mutant of *E. coli* which overproduces Phe [120] was purchased from the American Type Culture Collection (ATCC; Manassas, VA). *E. coli* strains JW2410-1, JW1843-2, and JW1666-3 were obtained from the Coli Genetic Stock Center (CGSC; New Haven, CT) and served as the genetic source for the *crr::FRT-kan^R-FRT, pykA::FRT-kan^R-FRT* and *pykF::FRT-kan^R-FRT* deletion cassettes. *E coli* W-variant LN6 [154], which served as the template for the cloning of mutations (R121C, P363S) into wild-type *xylR,* was a generous gift from the Xuan Wang lab. Chromosomal in-frame gene deletions in *E. coli* and subsequent *kan^R* marker removal were accomplished utilizing the plasmid pSIJ8 via a method adapted from Jensen et al. [157] with 5% (w/v) L-arabinose for induction of λ red recombinase and 50 mM rhamnose for induction of the FLP recombinase. *E. coli* W3110 variant T-SACK [158], which served as a template for *tetA-sacB*, was a generous gift from the Donald Court lab.

3.2.2 DNA Cassette Construction

Custom DNA oligonucleotides were synthesized by Integrated DNA Technologies (Coralville, IA). Genomic DNA (gDNA) was prepared from cell cultures using the ZR Fungal/Bacterial DNA MiniPrep (Zymo Research, Irvine, CA) according to vendor protocols. All genes were PCR amplified with Q5 High-Fidelity DNA Polymerase (NEB) using standard protocols. Amplified linear DNA fragments were purified using the Zymo Research DNA Clean & Concentrator Kit (Zymo Research) according to manufacturer protocols.

Table 3.1 shows the primers utilized for incorporation of mutations into *xylR*. Utilizing methods adapted from Datsenko and Wanner [121], as previously described [32], *tetA-sacB* was integrated into the *xylR* locus. Colonies were selected from on LB-agar plates containing 10 ng/uL tetracycline. Positive clones were checked for insertion of *tetA-sacB* into the *xylR* locus via colony PCR.

Subsequently, correct clones were then subjected to a secondary integration of *xylR* (R121C, P363S) from LN6 and screened for insensitivity to 10% (w/v) sucrose in liquid LB media followed by plating on LB-agar plates containing 6% (w/v) sucrose [158,159]. Colonies were subsequently verified via colony PCR.

Table 3.1 Primers for the Insertion of *xylR* (R121C, P363S) into Production Strains.

Primer Name	Sequence (5' -> 3')	Purpose
F - *xylR* (R121C, P363S) from LN6	gtgggaagcgttgccgg	Cloning of *xylR* (R121C, P363S) from LN6
R - *xylR* (R121C, P363S) from LN6	cctgatgtgacgccgacaattctc	
F - *tetA-sacB* into *xylR*	tttgagtttttgcatgattcagcaggaaaagaacctcctaatttttgttg acactctatc	Cloning of *tetA-sacB* from T-SACK
R - *tetA-sacB* into *xylR*	gttacctgatgtgacgccgacaattctcatcatcgatcaaaggga aaactgtccatatgc	
F - *xylR* (780 bp homology)	ctgtatcccccaccagcgcc	Cloning of homology arms for *tetA-sacB* from T-SACK and *xylR* (R121C, P363S) from LN6 and colony PCR
R - *xylR* (790 bp homology)	ggaaaaaggcgtttctccggaccg	
F - *xylR* helper	cgatgatgagaattgtcggcg	Helper primers for cloning of homology arms for *tetA-sacB* from T-SACK and *xylR* (R121C, P363S) from LN6
R - *xylR* helper	ggttcttttcctgctgaatcatgc	

3.2.3 Production of Phe by Engineered E. coli

Seed cultures were grown in 3 mL LB broth at 32°C for 12 – 16 h. Next, 0.25 mL of seed culture was used to inoculate 25 mL (in 125 mL shake flasks) of pH 6.8 MM1 – a phosphate-limited minimal media adapted from McKenna and Nielsen [117], with the following recipe (in g/L): $MgSO_4 \cdot 7H_2O$ (0.5),

$(NH_4)_2SO_4$ (4.0), MOPS (24.7), KH_2PO_4 (0.3), and K_2HPO_4 (1.0), as well as 1 mL/L of a trace mineral solution containing (in g/L): $MnCl_2 \cdot 4H_2O$ (1.584), $ZnSO_4 \cdot 7H_2O$ (0.288), $CoCl_2 \cdot 6H_2O$ (0.714), $CuSO_4$ (0.1596), H_3BO_3 (2.48), $(NH_4)_6Mo_7O_{24} \cdot 4H_2O$ (0.370), and $FeCl_3$ (0.050). The type of carbon source (i.e., glucose or xylose) and concentration used for each experiment is noted in the text.

Once inoculated, cultures were grown at 32°C while shaking at 200 RPM. Following inoculation, strains were cultured until the time stated in the text, during which time, samples were periodically withdrawn for cell growth and metabolite analysis. Meanwhile, intermittently throughout each culture, pH was increased back to its initial value by adding a minimal volume (typically ~0.1-0.3 mL) of 0.4 g/L K_2HPO_4 solution.

3.2.4 Analytical Methods

Cell growth was measured as OD_{600} using a UV/Vis spectrophotometer (Beckman Coulter DU800, Brea, CA). Culture samples were centrifuged at 11,000 x *g* for 4 min to pellet cells, after which 0.25 mL of the resulting supernatant was then transferred to a glass HPLC vial containing an equal volume of 1 N HCl before being sealed with a Teflon-lined cap. Analysis of Phe was performed via high performance liquid chromatography (HPLC; Agilent 1100 series HPLC, Santa Clara, CA) using a diode array (UV/Vis) detector. Separation and analysis of phenylalanine was achieved on a reverse-phase 5µm BDS Hypersil C18 column (3 mm x 250 mm; Thermo Electron, USA) operated at 45°C using a mobile phase consisting of 85% 5 mM H_2SO_4 and 15% acetonitrile, flowing at a constant rate of 0.5 mL/min for 6.5 min. The eluent was monitored using a diode array detector (DAD) set at 215 nm for detection of phenylalanine. Glucose, xylose and acetate analysis, meanwhile, was performed using the same HPLC system equipped with a refractive index detector (RID) and an Aminex HPX-87H column (BioRad, Hercules, CA) operated at 35ºC. The column was eluted using 5 mM H_2SO_4 as the mobile phase at a constant flow rate of 0.55 mL/min for 20 min. External calibrations were prepared and used to quantify each species of interest. Data reported here is a result of triplicate experiments, unless otherwise noted, along with one standard deviation.

3.3 Results and Discussion

3.3.1 Comparison Between Utilization of Glucose and Xylose for Production of L-Phenylalanine

The production of L-phenylalanine (Phe) in *E. coli* necessitates the production of two intracellular metabolites that funnel into the shikimic acid pathway – erythrose-4-phosphate (E4P) and phosphoenolpyruvate (PEP) – which are converted to 3-deoxy-D-arabino-heptulosonate-7-phosphate (DAHP), the precursor to all three aromatic amino acids (AAAs), via three enzymes in *E. coli* – AroG, AroF and AroH. **Figure 3.1** shows pertinent reactions, substrates, co-factors and products in *E. coli* to convert glucose and/or xylose to Phe (one of the AAAs). Therefore, to maximize production of aromatic amino acids – and the production of their derivatives – a careful balance between the pools of PEP and E4P must be maintained. While ideally, the production rates of both metabolites will be maximized, without a consistent, simultaneous supply of both PEP and E4P, final production of aromatic amino acids will suffer. Additionally, as a second PEP molecule is consumed during the production of the aromatic amino acids (i.e., shikimate-3-phosphate + PEP → 5-enolpyruvoyl-shikimate 3-phosphate + phosphate via AroA), the flux towards PEP and the buildup of a pool of this molecule is critical to enchancing production of AAAs.

While E4P is predominately utilized for production of aromatic amino acids and as a part of the pentose phosphate pathway, PEP plays a significant role in both glycolysis and glucose transport into the cell. While a large portion of PEP pools are predominantly produced during glycolysis, PEP also serves as the direct precursor to pyruvate (reaction catalyzed by pyruvate kinase – PykA and PykF in *E. coli*) where pyruvate is subsequently converted into acetyl-CoA and funneled into the TCA cycle. Additionally, PEP is converted to pyruvate via a different enzyme to facilitate glucose uptake in the phosphotransferase system (PTS) of *E. coli* which serves as another sink for PEP pools. Conversely, E4P is mainly produced in the pentose phosphate pathway. Additionally, E4P can serve as a substrate in the reversible transketolase reaction (encoded by *tktAB* in *E. coli*) which converts E4P and xylulose-5-phosphate (X5P) into fructose-6-phosphate (F6P) and glyceraldehyde-3-phosphate (G3P). In ^{13}C-flux analysis studies of wild-type cells, when grown on glucose, the flux through the pentose phosphate pathway, and ultimately, E4P, was quite low [160].

For glucose, the ratio of flux from S7P to E4P compared to the flux from 3-phosphoglycerate to PEP was ~1:23.7 while this ratio when grown on xylose was ~1:3.5 [160]. Therefore, even though the number of PEP molecules to produce one Phe is twice the number of E4P needed, the severe difference in flux towards PEP when grown on glucose may ultimately limit Phe production. The production of aromatic amino acids (such as Phe) representatives a potentially useful application and test case due to the need for two intracellular precursors (one E4P and two PEP molecules) to produce one molecule of the aromatic amino acid.

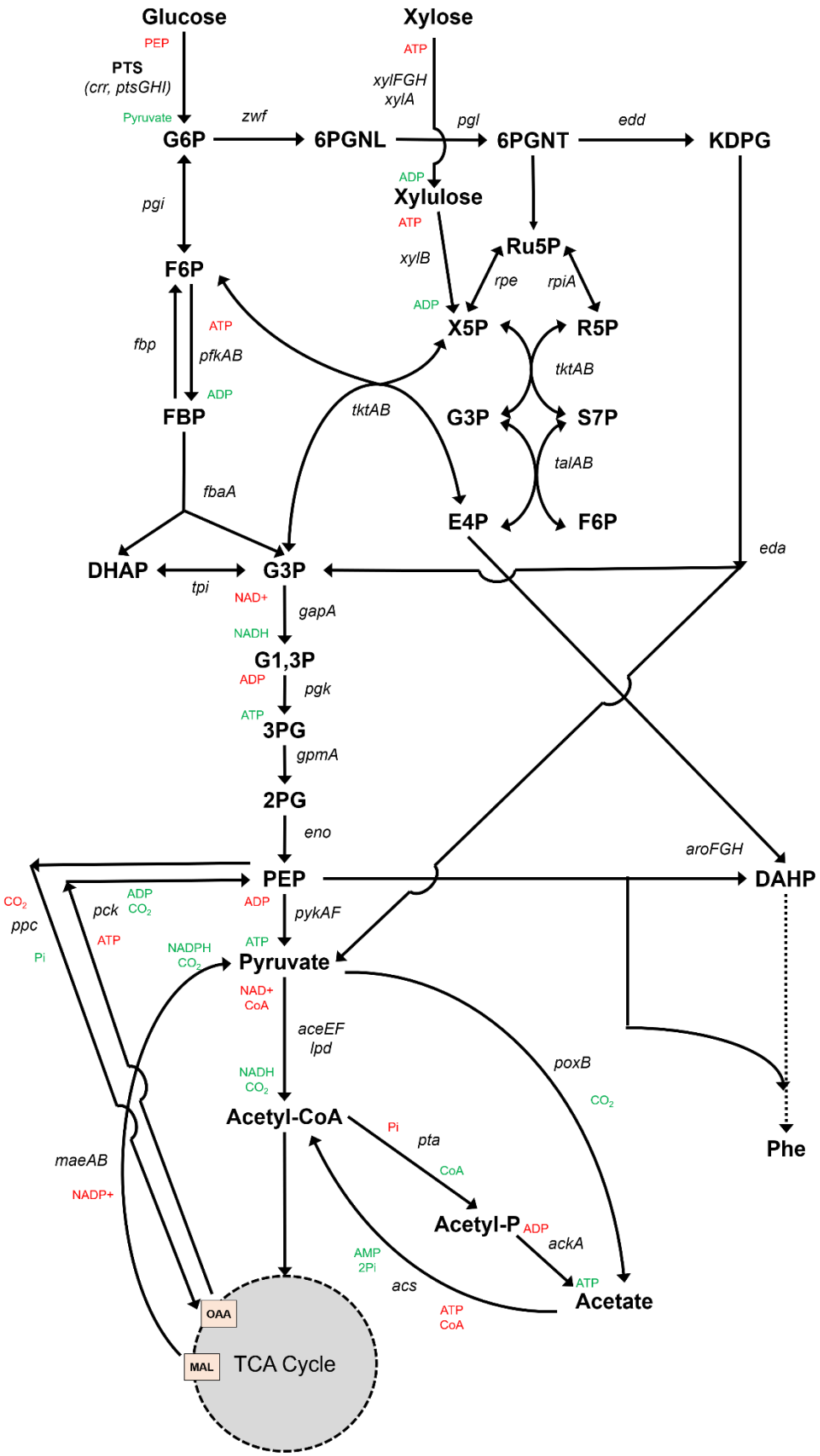
Glucose
PEP
PTS
(crr, ptsGHI)
Pyruvate
zwf
G6P
6PGNL
Xylose
ATP
xylFGH
xylA
pgl
6PGNT
edd
KDPG
ADP
Xylulose
ATP
xylB
pgi
F6P
Ru5P
rpe
rpiA
ADP
X5P
R5P
fbp
ATP
pfkAB
ADP
tktAB
FBP
tktAB
G3P
S7P
talAB
fbaA
E4P
F6P
eda
DHAP
tpi
G3P
NAD+
gapA
NADH
G1,3P
ADP
pgk
ATP
3PG
gpmA
2PG
eno
aroFGH
PEP
DAHP
CO2
ppc
ADP
CO2
pck
ADP
pykAF
Pi
ATP
NADPH
CO2
ATP
Pyruvate
NAD+
CoA
aceEF
lpd
poxB
NADH
CO2
CO2
Acetyl-CoA
Pi
pta
Phe
maeAB
NADP+
CoA
Acetyl-P
ADP
ackA
AMP
2Pi
acs
ATP
Acetate
ATP
CoA
OAA
MAL
TCA Cycle

Figure 3.1 Metabolic Pathway of *E. coli* from Glucose and Xylose to Phenylalanine.

Metabolic pathway of glucose and xylose metabolism to phenylalanine (Phe). Single enzymatic steps are shown as solid lines, pathways with multiple steps are shown as dashed lines. Lines which have arrows are either end illustrate reversible reactions. The genes which encode each step are shown next to the enzymatic line in italics. Co-factors for each reaction are shown in green (if produced) and red (if consumed). G6P = glucose-6-phosphate, F6P = fructose-6-phospate, FBP = fructose-1,6-biphosphate, DHAP = dihydroxy-acetone-phosphate, G3P = glyceraldehyde-3-phosphate, 6PGNL = 6-phosphogluconolactone, 6PGNT = 6-phosphogluconate, KDPG = 2-keto-3-deoxy-6-phosphogluconate, Ru5P = ribulose-5-phosphate, X5P = xylulose-5-phosphate, R5P = ribose-5-phosphate, S7P = seudoheptulose-7-phosphate, E4P = erythrose-4-phosphate, G1,3P = glyceraldehyde-1,3-phosphate, 3PG = 3-phosphoglycerate, 2PG = 2-phosphoglycerate, PEP = phosphoenolpyruvate, DAHP = 3-deoxy-D-arabino-heptulosonate-7-phosphate, Acetyl-P = acetyl-phosphate, OAA = oxaloacetate, MAL = malate. Note: G3P and F6P appear twice on this pathway map for clarity purposes.

3.3.2 Utilization of Xylose and Glucose for Production of Phenylalanine in E. coli

To analyze the production capacity of either xylose or glucose for the bioconversion to phenylalanine, NST74, a Phe overproducing strain, was utilized and the time course of pertinent performance metrics are shown in **Figure 3.2**. Either 2% (w/v) of glucose or xylose was fed to cells and with glucose as the sole substrate, NST74 produced 567 ± 25 mg/L Phe at a mass yield of 28.4 ± 2.8 mg-Phe/g-glucose after 96 h of culturing (cells were grown to 120 h but Phe titers were maximized after 96 h). Utilizing xylose as the sole substrate, NST74 produced 1315 ± 65 mg/L Phe at a mass yield of 63.1 ± 3.1 mg-Phe/g-xylose after 138.5 h of culturing. Other than the large differences in titer and yield, there were other variations observed when NST74 was grown on the two substrates such as those observed in terms of sugar consumption and Phe production rates. Overall, NST74 consumed 100% of the original glucose at an overall rate of 0.181 g glucose/L-h (after 120 h). When only xylose was fed, 100% of the original xylose was also consumed at a surprisingly quicker rate of 0.217 g xylose/L-h (after 95 h). In terms of overall rates, the production of Phe ran concurrently to the rate of sugar consumption. Cells produced Phe at a much slower degree as production from glucose occurred at an overall rate of 5.9 ± 0.3 mg Phe/L-h (after 96 h) while overall Phe production rates from xylose were 9.5 ± 0.5 mg Phe/L-h (over 138.5 h). While strains utilizing only glucose reached near maximum production levels at around 50 h after inoculation (i.e., ~92% of final titers of Phe was produced in the first 50 h of culturing), cells growing only on xylose took much longer to reach final production concentrations as only ~77% of total Phe production was accomplished in the first 50 h of culturing. Even so, the concentrations of Phe at

this time point (50 h) were 523 ± 27 and 1010 ± 45 mg/L Phe from glucose and xylose, respectively, indicating the high production capabilities of Phe overproducing strains from xylose. It is likely that the abundance of E4P plays a key role in the high production on xylose, as the availability of E4P is much higher on this substrate.

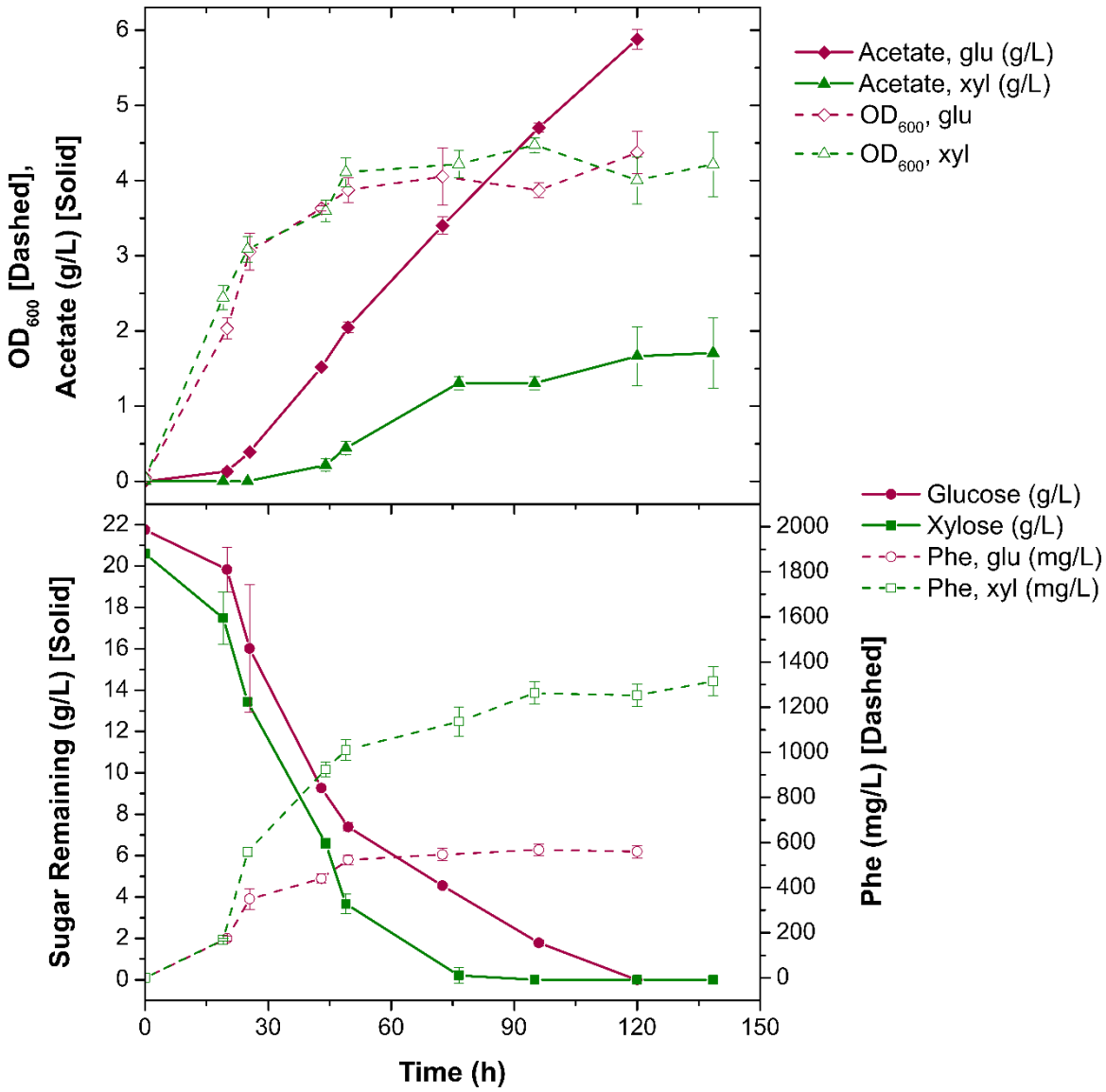

Figure 3.2 Time Course of NST74 Phe Production on 2% (w/v) Xylose or Glucose.

Time course of NST74 production of Phe on xylose or glucose as measured by (Top) OD_{600} (dashed line) and acetate (g/L; solid line) and (Bottom) sugar consumption (g/L; solid line) and Phe production (mg/L; dashed line). Data of strains grown on xylose are shown in green while data from glucose is shown in maroon. Error bars reported as one standard deviation from triplicate experiments.

While growth on 100% glucose or xylose is possible at the lab scale, as biomass sugars typically consist of sugar mixtures, this approach is likely less viable at the large scale. For typical sources of lignocellulosic biomass, the ratio between glucose and xylose is approximately 2:1 (glucose:xylose). Accordingly, this same ratio was next employed in model glucose-xylose mixtures and evaluated with respect to Phe production by NST74 (**Figure 3.3**). Here, 13.4 and 6.6 g/L of glucose and xylose, respectively, were initially fed to NST74 for an overall sugar concentration of 2% (w/v). After 141.5 h of culturing, 559 ± 105 mg/L Phe was produced at a mass yield of 37.8 ± 7.1 mg-Phe/g-total sugar. In this case, no xylose was consumed during the culture, even after 100% of glucose was utilized indicating the significant impact of CCR on cell growth. This ultimately limited Phe production, as the strain was unable to take advantage of the benefits of xylose for aromatic amino acid production.

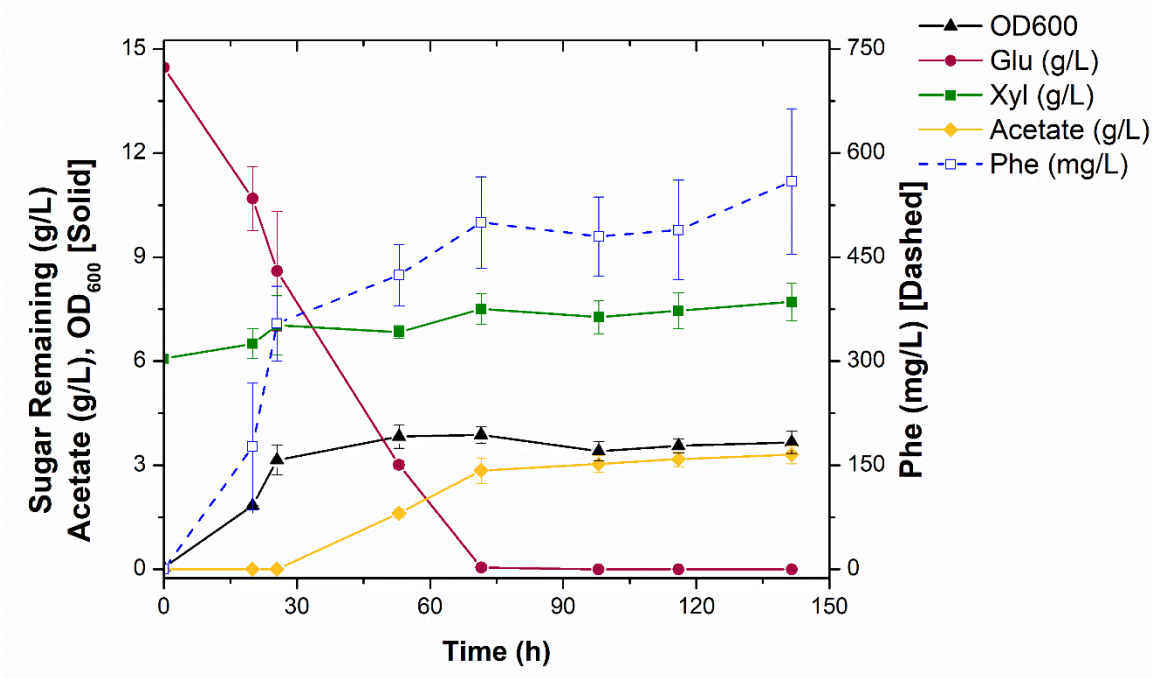

Figure 3.3 Time Course of NST74 Phe Production on Glucose-Xylose (67%-33%) Feed.

Time course of NST74 production of Phe on mixed sugar feed (67% glucose, 33% xylose; total sugar concentration = 20 g/L) as measured by OD_{600} (solid black line, triangle), acetate (g/L; solid gold line, diamond), glucose remaining (g/L; solid maroon line, circle), xylose remaining (g/L; solid green line, square) and Phe production (mg/L; dashed blue line, square). Error bars reported as one standard deviation from triplicate experiments.

3.3.3 Effect of xylR Mutation on Aerobic Xylose Consumption Rates and Phenylalanine Production

It was previously demonstrated under anaerobic conditions that the introduction of XylR* effectively eliminated glucose CCR, allowing for efficient and simultaneous consumption of both glucose and xylose [154,156]. To examine the effects of XylR* on aerobic growth and production of Phe, *xylR* (R121C, P363S) was integrated into NST74 at its native locus, resulting in NST74xylR*. When a sugar mixture of glucose (67%) and xylose (33%) was fed to these cells, xylose utilization was improved upon and Phe production increased as seen in **Figure 3.4**. When compared to NST74 (**Figure 3.3**), both strains consumed 100% of the supplied glucose fed, no xylose was consumed by NST74 whereas NST74xylR* utilized 100% of supplied xylose, occurring in parallel with glucose consumption. Consequently, it is clear that introduction of XylR* not only alleviates glucose CCR during anaerobic fermentations, but under aerobic conditions as well. Ultimately, the co-utilization of both sugars led to improved titers and yields for NST74xylR* when compared to NST74, as NST74xylR* produced over 3-fold more Phe (1755 ± 91 versus 559 ± 105 mg/L) at a significantly higher yield (83.1 ± 4.3 versus 37.8 ± 7.1 mg Phe/g sugar). This is due to the efficient co-utilization of xylose in NST74xylR* (100% xylose utilized by 71.5 h) compared to NST74 which consumed no xylose even after 141.5 h of culturing.

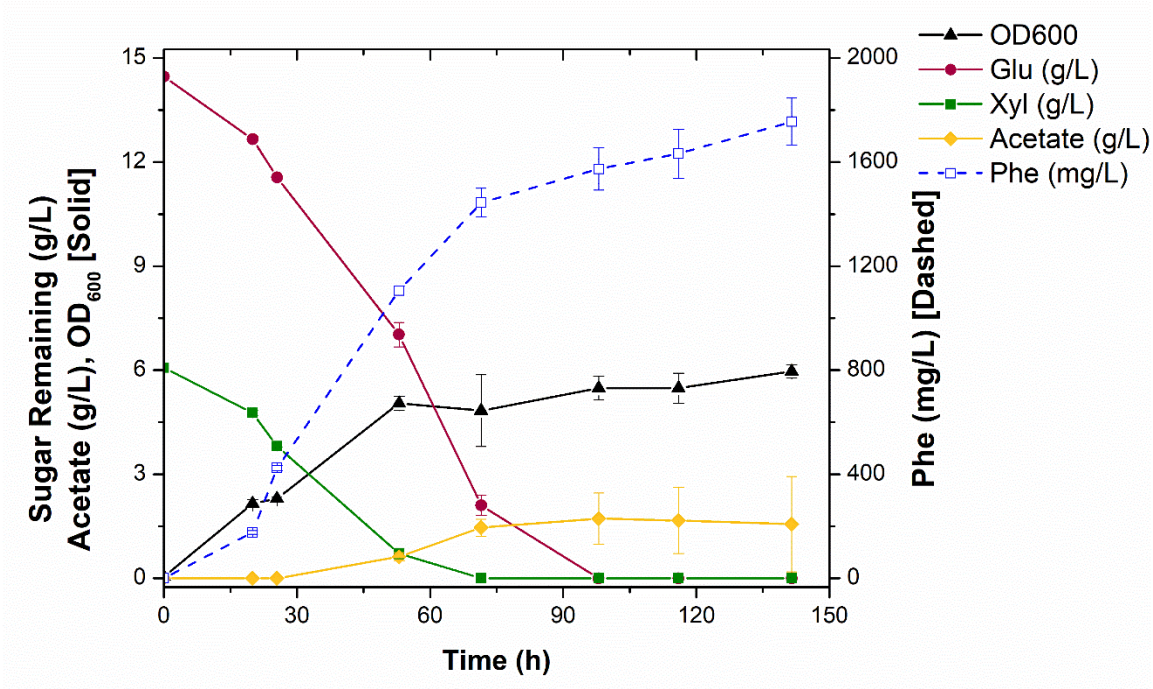

Figure 3.4 Time Course of NST74xylR* Phe Production on Glucose-Xylose (67%-33%) Feed.

Time course of NST74xylR production of Phe on mixed sugar feed (67% glucose, 33% xylose; total sugar concentration = 20 g/L) as measured by OD_{600} (solid black line, triangle), acetate (g/L; solid gold line, diamond), glucose remaining (g/L; solid maroon line, circle), xylose remaining (g/L; solid green line, square) and Phe production (mg/L; dashed blue line, square). Error bars reported as one standard deviation from triplicate experiments.*

3.3.4 Genetic Modifications to Improve Phe Production in Xylose-Utilizing Cells

Although NST74xylR* consumed more sugar by mass than NST74, it produced 53% less acetate even after 141.5 h. Along with differences in the metabolic pathways for conversion of glucose and xylose into central metabolism, the increased rate of glucose consumption compared to xylose may play a role in increased acetate accumulation [134]. Therefore, one reason that NST74xylR* may display reduced production of acetate compared to NST74, is a decrease in glucose assimilation rates. When compared **Figure 3.3** and **Figure 3.4**, it can be seen that the rate at which glucose is consumed from the culture media is slower in NST74xylR* compared to NST74. In fact, over the first 53 h of culturing, when xylose is still present, glucose is consumed at a rate of 0.140 ± 0.007 g glucose/L-h in NST74xylR* compared to 0.216 ± 0.002 g glucose/L-h for NST74. This difference in glucose consumption rates is only observed in the presence of xylose as NST74 and NST74xylR* grown in media containing only 2% (w/v) glucose showed similar consumption rates (data not

shown). In contrast, however, NST74xylR* accumulated ~61.4% more biomass when compared to NST74, an interesting phenomenon that may simply be due to an increase in total sugar consumed.

As the increased production of Phe depends on improving the availability of intracellular metabolites PEP and E4P, further genetic mutations were investigated for their effect on NST74 and NST74xylR* and the abilities of these strains to consume pure xylose and glucose-xylose feedstocks. Previously, *pykF* and *pykA*, which encode for pyruvate kinase enzymes, have been utilized to improve the production of a variety of compounds derived from the shikimic acid pathway and its derivatives as well as reduce acetate accumulation via reduced pyruvate production [18,129,152]. As two PEP molecules are needed to produce one Phe molecule (compared to only one E4P molecule), it is thought that improvements in PEP pools, rather than E4P, may be more effective at boosting titers of Phe, especially in feedstocks containing xylose due to its more significant flux through E4P [161].

Additionally, as the observed acetate accumulation arises as glucose is introduced into the feed, a genetic modification to reduce overflow metabolism from glucose catabolism was implemented. The *crr* gene encodes for IIA^{Glc}, an important member of the glucose:PTS [130], and can work to reduce acetate accumulation rates as discussed in Chapter 2 [130,131]. Previously, in a glucose-only feed, the introduction of this mutation reduced glucose uptake rates and acetate production in the media significantly decreased. This deletion may also have the effect of improving PEP availability with feedstocks containing glucose as the removal of *crr* seems to "slow down" glucose assimilation into the cell, allowing PEP pools to build up for further enzymatic conversion to the SA pathway. In an effort to investigate the effects of minimizing acetate production via upstream modifications and improve the availability of PEP, *crr, pykA* and *pykF* were deleted from NST74xylR* Δ*pykAF* to produce NST74xylR* Δ*crr* Δ*pykAF*. When comparing NST74xylR* to NST74xylR* Δ*crr* Δ*pykAF*, as seen in **Table 3.2**, it can be observed that 100% of sugar fed is consumed in both strains, however, NST74xylR* Δ*crr* Δ*pykAF* produceds almost 2 times the amount of Phe as NST74xylR*, indicating that these mutations are helpful in a mixed sugar feed scenario, not only with a pure

glucose feed. Additionally, a comparison between NST74 Δ*crr* Δ*pykAF* and NST74xylR* Δ*crr* Δ*pykAF* in terms of sugar consumption, acetate and biomass accumulation, and Phe production was investigating as shown in **Figure 3.5**.

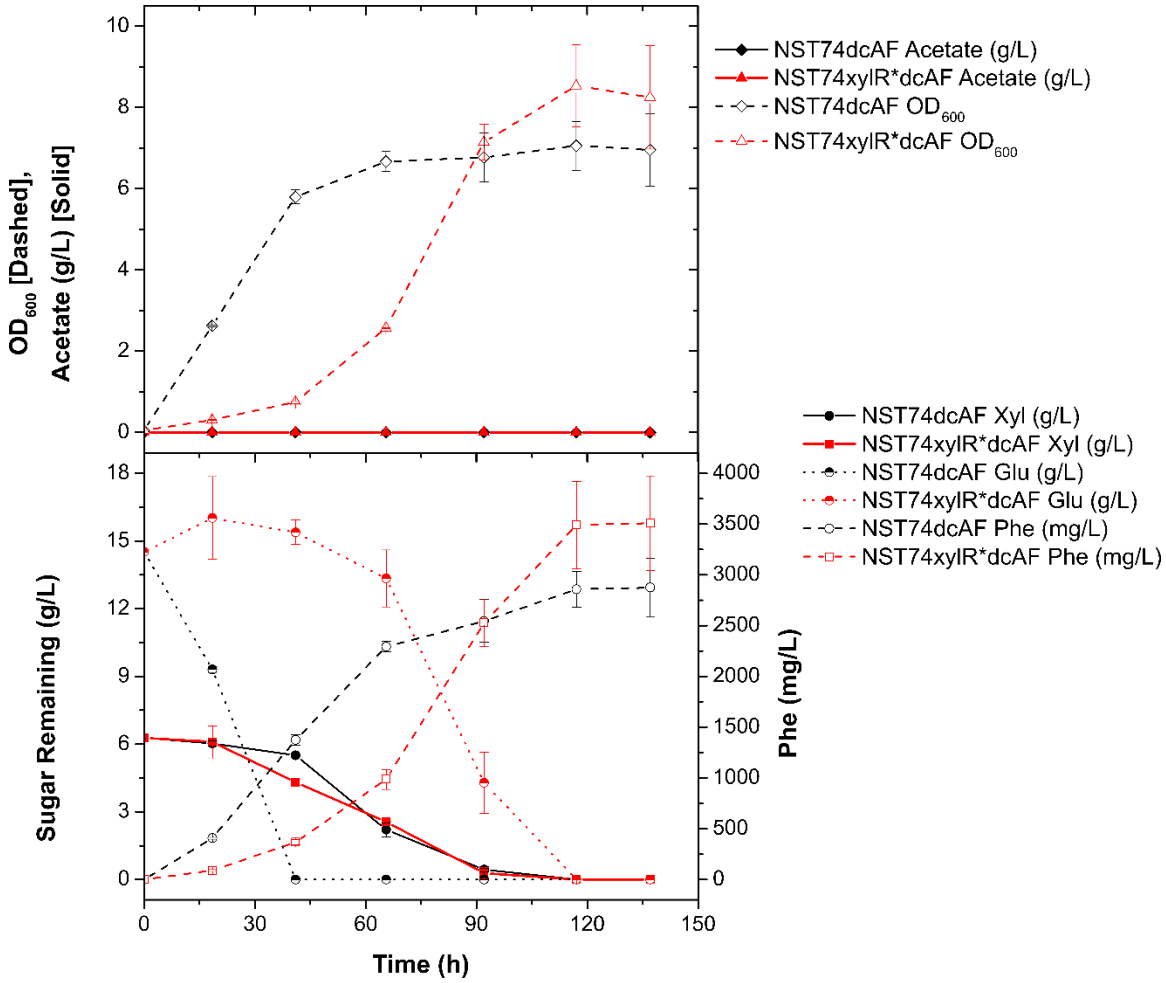

Figure 3.5 Time Course of NST74 Δcrr ΔpykAF and NST74xylR* Δcrr ΔpykAF Phe Production on Glucose-Xylose (67%-33%) Feed.

Time course of NST74 Δcrr ΔpykAF and NST74xylR Δcrr ΔpykAF production of Phe on mixed sugar feed (67% glucose, 33% xylose; total sugar concentration = 20 g/L) as measured by (Top) OD_{600} (dashed line) and acetate (g/L; solid line) and (Bottom) glucose consumption (g/L; double dashed line, half-moon), xylose consumption (g/L, solid line, square) and Phe production (mg/L; dashed line). Data of from NST74 Δcrr ΔpykAF is shown in black, data from NST74xylR* Δcrr ΔpykAF is shown in red. Error bars reported as one standard deviation from triplicate experiments.*

Here, the most obvious differences are observed in terms of glucose consumption and initial growth rate. For NST74 Δ*crr* Δ*pykAF*, 100% of glucose fed is consumed by 41 h into culturing while NST74xylR* Δ*crr* Δ*pykAF* has only consumed ~2 g/L glucose after 65.5 h of culturing.

Correspondingly, the growth rates show similar differences as NST74 Δ*crr* Δ*pykAF* and NST74xylR* Δ*crr* Δ*pykAF* have reached OD_{600} values of 5.80 ± 0.17 and 0.75 ± 0.03, respectively after 41 h. However, overall, 100% glucose is consumed by both strains after 137 h and the final OD_{600} values are relatively similar. For both strains, xylose consumption rates are nearly identical throughout culturing and interestingly, the changes in Phe production rates seem to be similar to the differences in growth rates throughout culturing. This may indicate that production of intermediates of interest (i.e., PEP and/or E4P) is somewhat tied to growth in these strains and conditions. Surprisingly, in contrast to previous results, the strain with the wild-type *xylR* gene was able to consume 100% of xylose, although seemingly only after glucose was fully utilized.

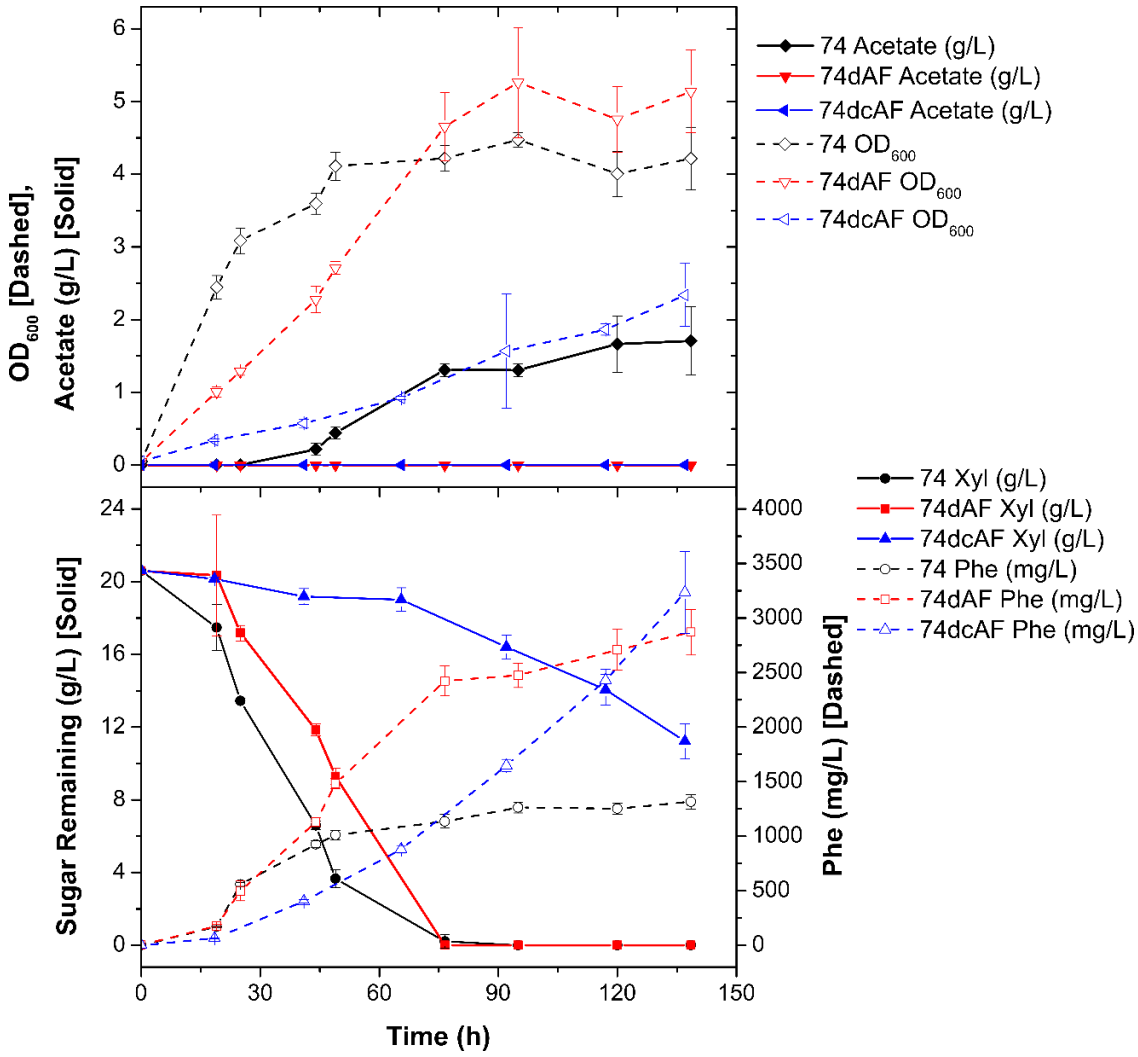

Figure 3.6 Time Course of NST74, NST74 ΔpykAF and NST74Δcrr ΔpykAF Phe Production on Xylose Feed.

Time course of NST74, NST74 ΔpykAF and NST74x Δcrr ΔpykAF production of Phe on 2% (w/v) xylose feed as measured by (Top) OD_{600} (dashed line) and acetate (g/L; solid line) and (Bottom) xylose consumption (g/L, solid line) and Phe production (mg/L; dashed line). Data of from NST74 is shown in black, data from NST74 ΔpykAF is shown in red and data from NST74 Δcrr ΔpykAF is shown in blue. Error bars reported as one standard deviation from triplicate experiments.

To further investigate the interesting effects of these genetic mutations on Phe titers and yields, the mutations (e.g., Δ*pykAF* and Δ*crr*) were placed into NST74 and grown on 2% (w/v) xylose. The performance metrics are shown in **Figure 3.6**. Here, it can be seen that upon introduction of each subsequent mutation xylose assimilation rates are reduced. For NST74, NST74 NST74 *ΔpykAF*, and NST74 *Δcrr ΔpykAF*, the xylose consumption rates over the first ~43 h were 0.318 ± 0.006,

0.199 ± 0.008, 0.035 ± 0.011 g xylose/L-h, respectively. However, the overall Phe production (in terms of titers and yields) showed corresponding increases upon addition of these mutations. Clearly a key aspect to enhance Phe production (i.e., yield) from xylose (and glucose), may be the ability to slow down sugar utilization rates and cell growth. A summary of all experiments and relevant production metrics is shown in **Table 3.2**.

Table 3.2 Summary of Phe Production Metrics for NST74 and Various Genetic Variations.

Summary of data showing the strain, percentage of sugar used, Phe titers, culture time, Mass yield, growth as measured by OD_{600} and acetate accumulation at the end of culturing. All data is with 2% (w/v) total sugar and error bars represent one standard deviation from triplicate experiments. "n.d." = "not detected".

Strain	*Time (h)*	*Phe Titer (mg/L)*	*Phe Mass Yield (mg-Phe/g-total sugar)*	*% Total Glucose Used*	*% Total Xylose Used*	*Final OD_{600}*	*Final Acetate (g/L)*
100% Glucose							
NST74	120	567 ± 29 (at 96 h)	28.4 ± 2.8 (at 96 h)	100%	N/A	4.37 ± 0.28	5.88 ± 0.13
100% Xylose							
NST74	138.5	1315 ± 65	63.1 ± 3.1	N/A	100%	4.22 ± 0.43	1.71 ± 0.47
NST74 ΔpykAF	138.5	2870 ± 209	137.7 ± 10.0	N/A	100%	5.14 ± 0.57	n.d.
NST74 Δcrr ΔpykAF	137	3234 ± 377	348.4 ± 70.7	N/A	45.6 ± 4.6%	2.34 ± 0.43	n.d.
67% Glucose/33% Xylose							
NST74	141.5	559 ± 105	37.8 ± 7.1	100%	0%	3.66 ± 0.32	3.30 ± 0.26
*NST74xylR**	141.5	1755 ± 91	83.1 ± 4.3	100%	100%	5.96 ± 0.19	1.56 ± 1.37
NST74 Δcrr ΔpykAF	137	2875 ± 286	127.8 ± 12.7	100%	100%	6.95 ± 0.88	n.d.
NST74xylR Δcrr ΔpykAF*	137	3509 ± 465	156.0 ± 20.7	100%	100%	8.25 ± 1.27	n.d.
Strain	*Time (h)*	*Phe Titer (mg/L)*	*Phe Mass Yield (mg-Phe/g-total sugar)*	*% Total Glucose Used*	*% Total Xylose Used*	*Final OD_{600}*	*Final Acetate (g/L)*

3.4 Discussion

One factor that may be severely limiting overall Phe production is the co-accumulation of byproduct acetate; a problem often exacerbated by higher rates of and overall consumption of sugars (especially glucose). For instance, NST74 grown on glucose produced 5.88 ± 0.13 g/L acetate after 120 h with levels reaching over 1 g/L (the level where reduction in cell growth and protein stability commonly occurs [137]) within 25 h of culturing (as seen in **Figure 3.2**). In contrast, for cells grown on xylose, overall accumulation of acetate only reached a maximum of 1.71 ± 0.47 g/L (occurring at the end of culturing). This may help play a role in the fact that NST74 continues to produce Phe into stationary phase when grown on xylose while cells grown on glucose stop producing significant levels of Phe at an earlier time point. As acetate accumulation is known to inhibit *E. coli* growth [137], additional strain engineering to reduce acetate production was expected to improve Phe production. Acetate production at levels of 0.5 g/L have been shown to reduce *E. coli* growth rates while concentrations above 2 g/L are severely inhibitory [162,163]. High levels of acetate production in these scenarios here may play an even more significant role here compared to glucose-based production as it has previously been observed that inhibition caused by acetic acid in *E. coli* production runs has a more pronounced effect on hindering xylose utilization than with glucose [164].

Additionally, one important by-product of the pyruvate kinase reaction is ATP. In wild-type, signficant carbon flux flows through this reaction [161] as it is one of the main pathways by which cells funnel carbon into the TCA cycle. While, in wild-type, significant levels of ATP is generated in this reaction, the removal of these enzymes may reduce intracellular ATP levels. As ATP is needed to import xylose into *E. coli* through XylFGH [155] (although, alternatively, XylE, a xylose:H^+ symporter, can also uptake xylose into the cell), the decrease in available intracellular pools of ATP may potentially limit the rate of xylose uptake and utilization and flux through the pentose phosphate pathway. In fact, through *in silico* models of shikimic acid (SA) production in *E. coli* from various carbon sources, researchers estimated that the the ATP demand for SA from xylose when utilizing XylFGH for import was 2.27 mol ATP/mol SA compared to that from glucose (utilzing the native

PTS system) which was 1.97 mol ATP/mol SA [165]. To further test this theory, the Δ*pykAF* mutation was placed in NST74 and grown on 100% xylose. Here, over the first 49 h, NST74 consumed xylose at a rate of 0.346 ± 0.010 g xylose/L-h. Comparatively, NST74 Δ*pykAF* only utilized xylose at a rate of 0.231 ± 0.009 g xylose/L-h (**Figure 3.6**).

In addition to the possible explanation of limited ATP availability to explain reduced titers, the production of pyruvate may also play a role. Pyruvate kinase is the main mechanism by which pyruvate is produced in growing, wild-type *E. coli* cells. Upon removal of this enzymatic reaction, other avenues through which pyruvate (and subsequently acetyl-CoA) can be be produced become vital. When cells are grown on glucose, pyruvate can be generated via the glucose:phosphotransferase system (PTS) which simultaneously phosphorylates and imports glucose by converting PEP into pyruvate. However, when grown on xylose, this reaction does not occur. In this scenario, pyruvate can be generated by two mechanisms (as seen in **Figure 3.1**): 1) conversion of PEP into oxaloacetate via phosphoenolpyruvate carboxylase (encoded by *ppc*; an essential gene in *E. coli* grown in minimal media on glucose) followed by a multi-step process in the TCA cycle to produce malate which can subsequently be converted in pyruvate via malate dehydrogenase (encoded by *maeA* and *maeB*), and 2) the catabolism of xylose via the pentose phosphate pathway [166], followed by gluconeogenic steps to produce glucose-6-phosphate (G6P) from fructose-6-phosphate via G6P isomerase (encoded by *pgi*), and subsequent conversion into glyceraldehyde-3-phosphate (G3P) and pyruvate in the Entner-Doudoroff pathway [167] (reactions: G6P → 6-phosphogluconolactone (6PGNL) via G6P dehydrogenase (encoded by *zwf*); 6PGNL → phosphogluconate (6PGNT) via 6-phosphoglucocnolactonase (encoded by *pgl*); 6PGNT → 2-keto-3-deoxy-6-phosphogluconate (KDPG) via phosphogluconate dehydratase (encoded by *edd*); KDPG → G3P + pyruvate via KDPG aldolase (encoded by *eda*). As these two mechanisms are complex, involving multiple enzymatic steps, it may be likely that pyruvate (and acetyl-CoA) limitations upon growth on a glucose-xylose mixed feed ultimately play a role in affecting Phe production.

The removal of *crr* led to increases in Phe yields and titers and as well as the elimination of acetate accumulation. Interestingly, *crr* (i.e., its gene product IIA^{Glc}) plays a pivotal role not only in the mechanism of glucose uptake via the PTS system but also affects xylose catabolism and is the central component of regulating carbon catabolite repression. The phosphorylation state of IIA^{Glc} regulates the levels of cAMP as IIA^{Glc}-P binds to and subsequently activates adenylate cyclase in the cell, which can then convert ATP into cAMP [147,168]. High levels of cAMP will bind to CRP which can later activate genes of other, non-glucose sugars (e.g., xylose). In the presence of glucose, the phosphate group from IIA^{Glc}-P is donated to the PTS system to allow for glucose to be imported into the cell and converted into glucose-6-phosphate. In this case, levels of IIA^{Glc}-P are low which no longer activates adenylate cyclase and subsequently, leaves xylose-utilizing genes inactive. However, when no glucose is present, IIA^{Glc}-P dominates, and the above cascade is induced leading to activation of xylose-utilizing genes (i.e., *xylAB, xylFGH*) [211]. Furthermore, CRP-cAMP coactivates these genes with XylR [155], indicating that, at least in a wild-type strain, both systems are necessary to fully induce the xylose-utilizing operons. However, upon deletion of *crr*, IIA^{Glc} is no longer present and activation of adenylate cyclase cannot occur in the manner previously described. So, while glucose uptake and utilization rates are reduced, the removal of *crr* may also negate the improvements seen in xylose utilization rates when the *xylR** mutation is introduced. Surprisingly, in NST74 Δ*crr* Δ*pykAF* with a mixed sugar feed, cells consumed 100% of both xylose and glucose fed, whereas in NST74 and NST74 Δ*pykAF*, cells utilized 100% of glucose but no consumption of xylose was detected. As the above discussion indicates that the presence of IIA^{Glc} plays a significant role in activating xylose-utilizing genes, it is unexpected that the removal of *crr* allows for the consumption of xylose in these feeds compared to its parent strains. This may indicate further mechanisms at play affecting xylose consumption post-glucose assimilation, such as the presence of significant acetate levels in the media.

Furthermore, as NST74 is a mutated strain maintain various single-nucleotide polymorphisms (SNPs), insertions and deletions, there may be differences in terms of regulatory mechanisms concerning glucose and xylose interactions compared to a wild-type strain. For example, in NST74, a mutation replacing two codons in the gene encoding for adenylate cyclase (i.e., *cyaA*) is present

(data not shown). Two codons starting 831 nucleotides into the gene (CCA and CGT encoding for proline and arginine, respectively) are replaced with GTC (encodes for valine). This change may play some effect on the activity and functionality of adenylate cyclase in NST74. Also, NST74 contains a codon change in the gene *crp* (K29T), which may affect the activity of this gene product on inducing xylose-utilizing genes. Nonetheless, introduction of the *xylR** mutation into NST74 allows for the co-utilization of both glucose and xylose as previously observed in other wild-type and production strains [154], indicating the complexity of the regulatory mechanisms which govern sugar utilization and carbon catabolite metabolism in *E. coli*.

3.5 Conclusions

While the co-consumption of industrially relevant carbon sources is critical to future efforts to enhance titers and yields of Phe-derived compounds, it seems that a delicate balance must be maintained. Sugar consumption at too rapid of a pace is inefficient for Phe production and ultimately leads to accumulation of inhibitory acetate levels. From the above results, a slower consumption of sugar (especially xylose), seems to be more beneficial for Phe titers and yields. However, as an ideal, economically viable production scenario would consist of rapid production and purification of Phe (or its derivatives), a strain that very slowly consumes sugars and produces the desired product may not be idyllic. Therefore, future efforts to improve Phe production metrics may focus on engineering strains to consume sugars at increased rates while maintaining high intracellular pools of E4P and PEP for Phe production-use only. By perhaps investigating methods to tie Phe production directly to growth, such as allowing sugar catabolism only upon conversion of E4P and PEP into DAHP, Phe titers and yields may be maximized.

CHAPTER 4. TRANSCRIPTIONAL ANALYSIS OF *ESCHERICHIA COLI* RESPONSE TO STYRENE EXPOSURE

Abstract

Transcriptomic profiling is an important tool that can help to reveal key insights regarding how cells react and respond to different environmental stimuli, including the presence of inhibitory biofuels and biochemicals. Here, the transcriptional response of *E. coli* to the aromatic biochemical styrene was determined by performing RNA sequencing (RNA-seq) analysis. Furthermore, the potential influence of the source of exposure was comparatively evaluated by applying RNA-seq analysis to both styrene-producing and styrene-exposed cells. In both cases a systems-level assessment of transcriptional response was performed, with special attention given to response and potential role of different general tolerance mechanisms, as well as to the identification of possible gene markers displaying unique patterns of differential expression in one exposure mode versus the other. Genes involved in the phage shock protein response (e.g., *pspABCDE/G)*, general stress regulators (e.g., *marA, rpoH*), and several membrane-altering genes (notably, *bhsA, ompR, ldtC*) showed up-regulation in response to styrene exposure. Overall, the expression profiles of external addition and internal production of styrene were similar with some differences observed in the magnitude of differential expression for some important genes (e.g., up-regulated genes such as *pspABCDE/G, recA, marA, micF*) and expression of some genes involved in amino acid biosynthesis.

4.1 Introduction

Through metabolic engineering and synthetic biology strategies, significant effort has been put into producing value-added chemicals or bioenergy alternatives from renewable sources. Through the engineering of industrially relevant strains to enhance the production of native metabolic precursors, remove pathways that produce harmful or unnecessary byproducts and alter native flux regulation processes, the bioproduction of both natural and non-natural compounds in microbes has been improved upon [169]. One significant group of potentially vital bioproducts are aromatics, which contain one or more substituted benzene rings. Aromatics have many industrially relevant purposes such as precursors to pharmaceuticals, plastic monomers and biofuel alternatives so recent research has focused on improving the diversity of aromatics that can be produced in microbes as well as developing methods which can improve production metrics of these chemicals as has been recently reviewed [5,6,170].

One limitation in the quest for improved microbial production of aromatics is end-product toxicity [21,117,171,172]. Often, aromatics are highly lipophilic and have many solvent-like properties that lend themselves to poor biocompatibility by causing changes in membrane integrity and inhibiting function of membrane proteins [173-176]. While the goal of tolerance engineering is ultimately to enhance production of the target biochemical, many times, chemical tolerance does not necessarily lead to production improvements. In some cases, the resulting fitness improvements enabled by tolerance engineering strategies do not lead to increases in titers and yields [177,178]. Clearly, such phenotypes are often very complex and multi-genic in nature, as well as difficult to fully and independently resolve.

One such complication pertains to understanding if, how, when and to what degree various tolerance-related mechanisms are turned on when exposed to various stresses. As the first steps in cellular adaptation to environmental changes involve sensing the change and performing alterations on the transcriptional level, transcriptomic data (obtained by microarray analysis or RNA sequencing) provides the most comprehensive datasets needed to elucidate and understand what role native tolerance strategies might play in solvent tolerance. Examination of gene families which

are up- or down-regulated can be utilized to illuminate mechanisms of toxicity and subsequently, help develop synthetic engineering strategies to improve tolerance and cell fitness. Transcriptomics-based strategies have been utilized to investigate the transcriptional effect of exposure to compounds such as isobutanol [179], acetate [180], 1,4-butanediol [181], ethanol [182] and free fatty acids [183] among others [184-186].

Several studies have investigated the transcriptional response of microbes when stressed with aromatic chemical toxicity such as in *E. coli*, with most research focusing on antibiotics (e.g., triclosan, sulfamethoxazole, tetracycline) [187]. However, the transcriptional effects of more industrially-relevant aromatic compounds have also been examined in *E. coli* such as toluene [188], *p*-hydroxybenzoic acid [189] and cinnamaldehyde [185,190] (along with the 2-phenylethanol stress response in *S. cerevisiae* [191]). In response to 0.02% (v/v) toluene exposure, for example, researchers found 641 differentially expressed genes, with many of them involved in Fe/S assembly and oxidative and universal stress responses (flagella biogenesis and assembly related genes were also significantly down-regulated) [188]. When exposed to salicylate, an industrially relevant aromatic acid, *E. coli* activated global stress response systems such those mediated by the *marRAB* operon [184].

To gain a more complete understanding of transcriptomic response to aromatic exposure, RNA-seq analysis has been performed on *E. coli* under styrene-induced stress and two distinct exposure modes: extracellular addition versus intracellular production. The differences between exogenously added solvent versus internally produced solvent may be significant as, for many industrial processes, the internal production condition is much more relevant. Fundamental modes of toxicity may be different within the cell versus outside the cell and tolerance engineering strategies that succeed in one scenario may not help in others. Toxicity of styrene in *E. coli*, for example, has previously been investigated in terms of these different conditions when exposed to the chemical. Using membrane leakage as an analogue for membrane integrity, researchers found that less than 10% of cells exposed to styrene addition demonstrated membrane leakage while more than 50% of styrene-producing cells showed damaged membranes (although researchers

found no membrane fluidity changes caused by styrene production) [192]. In said study, however, no comparisons of transcriptional responses between the two different styrene-exposure modes were performed.

In particular, specific emphasis has been given to: i) comparing and contrasting the effect of different styrene exposure modes (i.e., P vs. A) on the cellular response, ii) elucidating which known tolerance mechanisms *E. coli* attempts to employ for inherent styrene resistance and which remain unchanged or inactivated, and iii) understanding the overall physiological response of *E. coli* following exposure to inhibitory concentrations of styrene. Overall, the objective of this work is to obtain an improved understanding as to how *E. coli* naturally responds to styrene toxicity, gives input on how cells respond differently when producing a toxin versus when they are externally exposed to it, identifies native machinery that might serve to construct aromatic-inducible transcriptional elements, and provides clues on possible future directions for improvements to engineer *E. coli* for aromatic tolerance.

4.2 Materials and Methods

4.2.1 Strains and Cultivation Conditions Used

E. coli NST74 (a phenylalanine-overproducing strain) [120] carrying pTrcColaK-PAL2 and pTrc99A-FDC1 (expressing *PAL2* from *Arabidopsis thaliana* and *FDC1* from *Saccharomyces cerevisiae*, respectively, to collectively convert endogenous phenylalanine to styrene) was used as the styrene producing strain. *E. coli* NST74 cells carrying the empty vectors pTrcColaK and pTrc99A were utilized as a non-producing strain for exogenous styrene addition and unexposed control conditions. Seed cultures were grown in 3 mL LB broth supplemented with appropriate 100 μg/mL ampicillin and 30 μg/mL kanamycin at 32°C while shaking at 200 rpm for 12 – 16 h. Seed cultures were used to inoculate 50 mL of pH 6.8 MM1 minimal media supplemented with 1.5% glucose in 100 mL Teflon-capped corning bottles (to prevent styrene loss via evaporation) at a starting OD_{600} of ~0.01. MM1, a phosphate-limited minimal media adapted from McKenna and Nielsen [117], was prepared according to the following recipe (in g/L): $MgSO_4 \cdot 7H_2O$ (0.5), $(NH_4)_2SO_4$ (4.0), MOPS (24.7), KH_2PO_4 (0.3), and K_2HPO_4 (1.0), as well as 1 mL/L of a trace mineral solution containing

(in g/L): $MnCl_2 \cdot 4H_2O$ (1.584), $ZnSO_4 \cdot 7H_2O$ (0.288), $CoCl_2 \cdot 6H_2O$ (0.714), $CuSO_4$ (0.1596), H_3BO_3 (2.48), $(NH_4)_6Mo_7O_{24} \cdot 4H_2O$ (0.370), and $FeCl_3$ (0.050). Furthermore, exogenous phenylalanine (1 mL of 20 g/L stock) was added to all conditions to boost styrene production to even further toxic levels in the P condition (the C and A conditions do not contain pathway enzymes so phenylalanine addition would have no effect on styrene accumulation).

Upon reaching OD_{600} ~1.0 , all cultures were induced by the addition of 0.2 mM IPTG, after which culturing continued at 32°C and 200 rpm for a total of 27 h. In the case of exogenous styrene addition, styrene (99%, stabilized with 10-15ppm 4-tert-butyl-catechol; Alfa Aesar, Tewksbury, MA, USA) was added to the culture according to the following schedule (listed values represent final concentrations after each addition): 0 mg/L at 0 h, 25 mg/L at 13 h, 65 mg/L at 23 h, 165 mg/L at 25 h.

4.2.2 RNA-seq Data Collection and Analysis

At 27 h after inoculation, cells were harvested for RNA extraction using the RNeasy Mini Kit (Qiagen, Germantown, MD, USA) following vendor's protocols. Two biological replicates were pooled at equimolar concentrations to create a single sample and duplicates were sequenced for each condition. RNA degradation and contamination were monitored on 1% agarose gels. After rRNA depletion using a RiboZero kit (Illumina), random hexamer priming was used to generate cDNA and library preparation was performed using a Nextera library prep kit (Illumina) according to the manufacturer instructions. Paired end sequencing (2 x 150) was performed using an Illumina NextSeq at the DNASU Sequencing Core at Arizona State University. Reads had adapters removed and were quality trimmed using the default settings of Trim Galore prior to being mapped to the *E. coli* MG1655 genome using STAR. Differential gene expression analysis was performed using edgeR. From these RNA-seq results, comparisons were made for both styrene production/addition relative to the no styrene control. Differences in transcript levels are indicated as $\log_2$-fold changes with positive numbers indicating up-regulation in the styrene-exposed cells and negative numbers indicating down-regulation. Significant differential expression (DE) is reported as those genes which maintain a p-value < 0.05 when compared to the no styrene control.

4.2.3 Gene Ontology and KEGG Pathway Analysis

For gene ontology (GO) term analysis, GeneSCF [193] was utilized, employing all three databases for GO analysis (i.e., biological process, molecular function, cellular components) and the *E. coli* organism database. For KEGG pathway analysis and identification of enriched pathways, KOBAS 3.0 (KEGG Orthology Based Annotation System) was utilized [194,195]. Only differentially expressed genes below the p-value of 0.05 cut-off were included in the GO term and KEGG pathway analyses. Significantly over-represented GO terms or KEGG pathways are reported if, when compared to all the genes in the *E. coli* K-12 genome, the p-value was < 0.05.

4.3 Results

4.3.1 Characterizing the Overall Transcriptomic Response of E. coli to Styrene Exposure

To elucidate the effect of styrene exposure on *E. coli* cells, as depicted in **Figure 4.1A**, a total of three conditions representing different styrene exposure modes were investigated in this study: styrene production (P), styrene addition (A), and a no styrene (production or addition) control (C). During A, the schedule of styrene addition was designed to mimic the profile of its accumulation during a typical production culture (**Figure 4.1B**). In each case, cells were harvested after 27 h, after which their total RNA was extracted and sequenced. There were 30.59 and 37.15 M reads generated for C runs (83.3% and 82.3% of reads mapped to genome, respectively), 28.41 and 42.91 M reads generated for A runs (81.7% and 82.6% of reads mapped to genome, respectively) and 35.49 and 37.23 reads generated for P runs (83.9% and 83.3% of reads mapped to genome, respectively). Changes (all relative to C) in global transcriptomic patterns arising in each case were then identified via bioinformatic analysis of the obtained RNA-seq data.

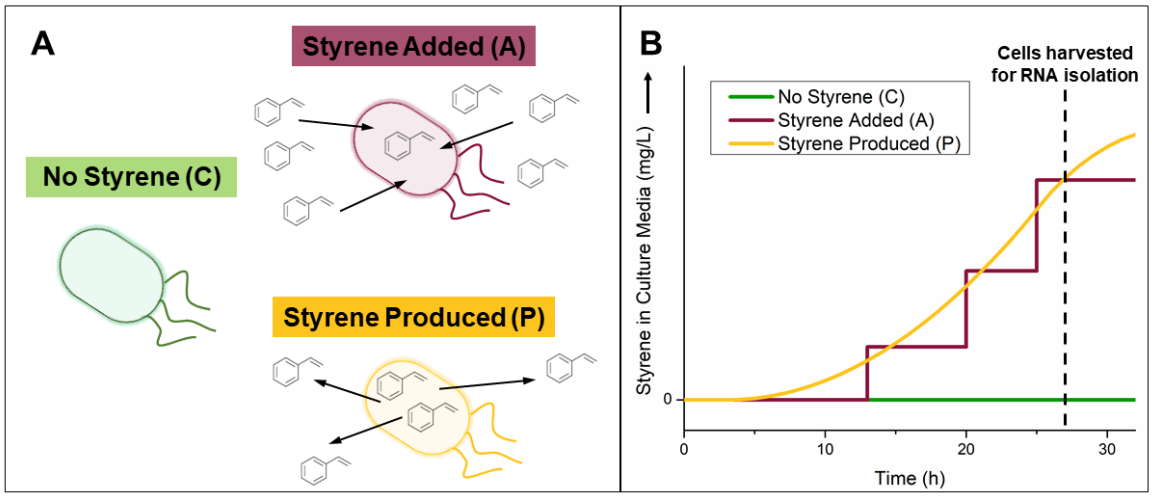

Figure 4.1 A) Three Conditions upon which RNA was Extracted and, B) Styrene Accumulation in Production Strain and Styrene Addition in Styrene-Added Strain.

A) Three conditions were used here: No styrene present (C), styrene added exogenously (A) and styrene produced internally (P). B) Approximate time-course of extracellular styrene concentration in the three conditions.

In total, 1,674 and 980 differentially expressed (DE) genes were identified for A and P (both relative to C), respectively (**Figure 4.2A**). Among these, approximately 50% of DE genes were up-regulated for A, compared to 56% in the case of P. Among up-regulated genes, the average magnitudes of differential expression were much higher for P than for A (~1.52 $\log_2$-fold change vs. ~1.11 $\log_2$-fold change) whereas, for down-regulated genes, the average magnitudes of differential expression were closer though still slightly higher for P compared to A (~-1.26 $\log_2$-fold change vs. ~-1.18 $\log_2$-fold change). The observed difference in magnitude, especially among up-regulated genes, could suggest that, at least amongst this subset of DE genes, sensitivity to styrene exposure is elevated when styrene originates from inside the cell, perhaps resulting due to its higher apparent intracellular concentration and/or limitations associated with its extracellular export. Meanwhile, a total of 652 genes were DE under both styrene exposure modes, compared to 1022 and 328 genes were only DE for P and A, respectively (**Figure 4.2B**).

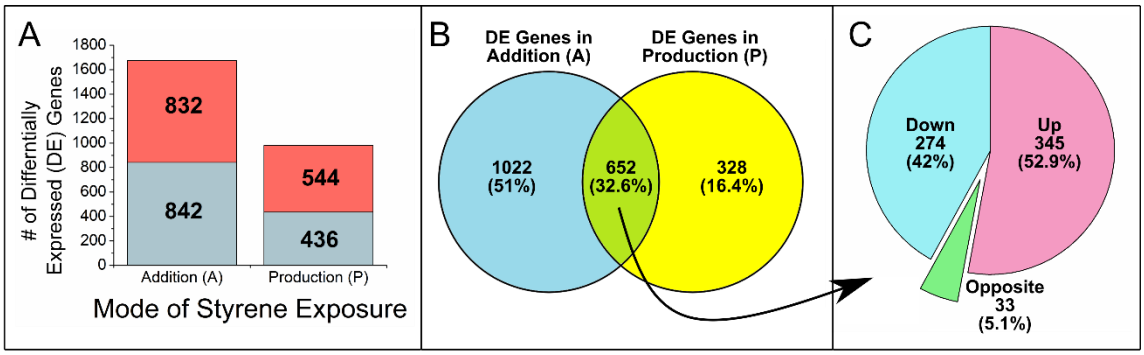

Figure 4.2 Overall Statistics for RNA-seq Analysis Showing DE Genes and Common DE Genes between Modes of Styrene Exposure.

A) The number of differentially expressed (DE) genes is shown for both modes of styrene exposure compared to the control. The red bars (and numbers inside) show the number of DE genes which were upregulated for that condition while the blue bars (and numbers inside) show the number of DE genes which were downregulated for that condition. Only genes which showed a p-value < 0.05 are included. B) Venn diagram (created with Venny 2.1.0 [196]) showing the number of genes which were DE in only the Addition condition (blue), the number of genes which were DE in only the Production condition (yellow) and the number of genes which were DE in both conditions (green). C) Of the genes which were DE in both conditions, the number of genes which were down-regulated under both conditions (light blue), the number of genes which were up-regulated under both conditions (pink) and the number of genes which showed DE in opposite directions for the two conditions (green). The percentage of common DE genes which are grouped in each category is also listed next to the number of genes.

Among the 652 commonly DE genes, 345 were up-regulated and 274 were down-regulated under both A and P (**Figure 4.2C**). Interestingly, however, 33 genes were DE in opposite directions for P versus A; a difference that again points to the likelihood that *E. coli* experiences styrene differently depending upon the source of exposure (i.e., internal vs. external). However, and perhaps unsurprisingly, the limited number of oppositely DE genes between P and A likely suggests that the overall experienced difference is relatively small.

The functions of DE genes were further analyzed based on gene ontology (GO) terms, revealing that, in total, 44 and 63 GO terms were over-represented for A and P, respectively, among which 26 were over-represented in both conditions. GO terms shared by both conditions unsurprisingly include those which are very broad (e.g., “GO:0005829~cytosol” and “GO:0005515~protein binding” which contain 1028 and 1016 genes in *E. coli*, respectively), but also more specific terms such as “GO:0017148~negative regulation of translation” and

"GO:0005525~GTP binding", which contain only 12 and 16 genes in *E. coli*, respectively. **Figure 4.3** shows some of the GO terms of particular interest for this study along with the percentage of genes in each term that were significantly repressed or induced upon styrene addition or production. Some noteworthy terms are those related to cell division, response to DNA damage via the SOS response and cellular response to various stresses (e.g., heat, radiation).

Additional KEGG pathway analysis, meanwhile, revealed that 8 and 17 KEGG pathways were over-represented for A and P, respectively. Of these, 5 KEGG pathways were over-represented in both conditions, including 'ribosome' (eco03010), 'metabolic pathways' (eco01100), 'homologous recombination' (eco03440), 'biosynthesis of secondary metabolites' (eco01110), and 'pyrimidine metabolism' (eco00240). Similarly to the GO terms, a multitude of relevant KEGG pathways and the percentage of genes that are induced or repressed for both styrene conditions are illustrated in **Figure 4.4.** KEGG pathways of significant interest include those related to the biosynthesis of amino acids, genes involved in central metabolism and those related to the production of membrane components (e.g., fatty acids, peptidoglycan). Further analysis and discussion regarding many of the GO terms and KEGG pathways, as well as the genes involved in each, is included in the following sections.

To gain a more detailed understanding of how *E. coli* responds to and is affected by styrene, a subset of the most statistically significant as well as generally interesting outcomes from the RNAseq results were selected for more detailed analysis and discussion in the following sections, as organized according to major cellular functions, systems, or roles. Overall, most behaviors were, at least qualitatively, conserved between A and P. Therefore, to facilitate the discussion the focus is first on the outcomes of just A, after which a comparison of notable differences between A and P is presented.

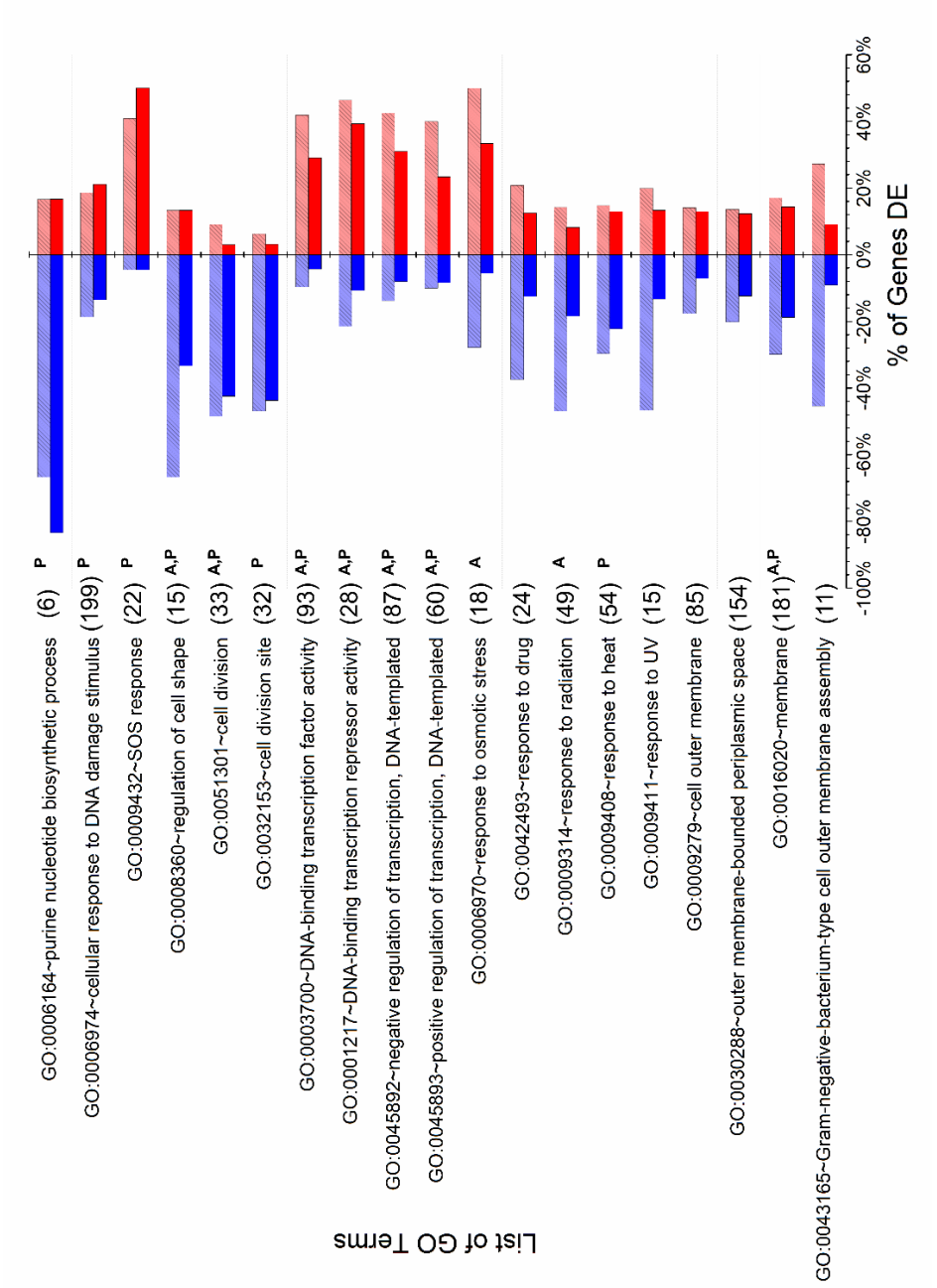

Figure 4.3 List of Relevant GO Terms for DE Genes after Exposure to Styrene.

A selection of Gene Ontology (GO) Terms. The total number of genes in each GO term in the E. coli genome is listed in parenthesis next to the GO term. The x-axis indicates the percentage of total genes in the GO term which were significantly repressed (left, blue) or induced (right, red) for each styrene exposure condition compared to the control. The addition condition is shown as light red or blue (with stripes) while the production condition is dark red or blue. The superscript 'A' or 'P' indicates that the GO term was significantly over-represented (p-value < 0.05) for the addition or production conditions, respectively, compared to the E. coli genome. GO term analysis was accomplished via GeneSCF [193].

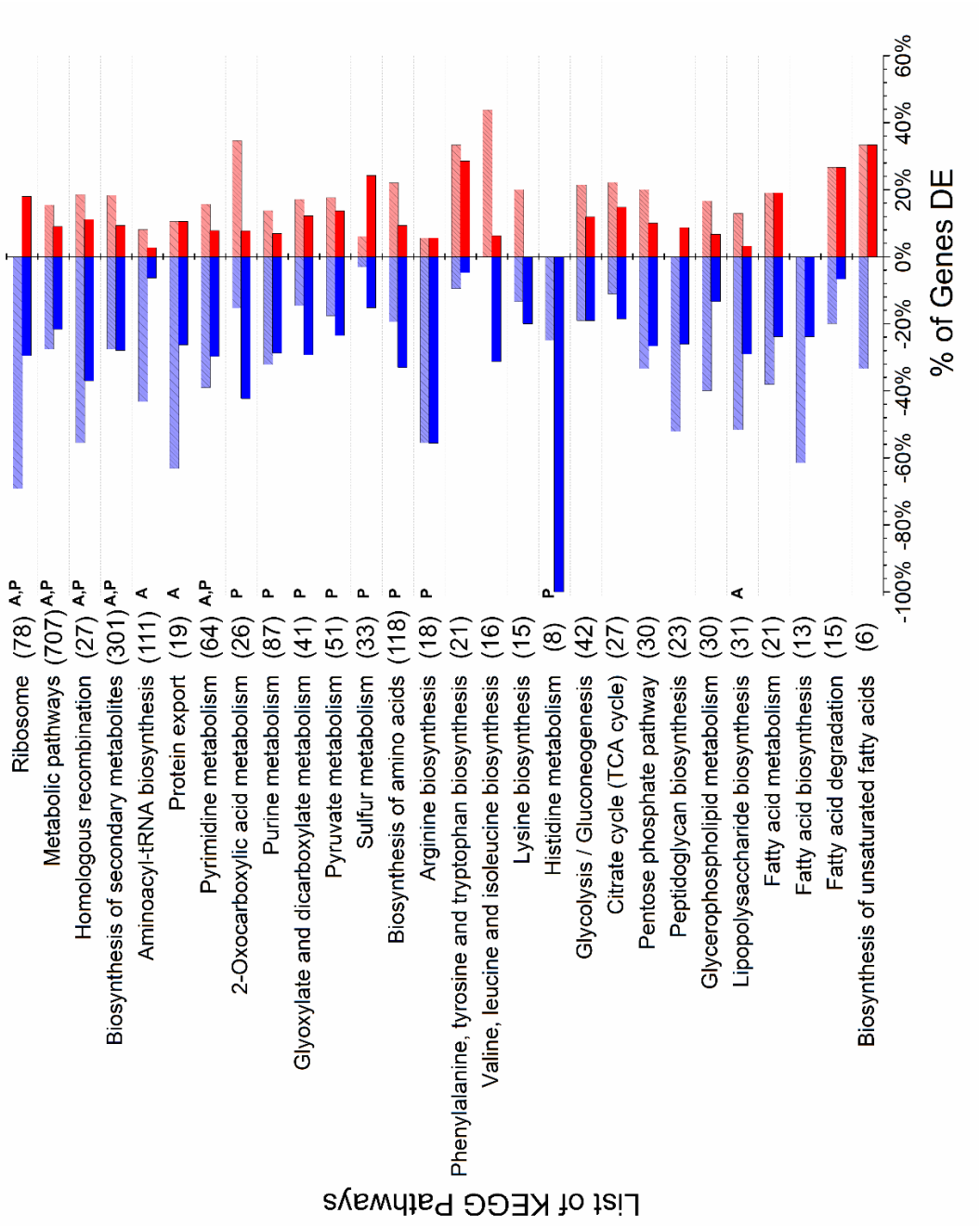

Figure 4.4 List of Relevant KEGG Pathways for DE Genes after Exposure to Styrene.

A selection of KEGG pathways. The total number of genes in each KEGG pathway in the E. coli genome is listed in parenthesis next to the KEGG pathway. The x-axis indicates the percentage of total genes in the KEGG pathway which were significantly repressed (left, blue) or induced (right, red) for each styrene exposure condition compared to the control. The addition condition is shown as light red or blue (with stripes) while the production condition is dark red or blue. The superscript 'A' or 'P' indicates that the GO term was significantly over-represented (p-value < 0.05) for the addition or production conditions, respectively, compared to the E. coli genome. GO term analysis was accomplished via KOBAS 3.0 [194,195].

4.3.2 DNA Synthesis, Replication, and Repair

One emergent pattern gleaned from overall dataset is that styrene exposure appears to trigger the shutdown of cell growth in a 'bottom up' manner, beginning with the synthesis and replication of DNA. Specifically, numerous DE genes were found to be associated with the "DNA replication" (GO:0006260) GO term, including those encoding for DNA polymerase (*dnaX*, DNA polymerase III subunit) and the replication initiator protein (*dnaA*), along with members of the primosome (*priA* and *priB*, primosomal replication factor and protein, respectively; which work to restart stalled DNA replication), all of which were significantly repressed. Meanwhile, pathways used to supply precursors to DNA synthesis were also repressed. For example, *purR* encodes a transcriptional repressor involved in regulating purine and pyrimidine nucleotide biosynthesis. While expression of *purR* was found to be mostly unchanged in the presence styrene, of the 31 known PurR-repressed genes, 23 were DE for A, all of which were downregulated. In concordance with the above data, the GO term "purine nucleotide biosynthetic process" (GO:0006164) showed 4 of the 6 total genes were down-regulated for the A condition. Since purine and pyrimidine biosynthesis is quite energy intensive, downregulation of these pathways may represent an attempt by the cell to conserve and possibly redistribute energy resources to other processes of more critical importance to aiding in survival.

Beyond simply inhibiting DNA replication, styrene exposure also appears to elicit DNA damage (e.g., double-strand breaks), in a manner similar to exposure to UV radiation or DNA-arresting chemicals [197,198]. In response to such damage, the SOS response is commonly activated as a mechanism to repair the damage through homologous recombination and DNA replication [198,199]. Analysis of genes associated with the "SOS response" (GO:0009432) GO term revealed that 10 of 22 were DE for A, 9 of which were upregulated. The gene *recA* ($\log_2$fold change = 0.46) encodes a recombinase that plays a major role of the SOS response [197]. Meanwhile, SOS-induced DNA polymerases (such as Pol IV and Pol V, encoded by *dinB* and *umuDC*, respectively), which enable replication through various damage and lesions that DNA polymerase III cannot [200], were also DE with *dinB* and *umuD* showing $\log_2$-fold changes of 0.82 and 0.80 for A, respectively. However,

since SOS-induced DNA polymerases are considered to be of lower fidelity [200], this suggest the cells might use this response as a mechanism to incorporate mutations that might improve the chance of survival.

4.3.3 Protein and Amino Acid Biosynthesis

Styrene exposure also caused the differential expression of several genes associated with ribosomal activity, suggesting that, like DNA synthesis, protein biosynthesis was also decreased. For example, in the case of A, 69% of all genes involved in the "ribosome" KEGG pathway (eco03010) were DE, 100% of which were repressed. Similarly, many genes associated with the biosynthesis of precursor amino acids were also DE, however, the resulting trends were not as clear or widespread. Specifically, analysis of the "biosynthesis of amino acids" KEGG pathway (eco01230) showed that 22% and 19% of the 118 total genes in this pathway were upregulated and downregulated, respectively, in response to styrene exposure. For example, of the 17 genes involved with converting α-ketoglutarate into the amino acids, L-glutamate, L-proline, L-arginine, L-glutamine, 12 were downregulated while none were upregulated. Genes such as *glnA* (encoding glutamine synthetase) and *argI* (encoding ornithine carbamoyltransferase) showed a $\log_2$-fold change of -4.77 and -3.27, respectively. Additionally, expression of all three subunits of the glutamine ABC transporter (encoded by *glnQHP*) were highly downregulated ($\log_2$-fold change = -3.58, -4.58 and -3.47, respectively). Shutdown of pathways competing for α-ketoglutarate might represent a strategy used by the cells to increase energy generation by enhancing flux through the TCA. Conversely, 7 genes involved in the biosynthesis of aromatic amino acids (i.e., L-phenylalanine, L-tyrosine, L-tryptophan) were upregulated while only two were downregulated. In fact, regarding the KEGG pathway for "phenylalanine, tyrosine and tryptophan biosynthesis" (eco00400), 33% of genes were upregulated for A, while only 10% were downregulated. This could, at least in part, be an experimental artifact, derived from the fact that the host strain (NST74) is a L-phenylalanine over-producing strain that carries a *tyrR* deletion, along with several additional point mutations in key shikimate pathway genes.

4.3.4 Cell Replication

In addition to its aforementioned role in facilitating DNA repair, the SOS response also influences cell division, notably via the inhibitor protein encoded by *sulA* (which disrupts cell division and can lead to loss of cell viability [201]), whose expression was also increased (log_2-fold change = 0.86) following styrene addition. Meanwhile, other genes associated with the GO term "cell division site" (GO:0032153), of which there are 32 in total, were also mostly repressed. Specifically, 15 genes were downregulated upon exposure to styrene, whereas 2 (*ftsL* and *zapC*) were upregulated. To date, over 3 dozen proteins have been identified to make up the so-called 'divisome' in *E. coli* [202]. Several vital components of the divisome belong to the *dcw* cluster: an operon consisting of 16 genes that each play key roles in controlling cell division, synthesizing cell wall components or the production/transport of peptidoglycan (PG) precursors (e.g., lipid II) [203]. Eight genes in this cluster were significantly downregulated following styrene exposure, including (log_2 fold change shown in parentheses): lpxC (-0.44), *mraY* (-0.54), *murE* (-0.56), *ftsW* (-0.95), *ddlB* (-0.95), *ftsQ* (-0.97), *murG* (-1.10) and *murC* (-1.11). Among these, *ftsW*, *ftsQ*, and *ftsL* all belong to the dozen total genes that are essential for cell division [202]. Other genes involved in synchronizing cell envelope division, controlling elongation machinery, and mediating cell wall synthesis also showed significant downregulation (log_2-fold change in parentheses), including *mreB* (-1.22; encoding a dynamic cytoskeletal protein that controls PG biosynthesis [204]), as well as those genes making up the Tol system (*tolA* (-1.50), *tolQ* (-1.11), *tolR* (-1.23), *tolB* (-1.04) and *pal* (-1.05)) which controls initiation of outer membrane (OM) constriction [204]. Previously, it has been shown that damage to any part of the Tol system leads to decreased OM integrity and periplasmic leakage, thus leading to increased sensitivity to drugs and other stresses [204]. As the initiation of cell division processes and constriction of the OM are often the most vulnerable moments for *E. coli* cells when exposed to various stresses [205], cells may be attempting to reduce expression of cell envelope organization genes upon styrene exposure to reduce times when cells are most susceptible to stress-induced damage. Furthermore, by downregulating genes involved in cell division and protein production, cells may be able to focus resources on stress responses and energy generation perhaps in an effort to move from a growth to survival mode.

4.3.5 Central Metabolic Pathways

The main KEGG pathways associated with central metabolism were also analyzed, revealing a wide distribution of genes were DE following styrene, including 21% upregulated and 19% downregulated for "glycolysis/gluconeogenesis" (eco00010; 42 genes total), 20% upregulated and 33% downregulated for "pentose phosphate pathway" (eco00030; 30 genes total), and 22% upregulated and 11% downregulated for "citrate cycle (TCA cycle)" KEGG pathway (eco00020; 27 genes total). One particularly interesting behavior revealed by this analysis pertains to the production (from pyruvate) and subsequent consumption (to citrate and into the TCA cycle) of acetyl-CoA by the pyruvate dehydrogenase complex (PDH; encoded by *aceEF-lpd*) and citrate synthase (encoded by *gltA*). Expression of PDH is negatively regulated by the dual regulator PdhR, whose own expression was also significantly upregulated (log_2-fold change = 2.12) in the case of A. Previously, activation of PdhR has been reported for *E. coli* in response to a variety of acid stresses [206]. Binding of PdhR to its cognate operator is influenced by the availability of pyruvate. More specifically, when present, pyruvate binds to and releases the transcriptional repression caused by PdhR. In the case of A, each of *aceE*, *lpd* and *gltA* were upregulated (log_2-fold change = 1.06, 0.89 and 1.30, respectively). In addition to PDH, meanwhile, PdhR has been also shown to negatively regulate *ndh* – a key gene involved in respiration – although its expression was upregulated in A (log_2-fold change = 0.82) perhaps in an effort to support flux through the TCA cycle. Overall, these collective behaviors suggest that the cells are attempting to increase energy generation by shuttling more carbon to pyruvate and, in turn, into the TCA cycle. Consistent with the above indicators of α-ketoglutarate preservation, these changes further support of a model suggesting that styrene exposure causes a shift towards increased energy generation by increasing carbon flux into and through the TCA cycle. Interestingly, this behavior differs from what has been previously reported for the case of octanoic acid stress in *E. coli*, for which flux analysis revealed a diversion of pyruvate flux from the TCA cycle and towards acetate via the more thermodynamically favorable pyruvate oxidase (PoxB) [207].

4.3.6 Global Stress Response

Unsurprisingly, several known and common stress response systems were also found to be activated in response to styrene addition. This included significant upregulation of several DE genes from GO terms including "response to radiation" (GO:0009314; 61% of 49 total genes), "response to UV" (GO:0009411; 67% of 15 total genes), "response to heat" (GO:0009498; 44% of 54 total genes), "response to osmotic stress" (GO:0006970; 78% of 18 total genes), and "response to drug" (GO:0042493; 58% of 24 total genes). The gene *marA*, for example, which is part of the *marRAB* locus and encodes a dual transcriptional regulator responsible for modulating expression of several genes involved in resistance to multiple antibiotics and other inhibitory compounds/conditions [208], was found to be up-regulated upon styrene addition (log_2-fold change = 1.08). This is consistent with previous transcriptomic analyses focused on characterizing the response of *E. coli* to a variety of inhibitory conditions, where *marA* expression was almost always upregulated (93% of the time), including in the case of exposure to phenolic compounds [187,209]. MarA has been shown to directly and indirectly activate expression of as many as 47 different genes while repressing expression of at least 15 additional genes, including OM proteins like the porin-encoding *ompF* [210]. Surprisingly, however, several genes whose expression is known to be regulated by MarA, and which typically play key roles in *E. coli*'s tolerance mechanisms, were not upregulated in the case of A. This includes *acrAB* and *tolC* (encoding for the multi-drug efflux transporter AcrAB-TolC), as well as and *soxS* (encoding for a stress-responsive transcriptional regulator). In fact, expression of *acrB* was actually repressed (log_2-fold change = -0.84) following styrene addition. This seemingly conflicting behavior may be due to the fact that the MarA regulon is governed by a "cascade"-like regulation where, for example, certain genes (e.g., *micF*, *sodA* and *marRAB*; all upregulated in A) are activated at low MarA levels whereas others (e.g., *tolC*) are induced only at higher concentrations [211,212].

The global stress response of *E. coli* is partially governed by the universal stress protein superfamily comprised of six proteins encoded by *uspACDEFG*, all of which are separately transcribed [213]. Increased transcription of these genes has been shown to be induced to a wide

variety of stresses, however, such as exposure to heat, ethanol and several antibiotics [213]. Meanwhile, whereas UspA and UspD have been implicated in protecting against superoxide stress, overall, the physiological roles of these genes are not well known. Here, styrene addition resulted in upregulation of each of *uspC*, *uspD*, *uspE* and *uspG*, however, *uspA* and *uspF* showed no DE. *E. coli*'s heat shock response also appears to be activated in response to styrene exposure. For instance, transcript levels for the heat shock responsive sigma factor, σ^{32} (encoded by *rpoH*), also showed significant upregulation ($\log_2$-fold change = 1.48). Expression of *rpoH* and its regulon have also been reported to respond to similar stresses, including ethanol [214] and *n*-butanol [215] addition. Two of the most upregulated genes in the dataset were *ibpA* and *ibpB*, both of which are part of the σ^{32} regulon and encode small heat shock chaperones [216] ($\log_2$-fold change = 2.27 and 3.94, respectively). Deletion of these genes is known to increase sensitivity to heat shock [217] while their overexpression correspondingly improves resistance [218]. Upregulation of the heat-responsive gene *yibA* ($\log_2$ fold change = 1.83) was also observed. While not well characterized, strains lacking YibA showed increased sensitivity to nalidixic acid, tetracycline, mitomycin [219], and UV- and X-radiation [220] while overexpression of *yibA* increased tolerance of *E. coli* to *n*-butanol by ~13% [221].

4.3.7 Membrane Stress Response

Aromatic chemicals, including styrene, have commonly be reported to cause membrane damage and stress [138,176,192]. Thus, unsurprisingly, several stress responses known to be associated with membrane-related damage were also found to be activated. For example, in *E. coli*, five main envelope stress response systems have been identified, including the Psp, Cpx, Bae, Rcs and σ^E signaling pathways, which collectively work to restore the cell envelope upon damage, as well as maintain cell envelope stability and integrity [222]. The conditions under which these pathways are activated have previously been studied via induction of representative promoters [223]. In this case, styrene addition was found to upregulate expression of both the Psp and σ^E signaling pathways. Conserved in multiple different bacteria, the Psp (phage shock protein) system has been shown to respond to multiple stresses, including exposure to ethanol, methanol and other hydrophobic solvents (e.g., *n*-hexane, cyclohexane) [224,225]. In the present study, those genes comprising the

pspABCDE and *pspG* operons (which, along with *pspF*, collectively make up the Psp system) were among the most highly upregulated overall (log_2 fold change = 5.18 to 5.99). Although the Psp system is responsive to a variety of stresses, unlike other cell envelope-based stress responses, its effect is self-contained (i.e., not global) [46]. Although several induction signals and mechanisms have been proposed for the Psp system, including dissipation of the proton motive force, changes in redox state of the quinone pool, and stored curvature elastic stress on the membrane, no one signal has been proven to be correct [47]. *E. coli* mutants lacking the *psp* operon, meanwhile, have been reported to display reduced biofilm formation, a common survival mechanism employed in response to solvent and other stresses [226]. Perhaps more interestingly, *psp* null mutants have also been found to display difficulties in maintaining proton motive force when exposed to different stresses, suggesting that this system plays a role in helping to maintain inner membrane stability and rigidity under stress [224,225].

The sigma factor σ^E (encoded by *rpoE*), meanwhile, has been shown to be responsive to outer membrane stresses and membrane protein misfolding and controls expression of several genes related to membrane stress [227]. Upon styrene exposure, *rpoE* expression was slightly up-regulated (log_2 fold change = 0.63). It has been shown that expression of *rpoE* is up-regulated upon misfolding of OM proteins, as well as in response to various forms of membrane stress [228,229]. The induction of *rpoE* can further up-regulate *rpoH* (the heat-shock sigma factor), which can further act to respond to misfolded membrane proteins [230]. Activation of *rpoE* expression plays a role in amplifying the rate of formation of double stranded DNA breaks and triggering induction of mutagenesis systems, which might facilitate *E. coli*'s ability to adapt and evolve in high-stress environments [231]. Ultimately, the activation of the σ^E sigma factor can improve the stability of the outer membrane by inducing the expression of genes that can re-fold membrane proteins, reduce the expression of new outer membrane proteins, and rapidly modify the cell envelope upon sensing stress [232].

4.3.8 Cell Envelope Modification

Since aromatic chemicals and other solvents are known to cause stress and damage to the cell envelope, adjustments made to its structure and composition have thus accordingly been found to significantly influence tolerance [233-238]. Numerous genes associated with several GO terms related to the cellular envelope were highly DE, including from "membrane" (GO:0016020; 47% of 181 total genes), "gram-negative-bacterium-type cell outer membrane assembly" (GO:0043165; 73% of 11 total genes), and "outer membrane-bounded periplasmic space" (GO:0030288; 34% of 154 total genes). Additionally, KEGG pathways which showing significant overrepresentation includes "lipopolysaccharide biosynthesis" (eco00540; 65% of 31 total genes) and "protein export" (eco03060; 74% of 19 total genes). One important component of the cell envelope stress response concerns the use of mechanisms to maintain proper cross-linking of the peptidoglycan (PG) layer. This can include intermolecular cross-linking via DacC, cross-linking of the PG to the OM lipoprotein (Lpp) via LdtC, or removal of intermolecular cross-linking via AmiA. Significant upregulated expression of both *lpp* and *ldtC* (log_2-fold change = 0.70 and 3.84, respectively) resulted following styrene exposure, suggesting that cells are attempting to increase production of Lpp while also decreasing the amount of free Lpp by anchoring it to PG [239]. This same mechanism has been reported to maintain or increase stability of the cell wall in response to penicillin-exposure and/or induction of the Cpx system [239-241]. Lpp plays an important role in the properties of the OM. Deleting *lpp*, for example, causes an increase in OM permeability [242], and has been shown to facilitate the uptake of the very hydrophobic organophosphorus compound coumaphos (logKow = 4.13 versus 2.95 for styrene) [242]. If the opposite is also true, *E. coli*'s response to styrene appears to perhaps include the use of strategies aimed at reducing membrane permeability and further stabilizing the OM to protect the cell from styrene-induced damage.

Overall, it has often been found that the composition and structure of the OM is a strong determinant of tolerance, especially in the case of hydrophobic solvents [178,234,243,244]. One of most important regulators of OM composition is the two-component signal transduction system composed of *ompR* and *envZ* [245] (log_2 fold change for A of 0.80 and 0.51, respectively), both of whose expression was

upregulated in the case of A. One function of this system has been shown to be its ability to provide variable control over the expression of two small RNAs (sRNAs) *omrA* and *omrB* [246], as well as the OM porins *ompF* and *ompC*, which it does in response to changes including those in osmolarity, pH or temperature [247]. Activation of *omrA* and *omrB* has previously been reported following exposure to several other bioproducts, including butanol, furfural, geraniol and succinic acid [248]. OmpF, meanwhile, belongs to the General Bacterial Porin (GBP) family and facilitates the diffusion of various small (600 Da or less; note: styrene is ~104 Da) molecules (e.g., ions, antibiotics, small proteins) through the OM [249,250]. In addition to its function as a porin, meanwhile, OmpF has also been reported to impose a significant impact on membrane composition, hydrophobicity and, ultimately, solvent tolerance [251]. For example, *ompF* expression was repressed in a series of isolated mutants with enhanced tolerance to a variety of hydrophobic solvents (e.g., cyclohexane, xylene) [252]. In a follow-up study, however, *ompF*-null mutants showed no improvement in solvent tolerance [251], suggesting that its relative abundance is a key factor. However, others have utilized the deletion of *ompF* with an overexpression of *fadL*, an OM ligand gated channel, to increase integrity of the membrane and consequently improve production of fatty acids by ~53% [253]. Here, expression of *ompF* was significantly downregulated following styrene exposure (log_2-fold change = -1.89). Furthermore, translation of *ompF* has been shown to be inhibited by an increase in expression of the sRNA *micF*, which concurrently was found to be upregulated in the case of A (log_2-fold change = 2.02).

Another of the most highly upregulated genes, meanwhile, was *bhsA* (log_2-fold change = 5.03), which encodes an OM protein. Induction of *bhsA* expression has often been associated with biofilm formation, and has been observed in response to various stresses (e.g., hydrogen peroxide [186], cadmium [254] and salicylate [184]). Null mutants of *bhsA*, meanwhile, have been found to suffer from increased sensitivity to acid, hydrogen peroxide and heat treatment, while displaying upregulation of a significant number of membrane proteins and downregulation several genes encoding cell surface proteins, ultimately leading to significant increases in both cell hydrophobicity and aggregation [255]. In contrast, overexpression of *bhsA* has been shown to reduce cell surface hydrophobicity, which lead to improved tolerance to and production of octanoic acid [256]. Separately,

while investigating several *E. coli* mutants tolerant to different organic solvents (e.g., *n*-hexane, *p*-xylene, cyclohexane), it was similarly reported that the cell surfaces of the more tolerant mutants were less hydrophobic then the parent strain (K-12) [252]. While several mechanisms remain to be elucidated, these collective observations at least suggest that *E. coli* is attempting to increase styrene tolerance via a multi-level strategy designed strengthen the membrane by modifying its structure and composition while also limiting styrene diffusion into the cell.

4.3.9 Efflux Transporters

One mechanism commonly utilized by various microbes to overcome the toxicity associated with small molecules involves the use of multi-drug resistant (MDR) efflux transporters to export species across the cell membrane and into the extracellular medium [257]. One of the most well-studied families of MDR transporters, in particular with respect to solvent-like hydrocarbons, are the RND (Resistance-Nodulation-Division) efflux pumps. In particular, it was previously reported that strains lacking *acrB* exhibited inhibited growth profiles when exposed to various concentrations of styrene relative to the wild-type control [258]. In another studies, *E. coli* strains which showing improved tolerance to added toluene showed 2.8- and 5.2-fold increases in transcript levels of *acrA* and *acrB*, respectively [259]. Interestingly, however in the case of A, of all known RND efflux transporters in *E. coli*, only 1 component was DE upon styrene addition (*acrB*) and transcript levels were, in fact, reduced relative to the control ($\log_2$-fold change = -0.84). Since efflux transporters activation typically involves by a transcription factor via a toxin dosage response [260,261], it is possible that intracellular styrene levels did not surpass the characteristic minima necessary for upregulation of RND transporters under the conditions examined.

Furthermore, the long-term exposure to styrene in this case may play a role in the lack of expression of RND efflux pumps as Molina-Santiago et al. demonstrated that in a toluene-sensitive strain (*P. putida* KT2440), transcriptional changes in efflux pump expression after short-term (one hour) exposure to toluene, were of a much higher magnitude compared to the long-term (several hours) exposure [262]. Furthermore, many efflux pumps which showed no DE upon short-term exposure, were subsequently DE after long-term exposure while many of the upregulated pumps in the short-

term demonstrated no DE after long-term exposure [262]. Therefore, the expression profile seen here under styrene exposure may be quite different from that seen directly after a sudden styrene shock as cells may utilize different mechanisms to survive a short-term exposure to styrene compared to a long-term exposure. An argument could be made that the utility of RND efflux transporters as a tolerance strategy is only feasible in the short-term due to consumption of energy (i.e., ATP) for molecule export.

One accessory protein related to active efflux that was upregulated upon styrene addition (log_2-fold change = 1.43) is the 49 amino acid-long small protein AcrZ, which was found to associate with AcrB in the AcrAB-TolC complex [263]. Researchers have shown that removal of the *acrZ* gene could negatively impact the minimum inhibitory concentrations (MIC) of chloramphenicol, for example, where while deletion of *acrB* may have lowered the MIC from 8 to 1 µg/mL, deletion of *acrZ* alone reduced the MIC from 8 to 4 µg/mL [263]. Not all AcrB-dependent compounds saw enhanced toxicity upon deletion of *acrZ*, however, including erythromycin and fusidic acid. Nevertheless, it is likely that AcrZ plays a noteworthy role in the AcrAB-TolC-dependent efflux of some compounds, and it has been suggested that AcrZ perhaps aids in determining substrate specificity and may serve as an interesting target for future engineering efforts.

The transcriptional responses of other MDR transporters were analyzed and most MDR pumps were not responsive to either external exposure of styrene. The expression of genes such as *emrE*, *fsr*, *ynfM*, *emrY*, *ydiM,* and *ydeA,* which encode for transporters, was increased upon styrene external exposure. **Table 4.1** shows a list of DE genes encoding for a variety of MDR efflux pumps and other transporters of interest in *E. coli* when cells were exposed to styrene via both modes. Of transporter-encoding genes which were upregulated under both modes of styrene exposure, *ydeA* and *mdtG*, which encode for a known L-arabinose exporter and a MDR efflux pump, respectively, are of particular interest. These results may indicate that the *ydeA* and *mdtG* promoters in *E. coli* have a natural positive response to styrene exposure.

Table 4.1 Differentially Expressed Efflux Transporters upon Styrene Exposure.

List of membrane transporter-encoding genes which were up- or down-regulated for each condition comparison (A or P) along with the efflux transporter family of each gene. The log_2 fold change (L_2FC) is also listed next to each gene along with a '-' if there was no significant DE of the gene in that condition. Only genes which showed a p-value < 0.5 in at least one condition when compared to the no styrene control were included. ABC = ATP-binding cassette, MATE = Multi antimicrobial extrusion, MFS = Major facilitator superfamily, SMR = Small multidrug resistance, RND = Resistance-nodulation-cell division, OM = Outer membrane.

UP			Efflux Family	**DOWN**		
A	P	Gene		Gene	A	P
0.60	1.23	*mdlA*	ABC	*macA*	-	-1.15
				macB	-	-1.17
				mdlB	-0.59	-
-	0.93	*mdtK*	MATE			
0.59	-	*fsr*	MFS	*emrK*	-0.72	-
1.15	1.02	*mdtG*		*emrD*	-0.98	-
	0.81	*mdtH*		*yajR*	-	-0.92
1.88	0.85	*ynfM*				
0.90	-	*emrY*				
1.43	-	*ydiM*				
1.83	2.23	*ydeA*				
-	0.83	*yebQ*				
-	0.95	*yghB*				
-	0.70	*yqjA*				
0.94	-	*emrE*	SMR	*sugE*	-0.89	-
				mdtI	-0.72	-
			RND	*acrB*	-0.84	-
0.55	1.52	*ompX*	OM Porins/ Proteins	*ompW*	-1.15	-
-	1.61	*slp*		*pal*	-1.05	-0.63
-	1.14	*ompA*		*ompF*	-1.89	-2.55
0.76	1.05	*tehA*	Other Exporters	*setA*	-0.59	-
1.09	-	*rhtC*		*ybjE*	-0.62	-
1.01	1.41	*yahN*		*dauA*	-0.84	-
1.11	-	*yhjX*		*rhtA*	-0.90	-
0.80	-	*aroP*		*dcuB*	-1.08	-1.44
0.69	-	*ygaZ*		*dctA*	-	-1.05
1.83	2.23	*ydeA*		*potG*	-0.84	-
0.76	1.58	*eamA*		*manX*	-	-1.29
0.66	-	*cydC*				
1.11	-	*cydD*				
0.57	-	*yhjE*				

4.3.10 Comparing E. coli's Response to Styrene Addition versus Styrene Production

One motivation in this study was to identify similarities and differences in the transcriptional response when cells were exposed to styrene via exogenous addition versus when cells internally produced styrene. Overall, the responses identified were largely the same with slight differences. Responses such as up-regulation of phage shock response, DNA damage response and cell envelope-altering genes as well as down-regulation of ribosomal and nucleotide biosynthesis genes were consistent between the two modes of exposure.

Although, the DE profile of genes in the two modes of exposure contain many similarities in terms of responses, a difference emerged in terms of the magnitude of DE between certain gene sets in the production and addition mechanisms of exposure. As discussed in section 4.3.1, the magnitude of DE for up-regulated genes was significantly higher in P compared to A. Among genes which were up-regulated under both modes of exposure, the average $\log_2$-fold changes for P and A were 1.58 and 1.38, respectively. When analyzing specific genes, these differences can become even larger. Among the highly up-regulated genes involved in the phage shock response (i.e., *pspABCDE*, *pspG*), the average $\log_2$-fold changes for P and A were 7.33 and 5.45, respectively. This was also prevalent in terms of cellular response to DNA damage mechanisms such as the SOS response. Genes such as *recA* and *sulA* showed increased responsiveness in styrene producing cells (*recA*: P $\log_2$-fold change = 0.90, A $\log_2$-fold change = 0.46; *sulA*: P $\log_2$-fold change = 1.90, A $\log_2$-fold change = 0.86). Other genes of interest saw similar DE magnitude differences such as *marA* (P $\log_2$-fold change = 2.52, A $\log_2$-fold change = 1.08), *lpp* (P $\log_2$-fold change = 1.77, A $\log_2$-fold change = 0.70), and *micF* (P $\log_2$-fold change = 2.75, A $\log_2$-fold change = 2.02). Additionally, up-regulation of genes associated with the heat shock response seem to be more prevalent upon styrene addition as $\log_2$-fold changes were 111% and 108% higher for *ibpA* and *ibpB*, respectively, than in production strains. Additionally, while *rpoH* was up-regulated ($\log_2$-fold change = 1.48) in the addition mode of exposure, it showed no DE in cells producing styrene.

A further difference between the two conditions is seen among amino acid biosynthesis. Overall, in the KEGG pathway "biosynthesis of amino acids" (eco01230; 118 genes total), the A condition

showed 22% of genes up-regulated and 19% of genes down-regulated. Conversely, in the P condition, only 9% of genes were up-regulated while 33% of genes in this KEGG pathway were down-regulated. While the expression of genes involved in the biosynthesis of some amino acids shows a similar profile (e.g., arginine biosynthesis, phenylalanine, tyrosine and tryptophan biosynthesis), there are larger differences among others. For example, in the KEGG pathway for "valine, leucine and isoleucine biosynthesis" (eco00290; 16 genes total), seven genes (44%) were DE for the A condition, with all of them being induced upon styrene addition. However, in the P condition, only one gene was induced in this KEGG pathway while 5 (31%) were repressed.

Exposure to certain aromatic compounds (e.g., *p*-coumaric acid) has previously been shown to result in DNA binding and damage [198]. In section 4.3.2, data showing the impact of styrene exposure to *E. coli* cells on DNA damage and repair mechanisms was illustrated. However, one key difference (namely, expression of *dps*) in this regard was identified between styrene-producing cells and cells where styrene was exogenously added. Dps is an important DNA-binding protein that works to protect DNA from a variety of stresses (most critically, oxidative stress) via prevention of DNA breakage, iron sequestration and ferroxidase activity [264]. Its encoding gene (*dps*) has been reported as one the most commonly DE genes, appearing in over 70 separate transcriptomic studies investigating the effects of exposure to compounds such as isobutanol, salicylate, and a variety of acids [187,209]. Interestingly, in the present study, *dps* showed no DE for A although it was up-regulated for P ($\log_2$-fold change = 1.95). Thus, the inhibition caused by styrene exposure is not likely due to any significant effect that it has on DNA damage.

As seen in **Figure 4.2C,** there were 33 genes which showed significant DE in opposite directions for the two modes of styrene exposure. These genes, as well as the $\log_2$ fold change in each condition is listed in **Table 4.2**. One gene of note is *mepS* which encodes for a DD-endopeptidase which functions to help expand the peptidoglycan layer by abolishing current cross-links to allow for incorporation of further peptidoglycan [265,266]. This is a vital process during growth and a reduction of MepS levels in the cell can inhibit synthesis of peptidoglycan (allow it is suggested that MepM/H are redundant of MepS in *E. coli*) [265,266]. Here, expression of *mepS* was significantly

repressed upon styrene addition while induced upon styrene production (log_2-fold change of -1.94 and 1.45, respectively). The expression of *mtgA*, which encodes for a peptidoglycan glycosyltransferase [267], shows a similar profile (log_2-fold change of -0.93 and 1.44 for A and P, respectively). The enzyme MtgA works to polymerize lipid II molecules for further synthesis of peptidoglycan [268]. This interesting expression of these two genes may indicate that, in production strains, cells are actually attempting to produce and incorporate more peptidoglycan even though cell division mechanisms are seemingly shutting down.

One interesting difference between the two modes of styrene exposure involves the various cold shock proteins found in *E. coli*. Overall, components of the CspA family of cold shock proteins were found to be down-regulated in cells exposed to exogenous styrene while up-regulated in cells producing styrene (**Table 4.2**). For example, cold shock proteins encoded by *cspB* and *cspG* were up-regulated in P (log_2-fold changes of 1.44 and 1.53, respectively) while showing down-regulation in A (log_2-fold changes of -1.37 and -2.84, respectively). Further differences were seen among genes in this family such as with the cases of *cspA* (log_2-fold change = -4.17 for A, no DE for P) and *cspE* (no DE for A, log_2-fold change = 1.72 for P).

Interestingly, expression of *ompT* (which encodes for an OM protease) was slightly down-regulated in the presence of styrene in the case of A, but up-regulated in the case of P (**Table 4.2**). Others have demonstrated that expression of *ompT* is often repressed upon up-regulation of *omrA/B* [246]. However, as OmpT has also been shown to be highly abundant in strains overexpressing recombinant proteins [269,270], this discrepant behavior may be an artifact of expressing the styrene pathway in P, and be unrelated to differences in the toxic action of styrene.

Table 4.2 Genes DE in Opposite Directions upon Styrene Addition or Production.

List of genes that were DE under both modes of styrene exposure but show DE in opposite directions (compared to the control). The log_2-fold change of expression between the styrene addition (A) or styrene production (P) compared to the no styrene control strain from our RNA-seq results is listed.

	log_2-fold change	
Gene	**A**	**P**
ilvM	0.85	-3.79
ilvE	0.66	-2.76
ilvX	0.80	-2.33
metQ	0.74	-1.40
mepS	-1.94	1.45
cspG	-2.84	1.53
ompT	-0.63	1.33
patA	-1.03	1.20
yeiH	0.82	-1.17
aceB	0.66	-1.18
rstA	-1.81	1.16
uxuA	0.56	-1.08
yeaQ	-0.73	0.97
ybgS	-0.69	1.17
csrC	0.76	-2.34
csrB	1.11	-2.24
elaB	-1.49	0.86
gadB	-1.05	1.17
hdeA	-1.04	1.31
gatY	0.80	-0.79
dacC	-0.58	0.87
yoaC	-0.74	0.82
yjdN	-0.52	0.91
yodD	-1.03	0.81
mgrB	-0.88	1.51
ybgA	-0.82	0.89
ycgB	-0.73	0.73
otsB	-1.29	0.84
mnmE	0.92	-0.75
cspB	-1.37	1.44
mtgA	-0.93	1.44
tusD	0.59	-0.75
thrU	-1.48	1.06

4.4 Discussion

While the present study represents the first to report on the transcriptome-wide response of *E. coli* to styrene, others have explored the impacts of other hydrophobic solvents on *E. coli* as well as different aromatic chemicals on other microorganisms. In terms of aromatic chemicals, Jin et al. recently performed a transcriptomic analysis of *Saccharomyces cereviasiae* following 2-phenylethanol exposure [191], whereas Molina-Santiago et al. previously compared the transcriptional response of two *P. putida* strains (KT2440 and DOT-T1E) to toluene exposure [262] and Yung et al. investigated the effect of sub-lethal levels of toluene on the transcriptome of *E. coli* [188].

As a result of styrene exposure, the collective responses demonstrate that *E. coli* alters expression of numerous membrane-related functions, the likes of which likely represent a concerted effort by the cell to repair and alter the membrane composition in order to minimize direct harmful interactions with or other indirect effects of styrene. This type of survival strategy is common across bacteria. For instance, in the case of toluene exposure to *P. putida* KT2440 and DOT-T1E (toluene tolerant), whereas the more tolerant DOT-T1E strain mostly altered the expression of "intracellular parts", the more sensitive KT2440 strain differentially expressed a greater number of genes involved with a variety of different membrane functions, especially those encompassing energy generation and iron uptake [262]. As with styrene and *E. coli*, this response postulated to constitute an overall effort by the cell to alter membrane permeability and protect the cell from the membrane-damaging effects of toluene. Meanwhile, to provide the energy and material resources needed to repair, stabilize, and alter the membrane, cells must also divert and reallocate such resources from elsewhere in the cell. In the case of KT2440, it was seen that energy-intensive processes such as flagellar assembly were highly down-regulated (unlike in DOT-T1E), allowing more resources to be focused on stress management [262]. A similar picture emerged for styrene and *E. coli*, as cells seem to have worked to shut down processes which require significant energy such as cell division and nucleotide and protein biosynthesis to focus efforts on global stress responses and membrane

altering strategies. Overall, these findings underscore the importance of developing engineering strategies aimed at increasing the robustness and reducing the permeability of the cell membrane.

Accordingly, many tolerance engineering strategies have been investigated to improve the fitness of cells when exposed to solvent-like chemicals. For example, tolerance engineering has led to successful improvements in product yields such as with ethanol production in *S. cerevisiae* [271,272], as well as both limonene [257] and isopentenol [273] in *E. coli*. Furthermore, by incorporating heterologous parts from solvent-tolerant sources, tolerance of *E. coli* towards industrially relevant chemicals can be obtained. Tan et al. improved the growth rate of *E. coli* in the presence of a variety of compounds (e.g., styrene, toluene, succinate, butanol, hexanoic acid) and stresses (e.g., heat shock, osmotic pressure) by expressing the heterologous cis-trans isomerase (*cti*) from *Pseudomonas aeruginosa* [234]. This enzyme introduces the non-native process of producing trans unsaturated fatty acids into *E. coli* and incorporating this into the membrane to alter membrane properties. This group further demonstrated the utility of membrane engineering by overexpressing the native phosphatidylserine synthase (encoded by *pssA* in *E. coli*) which increased the abundance of the phosphoethanolamine head group in the membrane [237]. This change led to differences in membrane integrity and fluidity along with surface potential and hydrophobicity. Ultimately, this strain showed improved growth rates in the presence of styrene, toluene, vanilic acid, ferulic acid, 4-hydroxybenzoate and several others. These examples demonstrate the importance of identifying and developing mechanisms that can alter important membrane properties to protect cells against cell envelope-damaging compounds.

The importance of multi-drug resistant efflux transporters to maintain or improve tolerance to a variety of compounds has been shown for several organisms, including *E. coli* [69,90,92,189,257,260,261,274,275]. Furthermore, the intracellular accumulation of toxic compounds can have a significant impact on the expression of different efflux transporters by their associated hosts. For example, pumps such as AcrAB-TolC (from *E. coli*), TtgABC and SrpABC (from *P. putida*) have all been shown to become induced upon solvent exposure to minimize intracellular concentrations [276]. In the case of styrene exposure, it is difficult to isolate any single efflux transporter or system that

shows high up-regulation in the presence of styrene (at least in the long-term). Interestingly, only one member of the RND families of efflux pumps in *E. coli* showed any differential expression upon styrene exposure (i.e., *acrB*: $\log_2$ fold change of -0.84 in A). Previously, the AcrAB-TolC efflux transporter was implicated as an important part of *E. coli* growth in the presence of styrene and removal of this transporter inhibited both growth and production of styrene in NST74 [258].

Interestingly, a recent evolution of *E. coli* K-12 to improve tolerance to the aromatic acid benzoate showed that cells with higher tolerance actually lost of MDR efflux pumps (e.g., *emrA/Y, mdtEF*) and important regulators of MDR pump expression (e.g., *marRAB*) [277]. This may help indicate that specific efflux transporters are needed for improved chemical tolerance and the energy-intensive expression and subsequent placement of transporters which have limited or no activity on said chemical is ultimately counter-productive. This makes the isolation and engineering of specific efflux pumps with high activity for individual compounds of interest (such as styrene) vital to reduce toxicity through efflux transporter-mediated methods. Several examples have previously been demonstrated through the expression of heterologous RND-family efflux transporters in *E. coli* to improve the tolerance of cells to *n*-butanol [236], limonene, geraniol and others [257].

Even considering these successful examples, it may be that significant improvements in tolerance for many biochemicals (i.e., enough to allow for economically viable production levels), may not be obtained simply through expression of one, highly active and specific efflux transporter. In the toluene and styrene tolerant *P. putida* strain DOT-T1E, three main RND efflux transporters (TtgABC, TtgDEF, TtgGHI) are up-regulated upon exposure to toluene or styrene and play a role in the strain's significant tolerance to organic solvents [278,279]. Researchers found that removal of even one of these efflux systems led to at least a two order-of-magnitude reduction in cell survival [278]. Additionally, other efflux transporters in this strain have been found to play a role in DOT-T1E tolerance towards toluene [280] along with differences in fatty acid biosynthesis [281] further implicating a complex mechanism in overcoming solvent toxicity. Therefore, engineering efforts which focus on multiple strategies and genes may be the most effective method for future tolerance improvements endeavors, as has been suggested elsewhere [233].

As it will likely be important to sense and respond to membrane stress caused by styrene to improve tolerance in this case, the engineering of global regulators which can affect change in the membrane composition and properties may be useful. For example, researchers saw a 3.19-fold increase in cell viability in the presence of toxic levels of the aromatic phloroglucinol when overexpressing the chaperone-encoding *groESL* (production of phloroglucinol was also improved by 39.5% utilizing this strategy) [282]. The sigma factor encoded by *rpoE*, which responds to cell envelope stress, has previously been mutated to provide a more robust and rapid response, allowing the cell to repair defects and alter the cellular envelope composition [283]. Incorporating this mutation may be useful in improving tolerance towards membrane-damaging compounds such as styrene.

A key aspect of this study is the transcriptional analysis of long-term exposure of *E. coli* cells to styrene. This allows for better understanding of how cells are attempting to survive styrene-induced toxicity after long periods of contact. However, there is a dearth of data and knowledge regarding the temporal effects of styrene exposure. As the styrene exposure time in this study is hours, rather than minutes, only certain conclusions can be made regarding the transcriptional response of *E. coli* to styrene. It may be that responses to styrene exposure in the short-term and long-term are similar, perhaps only changing in magnitude of response. However, it may be more likely that an entirely different expression profile is observed between the two cases. In the aforementioned study regarding exposure of *P. putida* KT2440 and DOT-T1E to toluene, the transcriptional response between both short-term and long-term was analyzed for both strains [262]. In this case, the number of DE genes and the magnitude of fold change in KT2440 was higher in the short-term compared to the long-term.

Although the current dataset does not enable delineation of a clear timeline of events, several styrene-induced behaviors support a response model that includes cell envelope damage, inhibition of cell wall biosynthesis, and disruption of normal cell division. I theorize that the cells are attempting to shuttle resources and energy from a “growth” mode before styrene addition to a “survival” mode once they have been stressed. For the most part, cells reduce the expression of

genes involved in DNA and protein biosynthesis to allow the cell to focus on mechanisms necessary to stop cell death induced by styrene. Stress response systems such the phage shock response, stress-responsive sigma factors and the MarA-mediated response are all turned on to respond to the damage caused by styrene. Furthermore, by up-regulating *bhsA, ompR*, *ldtC* and the sRNAs *omrA/B* and *micF*, it is proposed that the cell is attempting to significantly alter the membrane composition, rigidity and fluidity in order to survive in the presence of styrene. By focusing on these areas, future engineering strategies to improve the tolerance of *E. coli* to aromatics such as styrene, and perhaps even other hydrophobic compounds, may prove to be successful.

CHAPTER 5. FUTURE WORK AND DISCUSSION

Abstract

Biochemical production metrics are often limited by end-product and/or intermediate-induced toxicity to the cell. At this time, for many chemicals (e.g., styrene, 2-phenylethanol, phenol), current improvements in production levels are entirely or partially impeded by low tolerance to these compounds by bacteria, especially *E. coli*. In an effort to discover mechanisms to improve the tolerance of *E. coli* to toxic aromatics, this chapter discusses potential future work to utilize a high-throughput method to isolate mutant strains which harbor increased tolerance towards compounds of interest. Additionally, proposed works will involve the engineering of a highly tolerant strain of *P. putida* (i.e., DOT-T1E), to over-produce the aromatic amino acid, L-phenylalanine, and express heterologous enzymes for the production of styrene. Further engineering efforts will focus on constructing an efficient sucrose-utilizing strain of this styrene producer to allow for improved yields and titers.

5.1 Furthering the Understanding of Aromatic Toxicity in *E. coli* and Improving Tolerance towards Aromatics Using High-Throughout Methods

There is interest in further understanding and improving the ability of *E. coli* to produce toxic aromatics and one of the first steps is comprehending how cells respond to this toxicity. While the RNA-seq results and analysis generated for Chapter 4 of this dissertation is a useful guide to understand the impact of styrene-induced toxicity in *E. coli*, it is insufficient evidence for the complete understanding of aromatic-based tolerance mechanisms in *E. coli*. This research gives a starting point for constructing a model for aromatic toxicity but certainly does not tell the whole story. More research is needed to determine which of the mechanisms induced by styrene toxicity (e.g., phage shock response, membrane alterations) are conserved over other aromatics and which are not. It is likely that there will be some overlap here but that there will be many responses that are activated upon styrene exposure but lie dormant when exposed to other aromatics and vice versa.

Towards the aim of broadening the understanding of aromatic tolerance in *E. coli*, several studies are here proposed.

5.1.1 Transcriptomic Analysis of E. coli for Various Toxic Aromatics

To better understand the broad transcriptional response of *E. coli* to a broad number of aromatic species, additional and complementary methods are needed. To this end, a previously developed GFP-based promoter library represents a useful tool. This library could be utilized to investigate the transcriptional response of specific *E. coli* genes identified from the styrene RNA-seq data obtained and analyzed in Chapter 4 from the above enrichment screens to each of various aromatic species of industrial interest (e.g., styrene oxide, 2PE, phenol, naringenin) along with controls (e.g., antibiotics, butanol, ethanol). Although, the results in Chapter 4 indicate that some native genes are up-regulated upon exposure to styrene, it is not known if, naturally, these responses are aromatic-specific or respond to other stresses.

One method that is often used to understand promoter dynamics, is the fusion of that promoter to a reporter (e.g., GFP, mCherry) and tracking the expression of that reporter under various conditions. Therefore, by fusing the promoters for each gene of interest to a reporter such as GFP and exposing the cells to various aromatics at different concentrations, the response of that promoter can easily be observed utilizing a fluorescent plate reader. Fortunately, a library of fluorescent transcriptional reporters was constructed with over 2,000 different promoters fused to GFP on a low copy plasmid [284]. A model study was done here to demonstrate utility of the library, illustrating differences in promoter activity in a glucose-lactose diauxic shift. This library allows for a more high-throughput manner of analyzing transcriptional response and can be utilized to understand promoter dynamics under aromatic toxicity conditions.

This data will provide us with information regarding the evolutionary progression of various stress response genes and how *E. coli* activates them. Genes that are "turned on" under a variety of aromatic exposure, will help to illustrate how these stress response mechanisms have evolved to help alleviate toxicity brought on by these chemicals. Alternatively, genes that show no up-regulation under these conditions may indicate that transcriptional elements that control these genes are not responsive to these aromatics but are affected by some styrene-induced stress. Styrene-responsive transcriptional elements from *P. putida* S12 have previously been identified [69] along with the regulator DmpR from *Pseudomonas* CF600 which is responsive to phenol [285].

Unfortunately, not all promoters in *E. coli* are part of this GFP library so, therefore, plasmids harboring missing promoters from this library (e.g., P_{pspA}) can be constructed (in a manner analogous to others in the library). Screening can be completed utilizing high-throughput microplate assays, where increases to induction ratio (as determined by RFUs vs. no aromatics controls and promoterless plasmids) can be used to indicate and quantify expression levels.

Furthermore, as the knowledge gained via RNA-seq regarding styrene exposure to *E.coli*, as discussed in Chapter 4, only concerns styrene exposure at one concentration and is limited to a single point in time, utilization of this library will allow for the elucidation of promoter dynamics throughout the course of culturing and with different concentrations. Furthermore, these

experiments could help determine if the up- or down-regulated genes/operons found in the Chapter 4 are consistent amongst other aromatics, different time points in culturing and varying concentrations of toxin.

5.1.2 Directed Evolution Strategies to Improve Tolerance of E. coli to Aromatics

While the utilization of such methods as adaptive laboratory evolution allows for the broad perturbation of an entire genome, it can often be a slow, labor-intensive process that necessitates the investment of many research hours [286-289]. However, as the amount of knowledge about the functionality of proteins in *E. coli* and the ways in which compounds impart toxicity onto cells is amplified, other high-throughput methods can be utilized to elucidate mechanisms by which cells can gain tolerance. One such process involves directed evolution where a single, target single (or multiple genes) are altered either randomly, or at specific sites, to generate an altered phenotype [290].

One method for directed evolution is *in vitro* replication. Here, an error-prone polymerase is utilized to perform a polymerase chain reaction (PCR) over a specific length of DNA (often, a single gene) [291,292]. Due to the low fidelity of the polymerase, mutations are inserted into the sequence. The degenerate DNA is then introduced into the strain with the desired outcome of a changes in phenotype due to a mutation. One drawback of this method is that it can be limited by transformation efficiency as the mutated DNA must be put back into the desired strain, often via a selection step. Therefore, the speed of experimentation and library size of mutations is often restricted by the transformation and selection step which can hinder the ability to obtain phenotypic changes.

In an effort to eliminate the limiting step in error-prone PCR methods, an *in vivo* strategy for directed evolution has recently been demonstrated. The method, EvolvR, generates mutations *in vivo* utilizing a nicking-variant of Cas9 (nCas9) fused to a DNA polymerase with lowered fidelity to first introduce nicks into a DNA sequence followed by nick repair via the error-prone DNA polymerase (PolI3M) [293,294]. This system allows for the user to target a specific region of their choice while diversifying the nucleotide composition over a range of DNA. In the initial study, Halperin et al.

demonstrated the utility of this system to reintroduce the resistance capabilities of the spectinomycin resistance gene after it had been inactivated with a specific mutation. By plating cells that had been subjected to EvolvR on spectinomycin plates and comparing the number of strains which harbored spectinomycin resistance to the original number of cells, a mutation rate could be determined. Here, they determined that the mutation rate of wild-type *E. coli* cells was 10^{-10} mutations per nucleotide per generations, whereas the mutation rates of cells utilizing EvolvR were calculated from 24,500-fold to 7,770,000-fold higher (depending on if mutations were incorporated into nCas9 or PolI3M) at the target DNA location. In fact, the researchers suggest that 1 µL of cells expressing the EvolvR variant, enCas9-PolI3M-TBD, for 16 hours will contain all substitution possibilities in a 60-nucleotide window with over ten-fold coverage. While the tunable window over which mutations can be generated is not long (max of 350 bp from PAM start site), the high number of mutations that can be introduced in this range and the ease by which the window can be moved simply with a change in gRNA sequence, makes this a potentially valuable tool to directly evolve bacteria cells.

To introduce mutations to improve tolerance towards a variety of aromatics, specific genes in interest in *E. coli* will be targeted for mutagenesis utilizing high-throughput methods – chief among them, the EvolvR technique. As the EvolvR technology is relatively new in the biotechnological landscape, this will represent a novel use and may have implications for its utility in future tolerance engineering endeavors. By combining the high-throughput aspects of EvolvR with the growth-based selection process utilized to identify strains with improved tolerance, novel mutations will be identified which can help improve understanding of bacterial aromatic toxicity and mechanisms through which microbes survive. Plasmid parts of the EvolvR system are available on Addgene (pEvolvR-enCas90PolI5M – ID113078 and pEvolvR-enCas90PolI5M-TBD – ID113077) and will be purchased. The targeting gRNA part of this plasmid will be constructed for each separate gene target utilizing CPEC (Circular Polymerase Extension Cloning) [295]. A basic outline for the proposed protocol is illustrated in **Figure 5.1**. This will involve transformation of EvolvR plasmid with designed gRNA(s) expressed targeting region(s)/gene(s) of interest. The EvolvR system will be induced to generate a library of genetic variants. These variants will then be subjected to serial

transfers of increasing chemical (e.g., styrene) concentrations to kill any cells which have neutral or deleterious effects and eventually isolate those mutants which provide beneficial traits to the cells when exposed to the toxic compound (e.g., styrene). Variants can then be sequenced and tested further in terms of improving cell viability and growth as well as various structural protein changes that may be of interest to investigate.

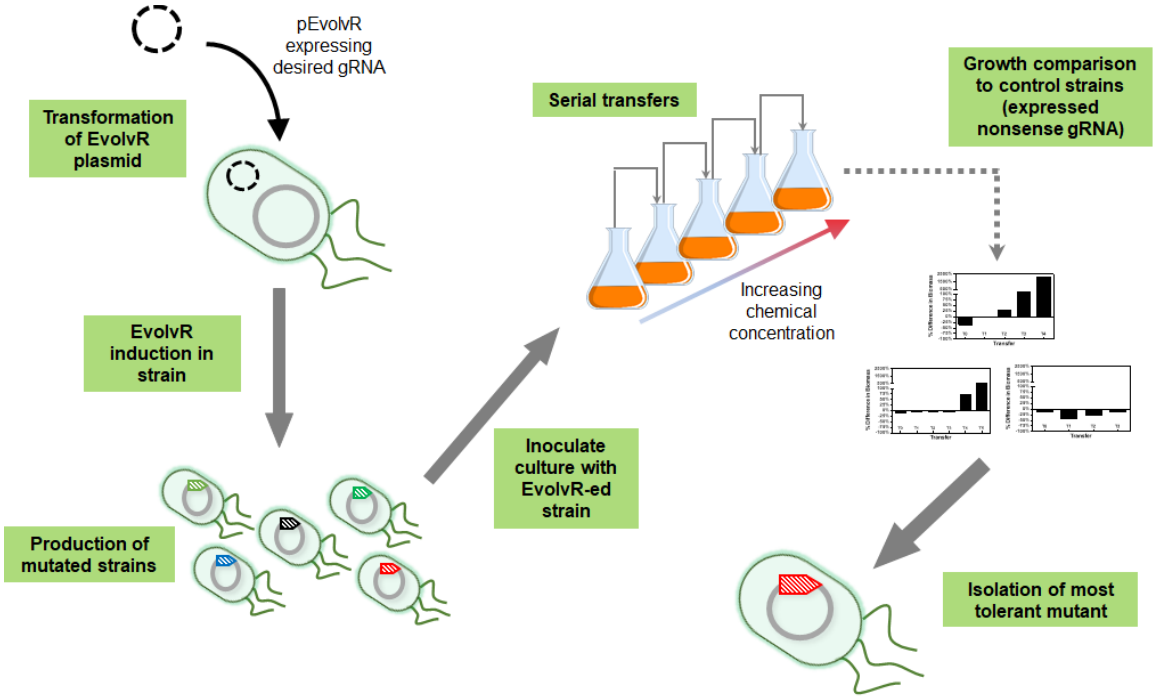

Figure 5.1 Proposed Protocol for Utilization of EvolvR System to Identify Genetic Mutants which Improve Tolerance to Biochemicals.

Procedure to utilize EvolvR to identify useful mutations that improve the tolerance of strains towards toxic chemicals of interest. This involves transforming the desired strain with the pEvolvR plasmid containing a gRNA targeting a gene of interest. Then, EvolvR will be induced and mutated strains will be exposed to the toxic compound, followed by growth and serial transfers in increasing concentrations of the toxin. Mutated strain growth will be compared to a control (e.g., strain harboring pEvolvR plasmid with a nonsense gRNA) followed by isolation and sequencing of useful mutants.

In Chapter 4, several genes were identified via RNA-seq which may serve an important role in the survival of *E. coli* to styrene. While not comprehensive or necessarily applicable to all aromatics, a survey of these genes will serve as a starting point for genes to target for mutagenesis. As these genes were identified in a screen against styrene, and styrene represents an important chemical upon which production in *E. coli* has reached near toxicity limits, it will serve as the initial compound

for screening this method. However, as this tool can be utilized for the entire genome in *E. coli*, this procedure could be optimized for other compounds such as antibiotics (to better understand mechanisms behind antibacterial resistances) and industrially relevant biochemicals (in efforts to improve tolerance and production).

Table 5.1 Genes to Investigate with EvolvR to Improve *E. coli* Tolerance Towards Styrene.

List of genes of interest identified in RNA-seq results of styrene-exposed cells. The length of gene in terms of bp in E. coli is listed along with regions of interest in the gene (as identified by UniProt [296]) and the functionality of the gene product in E. coli.

Gene Name	Gene Length (bp)	Regions of interest (#'s are bp from gene start)	Functionality
rpoE	576	144 -> 183 (Polymerase core binding)	Sigma Factor E
rpoH	855	159 -> 366 (Sigma-70 factor domain-2)	Sigma Factor H
pdhR	765	111 -> 168 (DNA binding region)	Transcriptional dual regulator
omrA	88	None	sRNA affecting outer membrane composition
omrB	82	None	sRNA affecting outer membrane composition
micF	93	None	sRNA affecting outer membrane composition
ompR	720	405 -> 702 (DNA binding region)	Member of EnvZ-OmpR signal transduction system; responsive to osmotic stress
marA	384	87 -> 150, 231-> 300 (DNA binding regions)	Stress responsive transcriptional regulator
soxS	324	72 -> 129 (DNA binding region)	Transcriptional dual regulator related stress response (e.g., superoxide, antibiotics)
acrR	648	99 -> 156 (DNA binding region)	Transcriptional repressor related to multidrug transport
fadR	720	102 -> 207 (DNA binding region); 645 -> 690 (acyl-CoA binding region)	Transcriptional dual regulator related to fatty acid degradation
lexA	609	84 -> 144 (DNA binding region)	Transcriptional repressor related to SOS response
rcsB	651	504 -> 561 (DNA binding region)	Transcriptional activator related to the Rcs-phosphorelay system
bhsA	258	1 -> 66 (Signal peptide)	Stress responsive outer membrane protein
pspA	669	None	Phage shock protein
acrZ	150	None	small protein affecting AcrAB-TolC

A potential list of genes is listed in **Table 5.1** along with the length of gene and the functionality of the gene product in *E. coli*. Furthermore, as the most effective mutation window of EvolvR is ~60 nucleotides, and many of genes selected are multiple folds longer than this window, judicious choice of PAM site is critical. Towards this end, some important enzymatic functionality sites are listed in **Table 5.1** as potential locations in the gene where mutations may produce the largest phenotypic impact. Additionally, it is proposed that multiple windows be targeted in each gene listed here (either in parallel strains or simultaneously in the same strain) in an effort to ensure significant coverage in each gene.

Of the genes listed, many are global regulators (e.g., *rpoE, rpoH*), specific transcriptional regulators (e.g., *marA, ompR*) or sRNA's (e.g, *omrAB*) and thus, it is more likely that changes in these genes will have wide ranging effects on all aspects of the cell. As it is probable that significant improvements in *E. coli* tolerance will arise from a broad change in cellular activity, rather than a deletion or mutation in one enzyme or transporter, the potential for full scale changes resulting from mutations in a regulator increases the chances of developing phenotypic changes which will improve tolerance. While chances are improved to isolate mutants with improved tolerances using these regulators, the task of determining the exact biochemical cause of phenotype changes is rendered more difficult. As these regulators affect the expression of many genes in *E. coli*, it may be necessary to utilize further RNA-seq or qPCR studies (compared to the wild-type control) to understand the total impact of these changes. To hedge against potential difficulties that may arise here, some genes whose products have fewer global effects will be investigated (e.g., *pspA*, *acrZ*).

5.1.3 Directed Evolution of Small Protein AcrZ for Modified Substrate Specificity of E. coli Efflux Pump AcrAB

One gene of interest that will be further investigated utilizing mutagenesis to explore changes in phenotype is *acrZ*. Many proteins exist that directly impact the translation and integration of efflux pumps into the membrane as well as substrate specificity/activity of these transporters (e.g., transcriptional regulators such as MarA and SoxS in *E. coli*) [69]. AcrZ is one of these proteins which was recently discovered in *E. coli* and was found to associate with AcrB in the AcrAB-TolC complex

as seen in **Figure 5.2** [263]. This 49 amino acid-long small protein (*E. coli* contains ~60 known small proteins [297]) is highly conserved among enterobacteria such as *Shigella* and *Klebsiella* sp and maintains a helical transmembrane domain. Additionally, transcription of *acrZ* is regulated by the same proteins as *acrAB* and *tolC*, namely, MarA, Rob and SoxS [263].

Furthermore, researchers showed that removal of the *acrZ* gene could negatively impact the minimum inhibitory concentrations (MIC) of several compounds. Concerning chloramphenicol, for example, while deletion of *acrB* may have lowered the MIC from 8 to 1 µg/mL, deletion of just *acrZ* alone reduced the MIC from 8 to 4 µg/mL [263]. Not all AcrB-dependent compounds saw enhanced toxicity upon deletion of *acrZ*, however, including erythromycin and fusidic acid. Nevertheless, it is apparent that AcrZ plays a noteworthy role in the AcrAB-TolC-dependent efflux of some compounds, and it has been suggested that AcrZ perhaps aids in determining substrate specificity. Researchers proposed two methods of action for AcrZ-mediated efflux activity – firstly, the binding of AcrZ confers conformational changes in AcrB, causing alterations in substrate specificity or secondly, AcrZ cooperates with other AcrB-interacting proteins to deliver chemicals to AcrAB-TolC for further efflux. Additionally, I believe that AcrZ may have an important role in mediating tolerance of certain aromatics such as styrene. In transcriptome-level experiments presented in the next chapter, expression of *acrZ* was up-regulated when exposed to styrene (log_2-fold changes ranging from +1.43 to +1.78 depending on the mode of exposure).

With the goal of further investigating the role of AcrZ in bacterial tolerance, I propose to use EvolvR to examine if AcrZ-derived mutants with improved specificity towards aromatic substrates can be isolated. As AcrZ is such a small protein (49 amino acids long), the number of iterations needed to cover a large part of the fitness landscape is relatively small. Firstly, Δ*acrZ* strains will be tested against wild-type strains to assess tolerance to a variety of aromatic chemicals such as styrene, 2-phenylethanol and phenol. Plasmid-based expression of *acrZ* will then be tested with chemicals that show enhanced sensitivity in the Δ*acrZ* strain, to test if native tolerance levels can be restored via plasmid-based complementation. Here, induction levels will be titrated to 1) analyze the effect of variations in AcrZ expression levels and 2) determine the optimal induction level that allows for

similar tolerance for most compounds. Finally, EvolvR will be utilized to generate a genomic "library" of *acrZ* mutants which will subsequently be used to screen for tolerance improvements.

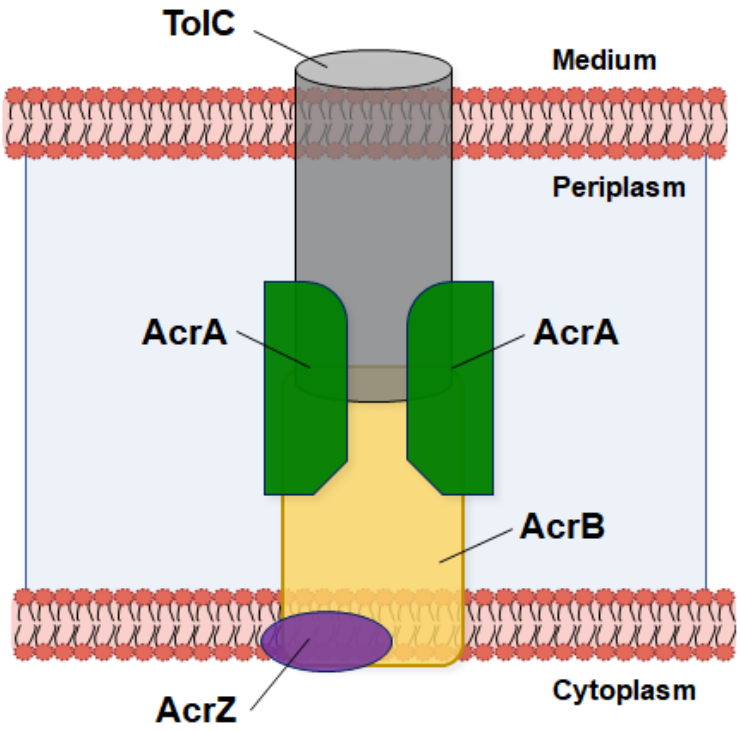

Figure 5.2 Interaction of AcrZ with the AcrAB-TolC Efflux Pump in *E. coli*.

As the desired phenotype is directly tied to improved growth under otherwise inhibitory conditions, enrichment screens with serial dilutions will be utilized. Controls will include: 1) Δ*acrZ* mutant strain and 2) wild-type *E. coli*. Ideally, cells harboring the *acrZ* "library" will display improved growth at inhibitory concentrations relative to both of these controls. Following enrichments, mutants will be isolated and sequenced to determine which *acrZ* mutations confer improved tolerance. As not much is known regarding AcrZ and its role in substrate specificity, these enrichments can be applied to toxins beyond the aromatic class such as antibiotics and compounds that have been linked to AcrAB-TolC mediated efflux (e.g., 1-hexene [258] and octane [298]). If AcrZ is indeed directly tied to substrate specificity of AcrAB-TolC, this screen may help to identify mutants which can shift the activity of the efflux pump from one chemical class to another. Additionally, another protein, YajC (part of the SecDF-YajC complex), was found to interact with AcrB, although, the extent of its

effect on bacterial tolerance was not examined thoroughly (strains harboring Δ*yajC* mutants showed decreased tolerance to β-lactam antibiotics) [299]. Depending on time constraints and the success seen by evolving AcrZ, further directed evolution of YajC may be investigated.

5.2 Engineering of a Solvent Tolerant Organism as a Host for Aromatic Bioproduction

With end-product toxicity representing a significant bottleneck in production of many industrially relevant chemicals, the previous sections of this chapter have focused on the engineering of *E. coli* for improved fitness when exposed to these compounds. Due to its ease of genetic manipulation and the demonstration of high levels of bioproduction in *E. coli* strains, it is sensible to explore avenues to enhance tolerance in these strains. On the other hand, there are bacterial species that have naturally evolved to grow in toxic environments and thrive in the presence of many solvents. Rather than engineering tolerance in product-making strains, pathways can be constructed in strains that already have high tolerance. As microbial tolerance is almost always not strictly limited to one mechanism (e.g., efflux pumps, membrane stabilization), but rather a multitude of factors, utilizing an already tolerant host for bioproduction is often the better path forward [300].

Perhaps the most well-known species of aromatic-tolerant microorganisms is the soil bacterium, *Pseudomonas putida*. Many strains of this species that thrive when exposed to a variety of solvents have been isolated, such as a strain of *P. putida,* IH-2000, which can grow in up to 50% (v/v) toluene (most bacteria cannot grow in higher than 0.3% (v/v) toluene) [301]. For many of these strains, efflux pumps play a crucial role, especially those in the RND family. The three RND complexes of note are TtgABC, TtgDEF and TtgGHI and are found in various combinations in different strains of *P. putida*. The solvent tolerant strain DOT-T1E[278] has all three while F1 has two (TtgABC and TtgDEF) and KT2440 only has one (TtgABC) of the three [301]. There seems to be significant variation in the transcriptional response of these strains when exposed to toluene, for example. With DOT-T1E, ~54% of the up-regulated genes under toluene exposure are not part of the core *P. putida* genome indicating that accessory proteins and their response under stressful conditions play a major role in solvent tolerance [301]. Additionally, many of these strains can utilize these solvents as a carbon source such as *P. putida* S12 which maintains the *styABCDE* operon,

allowing for styrene to be catabolized, providing the cells with carbon as well as reducing concentrations of the toxic solvent [125,302].

The utilization of *P. putida* as a chassis for production of industrially relevant biochemicals has recently garnered significant interest. While the use of *E. coli* and *S. cerevisiae* is much more prevalent in biochemical production processes due to the fast growth and breadth of knowledge regarding each species, the exploitation of *P. putida* has some advantages. As a bacterium isolated from soil, many *P. putida* strains have faced stresses and toxins from their naturally surrounding environment that make these members of these species tolerant to a variety of toxic compounds. Additionally, while not nearly at the levels of those for *E. coli*, a wide array of genetic tools has been developed for use in *P. putida* [303]. These include inducer-based expression systems such as NahR/P_{sal} (induced by salicylate) [304], MtlR/P_{mtlE} (induced by mannitol) [305] and more common systems such as LacI/P_{lac} [306] and P_{T7} [307] (induced by IPTG). Further genetic tools, such as the utilization of plasmids for gene overexpression [308] and the ability to "knockout" genes utilizing I-SceI [309,310] have been demonstrated as well as a method to incorporate heterologous expression cassettes onto the chromosome of *P. putida* via yTREX [311]. Furthermore, the incorporation of CRISPR/Cas9-based tools into the *P. putida* toolbox has led to other metabolic engineering strategies being possible including targeted chromosomal mutagenesis [312], targeted down-regulation [313,314] and plasmid curing [315]. The review by Martínez-García and Lorenzo outlines some of the recent advances in this field [316].

The continuous development and demonstration of genetic tools for *P. putida* engineering purposes has led to the established production of a variety of biochemicals. As many strains of *P. putida* are tolerant to aromatics and maintain aromatic-degrading mechanisms, a vast number of aromatic production studies have been demonstrated. One of the earliest uses of *P. putida* to produce aromatics was by Wierckx et al., engineering *P. putida* S12 for the production of phenol from glucose [26]. Here, a heterologous tyrosine phenol lyase from *Pantoea agglomerans* was expressed via plasmid to convert tyrosine into phenol. Then, flux towards tyrosine was improved via overexpression of *aroF-1* and random mutagenesis by introducing anti-metabolites for

phenylalanine and tyrosine. In batch culture, up to 1.5 mM phenol was produced while fed-batch runs led to accumulation of up to 5 mM phenol (~320 mg/L phenol; at this concentration, end-product toxicity limited further production). Additionally, researchers produced 1.73 g/L 4-hydroxybenzoic acid via the endogenous metabolite chorismate from glucose in *P. putida* KT2440 [317]. To improve flux towards chorismate (and ultimately, 4-hydroxybenzoic acid), the feedback resistant mutant of 3-deoxy-D-arabino-heptulosonate-7-phosphate synthase from *E. coli* (*aroG*^{D146N}) was overexpressed and the E4P supply was improved via deletion of *hexR*, a negative repressor of glucose metabolism. In *P. putida* S12, Verhoef et al. demonstrated the production of *p*-hydroxystyrene from glucose by expressing *pal* and *pdc* from *Rhodosporidium toruloides* and *Lactobacillus plantarum,* respectively [318]. These are just a few of the examples of bioproduction in *Pseudomonads* with many more referenced and discussed in section 1.3.3 of this dissertation.

5.2.1 Engineering of Pseudomonas putida DOT-T1E for the Production of Styrene

As DOT-T1E is a highly tolerant strain when exposed to aromatics such as toluene and styrene [319] and has no known styrene degradation mechanism, it is an attractive option to produce styrene. Some work has already been done to engineer DOT-T1E for the production of phenylalanine through toxic analog mutation, deletion of off-stream pathways and overexpression of feedback-resistant mutant enzymes in the phenylalanine production pathway [308]. Here, ~870 mg/L phenylalanine was produced from 1.5% (v/v) glucose in minimal media and the introduction of heterologous enzymes allowed for the production of 180 and 200 mg/L 2-phenylethanol and *trans*-cinnamic acid, respectively. Additionally, researchers demonstrated the enhanced tolerance of DOT-T1E to other aromatics of interest with 2-, 2-, 4- and 2- times higher MICs compared to *E. coli* (DH5α) for phenylalanine, 2-PE, phenylacetaldehyde and *trans*-cinnamic acid. While the titers obtained are not high compared to similar production in other organisms, these production levels are not near reaching completely inhibitory levels for *P. putida* or *E. coli*.

Towards the end of further demonstrating the potential of *P. putida* for efficient bioproduction, DOT-T1E will be engineered to first, overproduce the native aromatic precursor, L-phenylalanine, and second, introduce heterologous pathway enzymes to produce styrene, serving as a model for other

toxic aromatics. As styrene has a much lower toxicity limit (~300 mg/L) in *E. coli* and toxicity is likely the main bottleneck for improved production in this organism, transferring the styrene production pathway to DOT-T1E has high potential benefits. Additionally, previous researchers in the David Nielsen lab attempted to engineering *P. putida* S12 to overproduce styrene, however, deletion of the gene encoding the first step in styrene degradation, *styA*, removed any tolerance advantages it maintained over *E. coli* production strains (data not shown). This may indicate that the improved tolerance of *P. putida* S12 to styrene is mostly (or fully) due to the styrene degradation machinery in this strain. As DOT-T1E has no known styrene degradation-encoding genes, it is likely that tolerance is due solely to structural differences in DOT-T1E compared to other strains and is a superior potential host for styrene production. **Figure 5.3** shows the metabolism of aromatic amino acids (with specific details regarding phenylamine) as well as inherent phenylalanine catabolism processes present in DOT-T1E.

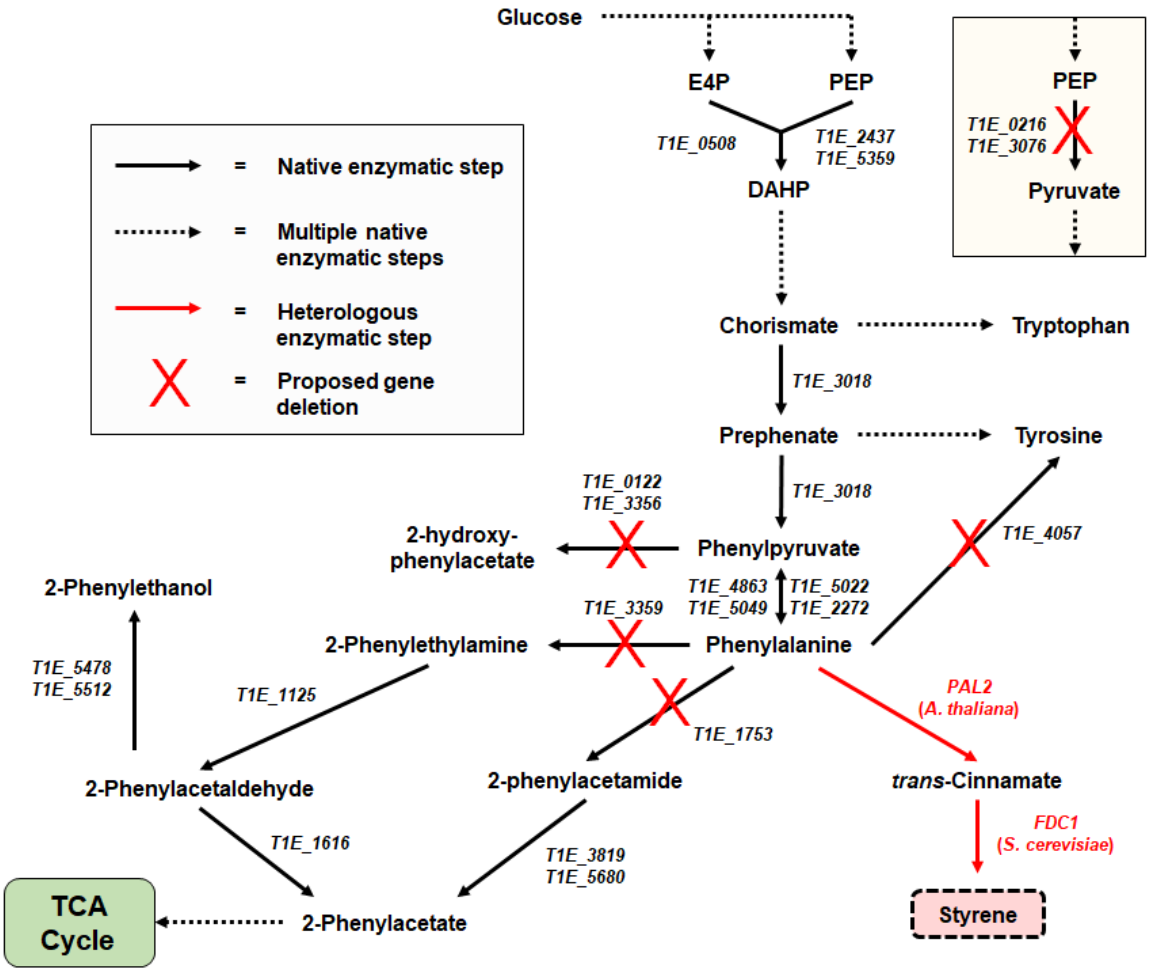

Figure 5.3 Pathway Map of Phenylalanine Biosynthesis and Metabolism in *P. putida* DOT-T1E.

A pathway map for P. putida DOT-T1E for aromatic amino acid biosynthesis and metabolism. Native enzymatic steps are shown as black arrows while proposed heterologous steps towards styrene production are shown as red arrows with proposed genes (and sources) listed. Genes which, upon deletion, it is believed will enhance to production of phenylalanine are shown with a red 'X' listed on the enzymatic step arrow. The insert in the upper right corner illustrates an enzymatic step for pyruvate kinase in central metabolism which is proposed to be deleted.

As phenylalanine is catabolized through several reactions in DOT-T1E, flux from phenylalanine to 2-hydroxy-phenylacetate, tyrosine and phenylacetamide must be reduced or removed. This includes the deletion of at least 5 genes in DOT-T1E: T1E_0122 and T1E_3356 (products catalyze the reaction from phenylpyruvate to 2-hydroxy-phenylacetate), T1E_1753 (product catalyzes the reaction from phenylalanine to phenylacetamide), T1E_1616 (product catalyzes the reaction from phenylacetaldehyde to phenylacetate) and T1E_4057 (product catalyzes the reaction from phenylalanine to tyrosine). Previously, Molina-Santiago et al. deleted these 5 genes from a DOT-

T1E mutant to improve production of phenylalanine by ~45% [308]. **Figure 5.3** shows the enzymatic deletions that will be investigated in DOT-T1E to enhance flux towards phenylalanine (and ultimately, styrene) along with the genes that produce enzymes associated with those reactions.

Other enzymes which consume phenylalanine will also be investigated and, if found, subsequently deleted. One reaction pathway of note is that from phenylalanine to phenylethylamine which can further be converted into phenylacetate. This will encompass one method to improve production of phenylalanine. Previous studies have made significant usage of toxic anti-metabolites (e.g., *p*-fluoro-DL-phenylalanine) along with chemical-induced mutagenesis to produce mutants which exhibit higher than normal levels of aromatic amino acids [26,308]. Additionally, through overexpression of genes encoding for limiting pathway enzymes (as well as feedback resistant mutants of such enzymes) such as *aroG* [317], further improvements in flux towards aromatic amino acid biosynthesis have been made. The incorporation of these methods into a phenylalanine overproducing strain of DOT-T1E will be investigated. **Figure 5.4** illustrates some of the methods that will be utilized to produce this strain.

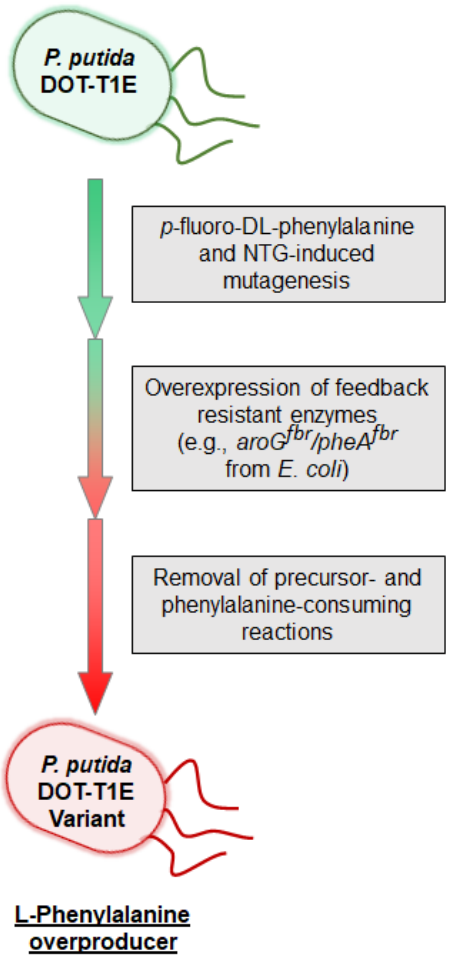

Figure 5.4 Overview of Procedure to Engineer *P. putida* DOT-T1E to Overproduce Phenylalanine. *The proposed procedure to develop a phenylalanine overproducer from DOT-T1E. Three strategies will be used which are shown in the grey boxes.*

While previous studies have demonstrated the enhanced tolerance of DOT-T1E towards styrene [319], further toxicity assays will be done to confirm previous results and investigate the effect of styrene on DOT-T1E in production-like conditions. Additionally, a comparison between wild-type DOT-T1E and the mutants engineered for enhanced phenylalanine production will be completed to investigate changes in tolerance towards styrene and other aromatics of interest (e.g., 2-phenylethanol, phenol). Further studies will be done to investigate the capacity of DOT-T1E (and its mutants) to catabolize important compounds in the biosynthesis of styrene (i.e., phenylalanine, *trans*-cinnamate, styrene). If degradation of any of the above compounds is observed, further

studies into possible enzymatic reactions which consume these compounds will be done and identified genes will be deleted.

Subsequently, *PAL2* from *A. thaliana* or *FDC1* from *S. cerevisiae* will be overexpressed in the final phenylalanine production strain to investigate the efficiency of conversion of phenylalanine to *trans*-cinnamate (for PAL2) and *trans*-cinnamate to styrene (for FDC1). Here, cells will be grown up expressing the heterologous enzyme and then resuspended in PBS buffer. Precursor (phenylalanine or *trans*-cinnamate) will be fed to cells and conversion will be tracked over time. This will allow for the confirmation of proper enzymatic expression in the cells. Additionally, utilizing random mutagenesis or codon-optimization strategies for *P. putida*, variants of each enzyme can easily be interrogated to achieve improved conversion. Once discovery of the most effective enzyme variant for each heterologous pathway is confirmed, both genes will be introduced in the production strain via several methods – overexpression via both heterologous (e.g., T_7, lacI/P_{lac}) and native (e.g., XylS/P_m, NahR/P_{sal}) expression systems using both plasmid-based expression and chromosomal integration strategies.

5.2.2 Utilization of Alternative Substrates for Styrene Production in P. putida DOT-T1E

The usage and development of tools for catabolizing alternative feedstocks is a significant field of study in the quest to make bioprocesses cost-effective and economical. Significant work has gone into demonstrating this for *E. coli* and *S. cerevisiae*, where cells have been engineered to introduce and/or improve utilization a variety of feedstocks such as starch [320], cellulose [321], lactose [322], sucrose [160,323], xylose [154], glycerol [324], and fructose [325].

While the utilization of glucose for biochemical production in *P. putida* has dominated, there is significant interest in incorporating alternative feedstocks. In fact, there are many studies which have illustrated the potential of utilizing other substrates as carbon sources. One such example is that of glycerol which has been used as a feedstock for *P. putida* fermentations due to its low cost and fewer carbons which need to be oxidized compared to glucose [326]. Kenny et al., for example, utilized glycerol to produce up to 6.3 g/L polyhydroxyalkanoate (PHA) in a fed-batch scenario in the *P. putida* strain GO16 [327]. PHA has been one of the most widely produced compounds from

glycerol in *P. putida* strains due to the fact that many *Pseudomonads* already produce PHA naturally and the structure of the monomer can be tuned depending on the carbon feedstock selection and availability [328,329]. Meanwhile, the demonstration of glycerol-conversion to aromatics of interest in *P. putida* strains has also been accomplished. Utilizing fed-batch principles, up to 1.8 g/L *p*-hydroxybenzoate was produced at a molar carbon yield of 8.5% from glycerol in *P. putida* S12 [330] while phenol has also been produced (0.4 g/L) in a *Pseudomonas taiwanensis* strain from glycerol [30].

One carbon source of high interest to the viability of future microbial bioproduction endeavors is sucrose (a disaccharide composed of one fructose residue and one glucose residue). As one of the major byproducts of the sugar industry, sucrose is inexpensive and there are vast, unused amounts available for biochemical conversion processes [331,332]. Furthermore, it can easily be fed to microbes as either the raw juice from sugarcane or as refined molasses (via sugar production) [160,333]. While *P. putida* is unable to naturally metabolize sucrose, previous studies have shown the high potential of using sucrose for bioproduction as theoretical yields for the production of rhamnolipids were higher for sucrose compared to glucose [334]. Therefore, Löwe et al. worked to engineer *P. putida* to metabolize sucrose by incorporating sucrose-utilizing enzymes from *E. coli* W [331]. The genes *cscA* and *cscB* (encoding for a sucrose hydrolase and permease, respectively) from *E. coli* W were expressed in *P. putida* KT2440 to allow for metabolization of sucrose into central metabolism. However, the growth rate of this engineered strain on sucrose was significantly lower than on a mixture of glucose and fructose (0.27 and 0.45 h^{-1}, respectively). Therefore, to improve sucrose utilization rates, Löwe et al. demonstrated another method to introduce sucrose into the metabolism of *P. putida* [335]. Here, researchers identified a sucrose-utilizing gene cluster from *Pseudomonas protegens* Pf-5 which was composed of four genes named *cscR* (AKA PFL_3236; encoding for a repressor of genes encoding for sucrose-utilizing proteins), *cscA* (AKA PFL_3237; encoding for a sucrose hydrolase), *cscB* (AKA PFL_3238; encoding for a sucrose/H^+ symporter) and *cscY* (AKA PFL_3239; encoding for a sucrose-specific porin) [335]. The gene cluster from *P. protogens* Pf-5 as well as the functionality of the gene products in *P. putida* metabolism are shown in **Figure 5.5**. Compared to the *E. coli*-derived sucrose utilization system, the *cscRABY*

system allowed for much higher growth rates on sucrose. Furthermore, the importance of the porin for sucrose metabolism was here demonstrated (when *cscY* was absent, growth rates decreased significantly) as researchers hypothesized that the outer membrane of *P. putida* was not permeable to sucrose. Unlike *E. coli*, which has broad-spectrum porins (e.g., OmpC, OmpF), porins in *P. putida* are more specific and less permeable which may account for the high level of solvent tolerance present in *Pseudomonads* [336].

Utilizing similar methods to those implemented by Löwe et al. in the aforementioned study [335], sucrose metabolism will be incorporated in the phenylalanine overproducing variant of *P. putida* DOT-T1E constructed in section 5.3.1 above. This will involve cloning the sucrose metabolism gene cluster from *P. protogens* Pf-5 into a plasmid suitable for *P. putida* (e.g., pSEVA221) for initial examination of whether or not this system will function in the engineered DOT-T1E strain. Following initial testing, the gene cluster will be transferred to a plasmid which can easily be manipulated to incorporate this cluster onto the genome. This can be done via conjugation methods with DNA transfer from *E. coli* [335] or utilizing a recent method to incorporate heterologous expression cassettes onto the chromosome of *P. putida* with yTREX, as previously mentioned [311]. Once onto the genome, the effect of the presence of the gene cluster will be compared to expression from the plasmid to evaluate differences in growth rate and sugar consumption. Additionally, comparisons between the two scenarios will be evaluated for phenylalanine production titers and yields. Furthermore, these metrics will be utilized to compare the engineered phenylalanine-overproducing DOT-T1E strain for production on sucrose versus other carbon sources, especially glucose.

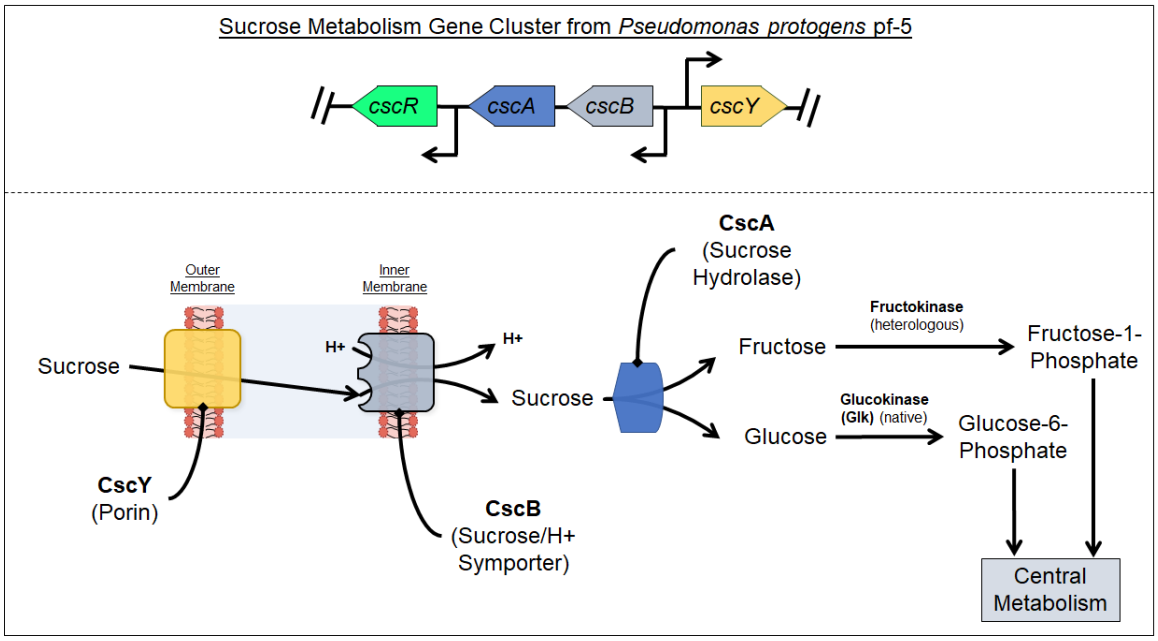

Figure 5.5 Sucrose Metabolism Gene Cluster *cscRABY* from *P. protogens* pf-5 and Potential Metabolism of Sucrose with CscRABY in *P. putida* DOT-T1E.

(Top) The sucrose-utilizing operon(s) cscRABY from P. protogens pf-5 is shown. (Bottom) The proteins and enzymes encoded by cscRABY are shown when implemented in DOT-T1E. The cscY encodes for a sucrose-specific porin, cscB encodes for a sucrose/H⁺ symporter, cscA encodes for a sucrose hydrolase, cscR encodes for a regulator of the previous three genes. The mechanism to uptake fructose and glucose into central metabolism in this strain is also shown utilizing a heterologous fructokinase and native glucokinase, respectively.

Additionally, further engineering efforts can be done to improve sucrose utilization in *P. putida.* One phenomenon of interest observed by Löwe et al. was the accumulation of fructose in the culture media during cell growth [335]. This supports the fact that *P. putida* has no known fructokinase activity (although it does maintain a native glucokinase) and can only incorporate fructose into the metabolism via a native phosphotransferase system [336]. Therefore, to uptake fructose into central metabolism, it must first be exported outside the cell, before it can then be imported via the fructose-PTS system [336]. This is undesirable for two reasons: 1) the process of first importing sucrose, hydrolyzing it into fructose and glucose, exporting the fructose and then importing it is an inefficient process and 2) the utilization of PEP in the fructose-PTS system for fructose import limits the availability of PEP that can be converted into phenylalanine. Therefore, to improve utilization of fructose derived from sucrose hydrolyzation, I propose implementing a heterologous fructokinase into the engineered DOT-T1E strain. In the sucrose-utilizing gene cluster in *E. coli* W, the gene

cscK encodes for a fructokinase which could be expressed in *P. putida* DOT-T1E alongside the *cscRABY* gene cluster to efficiently import fructose into the central metabolism. **Figure 5.5** illustrates the full metabolism of sucrose into central metabolism in DOT-T1E upon expression of *cscRABY* along with a functional fructokinase (e.g., *cscK*). The expression of these genes in a phenylalanine overproducing variant of DOT-T1E will allow for efficient utilization of the inexpensive feedstock sucrose to produce phenylalanine and demonstrate the utility of sucrose as a valuable potential carbon source for future efforts to produce value-added aromatics in *P. putida*. Alternatively, *cscRABY* and fructokinase gene can be placed into the native DOT-T1E strain before phenylalanine engineering strategies are utilized. By incorporating sucrose importing genes both before and after the engineering of phenylalanine over-production, the most efficient utilizer of sucrose and producer of phenylalanine can be isolated.

5.3 Conclusions

The above proposed works demonstrate the potential to utilize synthetic biology and metabolic engineering principles and strategies to overcome end-product-induced toxicity. By utilizing high throughput methods to engineer and isolate mutants of strains (e.g., *E. coli* NST74) which already maintain the capacity to highly produce industrially relevant compounds (or intermediates for those compounds), inherent stress response mechanisms in these strains can be improved upon to allow for enhanced tolerance and production metrics. Alternatively, strains which already possess the capacity to be highly tolerant to these compounds (e.g., *P. putida* DOT-T1E) can be engineered to over-produce important biochemicals such as styrene. By utilizing both methods in parallel, there is a greater chance for success. Through tolerance engineering strategies, greater knowledge can be gained about native mechanisms to overcome toxicity and what systems may have the most impact on tolerance towards toxic compounds. By using metabolic engineering strategies, highly tolerant microbes can not only be engineered to produce deadly biochemicals in large quantities, but greater insight on best practices to engineer lightly used strains such as DOT-T1E and further understanding strategies to broadly allow these types of strains to become versatile chassis for biochemical production can be gained.

REFERENCES

1 van Haveren J, Scott EL, Sanders J. Bulk chemicals from biomass. *Biofuel Bioprod Bior*. **2**(1):41-57 (2008).

2 King, J., Edgar, S., Qiao, K. & Stephanopoulos, G. Accessing Nature's diversity through metabolic engineering and synthetic biology. *F1000Research*, doi:10.12688/f11000research.17311.12681, doi:doi:10.12688/f1000research.7311.1. (2016).

3 Smanski, M. J. *et al.* Synthetic biology to access and expand nature's chemical diversity. *Nat Rev Microbiol* **14**, 135-149, doi:10.1038/nrmicro.2015.24 (2016).

4 Wang, J., Shen, X. L., Rey, J., Yuan, Q. P. & Yan, Y. J. Recent advances in microbial production of aromatic natural products and their derivatives. *Appl Microbiol Biot* **102**, 47-61, doi:10.1007/s00253-017-8599-4 (2018).

5 Thompson, B., Machas, M. & Nielsen, D. R. Creating pathways towards aromatic building blocks and fine chemicals. *Current opinion in biotechnology* **36**, 1-7, doi:10.1016/j.copbio.2015.07.004 (2015).

6 Noda, S. & Kondo, A. Recent Advances in Microbial Production of Aromatic Chemicals and Derivatives. *Trends Biotechnol* **35**, 785-796, doi:10.1016/j.tibtech.2017.05.006 (2017).

7 Gosset, G. Production of aromatic compounds in bacteria. *Current opinion in biotechnology* **20**, 651-658, doi:10.1016/j.copbio.2009.09.012 (2009).

8 Rodriguez, A. *et al.* Engineering Escherichia coli to overproduce aromatic amino acids and derived compounds. *Microbial cell factories* **13**, 126, doi:10.1186/s12934-014-0126-z (2014).

9 Averesch, N. J. & Kromer, J. O. Metabolic Engineering of the Shikimate Pathway for Production of Aromatics and Derived Compounds—Present and Future Strain Construction Strategies. *Front. Bioeng. Biotechnol.* **26**, https://doi.org/10.3389/fbioe.2018.00032, doi:https://doi.org/10.3389/fbioe.2018.00032 (2018).

10 Wang, Y. C., Chen, S. & Yu, O. Metabolic engineering of flavonoids in plants and microorganisms. *Appl Microbiol Biot* **91**, 949-956 (2011).

11 Trantas, E. A., Koffas, M. A. G., Xu, P. & Ververidis, F. When plants produce not enough or at all: metabolic engineering of flavonoids in microbial hosts. *Front Plant Sci* **6**, doi:UNSP 710.3389/fpls.2015.00007 (2015).

12 Katsuyama, Y., Funa, N., Miyahisa, I. & Horinouchi, S. Synthesis of unnatural flavonoids and stilbenes by exploiting the plant biosynthetic pathway in Escherichia coli. *Chem Biol* **14**, 613-621, doi:10.1016/j.chembiol.2007.05.004 (2007).

13 Lim, C. G., Fowler, Z. L., Hueller, T., Schaffer, S. & Koffas, M. A. High-yield resveratrol production in engineered Escherichia coli. *Appl Environ Microbiol* **77**, 3451-3460, doi:10.1128/AEM.02186-10 (2011).

14 Yang, S. M., Shim, G. Y., Kim, B. G. & Ahn, J. H. Biological synthesis of coumarins in Escherichia coli. *Microbial cell factories* **14**, 65, doi:10.1186/s12934-015-0248-y (2015).

15 Lin, Y., Sun, X., Yuan, Q. & Yan, Y. Combinatorial biosynthesis of plant-specific coumarins in bacteria. *Metab Eng* **18**, 69-77, doi:10.1016/j.ymben.2013.04.004 (2013).

16 Koma, D., Yamanaka, H., Moriyoshi, K., Ohmoto, T. & Sakai, K. Production of aromatic compounds by metabolically engineered Escherichia coli with an expanded shikimate pathway. *Appl Environ Microbiol* **78**, 6203-6216, doi:10.1128/aem.01148-12 (2012).

17 Kunjapur, A. M., Tarasova, Y. & Prather, K. L. Synthesis and accumulation of aromatic aldehydes in an engineered strain of Escherichia coli. *J Am Chem Soc* **136**, 11644-11654, doi:10.1021/ja506664a (2014).

18 Machas, M., McKenna, R. & Nielsen, D. R. Expanding Upon Styrene Biosynthesis to Engineer a Novel Route to 2-Phenylethanol. *Biotechnol J* **doi: 10.1002/biot.201700310** (2016).

19 Pugh, S., McKenna, R., Halloum, I. & Nielsen, D. R. Engineering Escherichia coli for renewable benzyl alcohol production. *Metabolic Engineering Communications* **2**, 39-45, doi:http://dx.doi.org/10.1016/j.meteno.2015.06.002 (2015).

20 Gottardi, M. *et al.* De novo biosynthesis of trans-cinnamic acid derivatives in Saccharomyces cerevisiae. *Appl Microbiol Biotechnol* **101**, 4883-4893, doi:10.1007/s00253-017-8220-x (2017).

21 Vargas-Tah, A. *et al.* Production of cinnamic and p-hydroxycinnamic acid from sugar mixtures with engineered Escherichia coli. *Microb Cell Fact* **14**, 6, doi:10.1186/s12934-014-0185-1 (2015).

22 Qi, W. W. *et al.* Functional expression of prokaryotic and eukaryotic genes in Escherichia coli for conversion of glucose to p-hydroxystyrene. *Metab Eng* **9**, 268-276 (2007).

23 McKenna, R. & Nielsen, D. R. Styrene biosynthesis from glucose by engineered E. coli. *Metab Eng* **13**, 544-554 (2011).

24 Kang, S. Y. *et al.* Artificial de novo biosynthesis of hydroxystyrene derivatives in a tyrosine overproducing Escherichia coli strain. *Microbial cell factories* **14**, 78, doi:10.1186/s12934-015-0268-7 (2015).

25 Liu, C. *et al.* A systematic optimization of styrene biosynthesis in Escherichia coli BL21(DE3). *Biotechnol Biofuels* **11**, 14, doi:10.1186/s13068-018-1017-z (2018).

26 Wierckx, N. J., Ballerstedt, H., de Bont, J. A. & Wery, J. Engineering of solvent-tolerant Pseudomonas putida S12 for bioproduction of phenol from glucose. *Applied and environmental microbiology* **71**, 8221-8227 (2005).

27 Miao, L., Li, Q., Diao, A., Zhang, X. & Ma, Y. Construction of a novel phenol synthetic pathway in Escherichia coli through 4-hydroxybenzoate decarboxylation. *Appl Microbiol Biotechnol*, doi:10.1007/s00253-015-6497-1 (2015).

28 Ren, Y. X., Yang, S., Yuan, Q. P. & Sun, X. X. Microbial production of phenol via salicylate decarboxylation. *Rsc Adv* **5**, 92685-92689 (2015).

29 Thompson, B., Machas, M. & Nielsen, D. R. Engineering and comparison of non-natural pathways for microbial phenol production. *Biotechnol Bioeng* **113**, 1745-1754, doi:10.1002/bit.25942 (2016).

30 Wynands, B. *et al.* Metabolic engineering of Pseudomonas taiwanensis VLB120 with minimal genomic modifications for high-yield phenol production. *Metab Eng* **47**, 121-133, doi:10.1016/j.ymben.2018.03.011 (2018).

31 Weber, C. *et al.* Biosynthesis of cis,cis-muconic acid and its aromatic precursors, catechol and protocatechuic acid, from renewable feedstocks by Saccharomyces cerevisiae. *Appl Environ Microbiol* **78**, 8421-8430, doi:10.1128/AEM.01983-12 (2012).

32 Pugh, S., McKenna, R., Osman, M., Thompson, B. & Nielsen, D. R. Rational engineering of a novel pathway for producing the aromatic compounds p-hydroxybenzoate, protocatechuate, and catechol in Escherichia coli. *Process Biochemistry* **49**, 1843-1850, doi:http://dx.doi.org/10.1016/j.procbio.2014.08.011 (2014).

33 Wang, J. *et al.* Exploring the Promiscuity of Phenol Hydroxylase from Pseudomonas stutzeri OX1 for the Biosynthesis of Phenolic Compounds. *ACS Synth Biol*, doi:10.1021/acssynbio.8b00067 (2018).

34 Xu, P. *et al.* Modular optimization of multi-gene pathways for fatty acids production in E. coli. *Nature communications* **4**, 1409, doi:10.1038/ncomms2425 (2013).

35 Jiang, W., Qiao, J. B., Bentley, G. J., Liu, D. & Zhang, F. Modular pathway engineering for the microbial production of branched-chain fatty alcohols. *Biotechnol Biofuels* **10**, 244, doi:10.1186/s13068-017-0936-4 (2017).

36 Ajikumar, P. K. *et al.* Isoprenoid pathway optimization for Taxol precursor overproduction in Escherichia coli. *Science* **330**, 70-74, doi:10.1126/science.1191652 (2010).

37 Juminaga, D. *et al.* Modular Engineering of L-Tyrosine Production in Escherichia coli. *Appl Environ Microb* **78**, 89-98 (2012).

38 Trantas, E. A., Koffas, M. A., Xu, P. & Ververidis, F. When plants produce not enough or at all: metabolic engineering of flavonoids in microbial hosts. *Front Plant Sci* **6**, 7, doi:10.3389/fpls.2015.00007 (2015).

39 Wu, J., Zhou, T., Du, G., Zhou, J. & Chen, J. Modular optimization of heterologous pathways for de novo synthesis of (2S)-naringenin in Escherichia coli. *PLoS One* **9**, e101492, doi:10.1371/journal.pone.0101492 (2014).

40 Santos, C. N., Koffas, M. & Stephanopoulos, G. Optimization of a heterologous pathway for the production of flavonoids from glucose. *Metab Eng* **13**, 392-400, doi:10.1016/j.ymben.2011.02.002 (2011).

41 Noda, S., Shirai, T., Oyama, S. & Kondo, A. Metabolic design of a platform Escherichia coli strain producing various chorismate derivatives. *Metabolic Engineering* **33**, 119-129, doi:http://dx.doi.org/10.1016/j.ymben.2015.11.007 (2016).

42 Shen, X. *et al.* Establishment of novel biosynthetic pathways for the production of salicyl alcohol and gentisyl alcohol in engineered Escherichia coli. *ACS Synth Biol*, doi:10.1021/acssynbio.8b00051 (2018).

43 Sharma, V., Yamamura, A. & Yokobayashi, Y. Engineering artificial small RNAs for conditional gene silencing in Escherichia coli. *ACS Synth Biol* **1**, 6-13, doi:10.1021/sb200001q (2012).

44 Na, D. *et al.* Metabolic engineering of Escherichia coli using synthetic small regulatory RNAs. *Nat Biotechnol* **31**, 170-174, doi:10.1038/nbt.2461 (2013).

45 Kim, B., Park, H., Na, D. & Lee, S. Y. Metabolic engineering of Escherichia coli for the production of phenol from glucose. *Biotechnol J* **9**, 621-629, doi:10.1002/biot.201300263 (2014).

46 Wu, J., Yu, O., Du, G., Zhou, J. & Chen, J. Fine-Tuning of the Fatty Acid Pathway by Synthetic Antisense RNA for Enhanced (2S)-Naringenin Production from l-Tyrosine in Escherichia coli. *Appl Environ Microbiol* **80**, 7283-7292, doi:10.1128/AEM.02411-14 (2014).

47 Yang, Y., Lin, Y., Li, L., Linhardt, R. J. & Yan, Y. Regulating malonyl-CoA metabolism via synthetic antisense RNAs for enhanced biosynthesis of natural products. *Metab Eng* **29**, 217-226, doi:10.1016/j.ymben.2015.03.018 (2015).

48 Qi, L. *et al.* Repurposing CRISPR as an RNA-Guided Platform for Sequence-Specific Control of Gene Expression. *Cell* **152**, 1173-1183 (2013).

49 Larson, M. H. *et al.* CRISPR interference (CRISPRi) for sequence-specific control of gene expression. *Nat Protoc* **8**, 2180-2196, doi:10.1038/nprot.2013.132 (2013).

50 Wu, J., Du, G., Chen, J. & Zhou, J. Enhancing flavonoid production by systematically tuning the central metabolic pathways based on a CRISPR interference system in Escherichia coli. *Sci Rep* **5**, 13477, doi:10.1038/srep13477 (2015).

51 Wu, J., Zhang, X., Zhou, J. & Dong, M. Efficient biosynthesis of (2S)-pinocembrin from d-glucose by integrating engineering central metabolic pathways with a pH-shift control strategy. *Bioresour Technol* **218**, 999-1007, doi:10.1016/j.biortech.2016.07.066 (2016).

52 Liang, J. L. *et al.* A novel process for obtaining pinosylvin using combinatorial bioengineering in Escherichia coli. *World J Microbiol Biotechnol* **32**, 102, doi:10.1007/s11274-016-2062-z (2016).

53 Vanegas, K. G., Lehka, B. J. & Mortensen, U. H. SWITCH: a dynamic CRISPR tool for genome engineering and metabolic pathway control for cell factory construction in Saccharomyces cerevisiae. *Microbial cell factories* **16**, 25, doi:10.1186/s12934-017-0632-x (2017).

54 Cress, B. F. *et al.* CRISPathBrick: Modular Combinatorial Assembly of Type II-A CRISPR Arrays for dCas9-Mediated Multiplex Transcriptional Repression in E. coli. *ACS Synth Biol* **4**, 987-1000, doi:10.1021/acssynbio.5b00012 (2015).

55 Ghosh, S., Chisti, Y. & Banerjee, U. C. Production of shikimic acid. *Biotechnology advances* **30**, 1425-1431, doi:10.1016/j.biotechadv.2012.03.001 (2012).

56 Gu, P., Fan, X., Liang, Q., Qi, Q. & Li, Q. Novel technologies combined with traditional metabolic engineering strategies facilitate the construction of shikimate-producing Escherichia coli. *Microbial cell factories* **16**, 167, doi:10.1186/s12934-017-0773-y (2017).

57 Gu, P., Su, T., Wang, Q., Liang, Q. & Qi, Q. Tunable switch mediated shikimate biosynthesis in an engineered non-auxotrophic Escherichia coli. *Sci Rep* **6**, 29745, doi:10.1038/srep29745 (2016).

58 Williams, T. C. *et al.* Quorum-sensing linked RNA interference for dynamic metabolic pathway control in Saccharomyces cerevisiae. *Metab Eng* **29**, 124-134, doi:10.1016/j.ymben.2015.03.008 (2015).

59 Drinnenberg, I. A. *et al.* RNAi in budding yeast. *Science* **326**, 544-550, doi:10.1126/science.1176945 (2009).

60 Stanton, B. C. *et al.* Genomic mining of prokaryotic repressors for orthogonal logic gates. *Nat Chem Biol* **10**, 99-105, doi:10.1038/nchembio.1411 (2014).

61 van Sint Fiet, S., van Beilen, J. B. & Witholt, B. Selection of biocatalysts for chemical synthesis. *Proc Natl Acad Sci U S A* **103**, 1693-1698, doi:10.1073/pnas.0504733102 (2006).

62 Liu, D., Xiao, Y., Evans, B. S. & Zhang, F. Negative feedback regulation of fatty acid production based on a malonyl-CoA sensor-actuator. *ACS Synth Biol* **4**, 132-140, doi:10.1021/sb400158w (2015).

63 Li, H., Chen, W., Jin, R., Jin, J. M. & Tang, S. Y. Biosensor-aided high-throughput screening of hyper-producing cells for malonyl-CoA-derived products. *Microbial cell factories* **16**, 187, doi:10.1186/s12934-017-0794-6 (2017).

64 Binder, S. *et al.* A high-throughput approach to identify genomic variants of bacterial metabolite producers at the single-cell level. *Genome Biol* **13**, doi:ARTN R4010.1186/gb-2012-13-5-r40 (2012).

65 Tropel, D. & van der Meer, J. R. Bacterial transcriptional regulators for degradation pathways of aromatic compounds. *Microbiology and molecular biology reviews : MMBR* **68**, 474-500, table of contents, doi:10.1128/MMBR.68.3.474-500.2004 (2004).

66 Diaz, E. & Prieto, M. A. Bacterial promoters triggering biodegradation of aromatic pollutants. *Current opinion in biotechnology* **11**, 467-475 (2000).

67 Shingler, V., Bartilson, M. & Moore, T. Cloning and nucleotide sequence of the gene encoding the positive regulator (DmpR) of the phenol catabolic pathway encoded by pVI150 and identification of DmpR as a member of the NtrC family of transcriptional activators. *J Bacteriol* **175**, 1596-1604 (1993).

68 Fillet, S. *et al.* Transcriptional control of the main aromatic hydrocarbon efflux pump in Pseudomonas. *Environ Microbiol Rep* **4**, 158-167, doi:10.1111/j.1758-2229.2011.00255.x (2012).

69 Sun, X., Zahir, Z., Lynch, K. H. & Dennis, J. J. An antirepressor, SrpR, is involved in transcriptional regulation of the SrpABC solvent tolerance efflux pump of Pseudomonas putida S12. *J Bacteriol* **193**, 2717-2725, doi:10.1128/JB.00149-11 (2011).

70 Xue, H. *et al.* Design, construction, and characterization of a set of biosensors for aromatic compounds. *ACS Synth Biol* **3**, 1011-1014, doi:10.1021/sb500023f (2014).

71 Kubota, T. *et al.* Chorismate-dependent transcriptional regulation of quinate/shikimate utilization genes by LysR-type transcriptional regulator QsuR in Corynebacterium glutamicum: carbon flow control at metabolic branch point. *Mol Microbiol* **92**, 356-368, doi:10.1111/mmi.12560 (2014).

72 Martin, R. G. & Rosner, J. L. Binding of purified multiple antibiotic-resistance repressor protein (MarR) to mar operator sequences. *Proc Natl Acad Sci U S A* **92**, 5456-5460 (1995).

73 Salis, H., Tamsir, A. & Voigt, C. Engineering bacterial signals and sensors. *Contrib Microbiol* **16**, 194-225, doi:10.1159/000219381 (2009).

74 Yang, J. *et al.* Synthetic RNA devices to expedite the evolution of metabolite-producing microbes. *Nature communications* **4**, 1413, doi:10.1038/ncomms2404 (2013).

75 Borujeni, A. E., Mishler, D. M., Wang, J. Z., Huso, W. & Salis, H. M. Automated physics-based design of synthetic riboswitches from diverse RNA aptamers. *Nucleic Acids Res* **44**, 1-13, doi:10.1093/nar/gkv1289 (2016).

76 Morgan, S. A., Nadler, D. C., Yokoo, R. & Savage, D. F. Biofuel metabolic engineering with biosensors. *Curr Opin Chem Biol* **35**, 150-158, doi:10.1016/j.cbpa.2016.09.020 (2016).

77 Liu, Y. *et al.* Biosensor-Based Evolution and Elucidation of a Biosynthetic Pathway in Escherichia coli. *ACS Synth Biol* **6**, 837-848, doi:10.1021/acssynbio.6b00328 (2017).

78 Singh, P. *et al.* Application of targeted proteomics to metabolically engineered Escherichia coli. *Proteomics* **12**, 1289-1299, doi:10.1002/pmic.201100482 (2012).

79 Liu, C., Zhang, B., Liu, Y. M., Yang, K. Q. & Liu, S. J. New Intracellular Shikimic Acid Biosensor for Monitoring Shikimate Synthesis in Corynebacterium glutamicum. *ACS Synth Biol* **7**, 591-601, doi:10.1021/acssynbio.7b00339 (2018).

80 Wang, H. H. *et al.* Programming cells by multiplex genome engineering and accelerated evolution. *Nature* **460**, 894-898, doi:10.1038/nature08187 (2009).

81 Raman, S., Rogers, J. K., Taylor, N. D. & Church, G. M. Evolution-guided optimization of biosynthetic pathways. *Proc Natl Acad Sci U S A* **111**, 17803-17808, doi:10.1073/pnas.1409523111 (2014).

82 Chou, H. H. & Keasling, J. D. Programming adaptive control to evolve increased metabolite production. *Nature communications* **4**, 2595, doi:10.1038/ncomms3595 (2013).

83 Beller, H. R. *et al.* Discovery of enzymes for toluene synthesis from anoxic microbial communities. *Nat Chem Biol*, doi:10.1038/s41589-018-0017-4 (2018).

84 Wallace, S. & Balskus, E. P. Interfacing microbial styrene production with a biocompatible cyclopropanation reaction. *Angew Chem Int Ed Engl* **54**, 7106-7109, doi:10.1002/anie.201502185 (2015).

85 Lane, A. B. *et al.* Enzymatically Generated CRISPR Libraries for Genome Labeling and Screening. *Dev Cell* **34**, 373-378, doi:10.1016/j.devcel.2015.06.003 (2015).

86 Köferle, A. *et al.* CORALINA: a universal method for the generation of gRNA libraries for CRISPR-based screening. *BMC Genomics* **17**, 917, doi:10.1186/s12864-016-3268-z (2016).

87 Kaya-Okur, H. S. & Belmont, A. S. CRISPR EATING on a Low Budget. *Dev Cell* **34**, 253-254, doi:10.1016/j.devcel.2015.07.013 (2015).

88 Arakawa, H. A method to convert mRNA into a gRNA library for CRISPR/Cas9 editing of any organism. *Sci Adv* **2**, e1600699, doi:10.1126/sciadv.1600699 (2016).

89 Marmann, A., Aly, A. H., Lin, W., Wang, B. & Proksch, P. Co-cultivation--a powerful emerging tool for enhancing the chemical diversity of microorganisms. *Mar Drugs* **12**, 1043-1065, doi:10.3390/md12021043 (2014).

90 Turner, W. J. & Dunlop, M. J. Trade-Offs in Improving Biofuel Tolerance Using Combinations of Efflux Pumps. *ACS Synth Biol* **4**, 1056-1063, doi:10.1021/sb500307w (2015).

91 Boyarskiy, S., Davis Lopez, S., Kong, N. & Tullman-Ercek, D. Transcriptional feedback regulation of efflux protein expression for increased tolerance to and production of n-butanol. *Metab Eng* **33**, 130-137, doi:10.1016/j.ymben.2015.11.005 (2016).

92 Siu, Y., Fenno, J., Lindle, J. M. & Dunlop, M. J. Design and Selection of a Synthetic Feedback Loop for Optimizing Biofuel Tolerance. *ACS Synth Biol* **7**, 16-23, doi:10.1021/acssynbio.7b00260 (2018).

93 Huffer, S., Clark, M. E., Ning, J. C., Blanch, H. W. & Clark, D. S. Role of alcohols in growth, lipid composition, and membrane fluidity of yeasts, bacteria, and archaea. *Appl Environ Microbiol* **77**, 6400-6408, doi:10.1128/AEM.00694-11 (2011).

94 Knoshaug, E. P. & Zhang, M. Butanol tolerance in a selection of microorganisms. *Applied biochemistry and biotechnology* **153**, 13-20, doi:10.1007/s12010-008-8460-4 (2009).

95 Swings, J. & De Ley, J. The biology of Zymomonas. *Bacteriol Rev* **41**, 1-46 (1977).

96 Lange, C. C., Wackett, L. P., Minton, K. W. & Daly, M. J. Engineering a recombinant Deinococcus radiodurans for organopollutant degradation in radioactive mixed waste environments. *Nat Biotechnol* **16**, 929-933, doi:10.1038/nbt1098-929 (1998).

97 Sonoki, T. *et al.* Enhancement of protocatechuate decarboxylase activity for the effective production of muconate from lignin-related aromatic compounds. *J Biotechnol* **192 Pt A**, 71-77, doi:10.1016/j.jbiotec.2014.10.027 (2014).

98 Johnson, C. W. *et al.* Enhancing muconic acid production from glucose and lignin-derived aromatic compounds via increased protocatechuate decarboxylase activity. *Metabolic Engineering Communications* **3**, 111-119, doi:https://doi.org/10.1016/j.meteno.2016.04.002 (2016).

99 Hua, D. & Xu, P. Recent advances in biotechnological production of 2-phenylethanol. *Biotechnol Adv* **29**, 654-660, doi:10.1016/j.biotechadv.2011.05.001 (2011).

100 Tieman, D. *et al.* Tomato aromatic amino acid decarboxylases participate in synthesis of the flavor volatiles 2-phenylethanol and 2-phenylacetaldehyde. *Proc Natl Acad Sci U S A* **103**, 8287-8292, doi:10.1073/pnas.0602469103 (2006).

101 Atsumi, S., Hanai, T. & Liao, J. C. Non-fermentative pathways for synthesis of branched-chain higher alcohols as biofuels. *Nature* **451**, 86-89, doi:10.1038/nature06450 (2008).

102 Tian, M., Van Haaren, R., Reijnders, J. & Boot, M. Lignin Derivatives as Potential Octane Boosters. *SAE Int. J. Fuels Lubr.* **8**, 415-422, doi:10.4271/2015-01-0963 (2015).

103 Shankar, V. S. B. *et al.* Antiknock quality and ignition kinetics of 2-phenylethanol, a novel lignocellulosic octane booster. *Proceedings of the Combustion Institute* **36**, 3515-3522, doi:10.1016/j.proci.2016.05.041 (2017).

104 Suastegui, M. & Shao, Z. Yeast factories for the production of aromatic compounds: from building blocks to plant secondary metabolites. *J Ind Microbiol Biotechnol* **43**, 1611-1624, doi:10.1007/s10295-016-1824-9 (2016).

105 Etschmann, M. M., Bluemke, W., Sell, D. & Schrader, J. Biotechnological production of 2-phenylethanol. *Appl Microbiol Biotechnol* **59**, 1-8, doi:10.1007/s00253-002-0992-x (2002).

106 Lee, C.-W. & Richard, J. Catabolism of L-phenylalanine by some microorganisms of cheese origin. *Journal of Dairy Research* **51**, 461-469, doi:10.1017/s0022029900023761 (1984).

107 Kieser, M. E., Pollard, A., Stevens, P. M. & Tucknott, O. G. Determination of 2-Phenylethanol in Cider. *Nature* **204**, 887 (1964).

108 Hazelwood, L. A., Daran, J. M., van Maris, A. J., Pronk, J. T. & Dickinson, J. R. The Ehrlich pathway for fusel alcohol production: a century of research on Saccharomyces cerevisiae metabolism. *Appl Environ Microbiol* **74**, 2259-2266, doi:10.1128/aem.02625-07 (2008).

109 Ehrlich, F. Concerning the conditions for fusel oil formation and concerning its connection with the protein formation of yeast. *Berichte Der Deutschen Chemischen Gesellschaft* **40**, 1027-1047, doi:DOI 10.1002/cber.190704001156 (1907).

110 Vuralhan, Z. *et al.* Physiological characterization of the ARO10-dependent, broad-substrate-specificity 2-oxo acid decarboxylase activity of Saccharomyces cerevisiae. *Appl Environ Microbiol* **71**, 3276-3284, doi:10.1128/aem.71.6.3276-3284.2005 (2005).

111 Dickinson, J. R., Salgado, L. E. & Hewlins, M. J. The catabolism of amino acids to long chain and complex alcohols in Saccharomyces cerevisiae. *J Biol Chem* **278**, 8028-8034, doi:10.1074/jbc.M211914200 (2003).

112 Kim, B., Cho, B.-R. & Hahn, J.-S. Metabolic engineering of Saccharomyces cerevisiae for the production of 2-phenylethanol via Ehrlich pathway. *Biotechnology and Bioengineering* **111**, 115-124, doi:10.1002/bit.24993 (2014).

113 Etschmann, M. M. W., Sell, D. & Schrader, J. Screening of yeasts for the production of the aroma compound 2-phenylethanol in a molasses-based medium. *Biotechnology Letters* **25**, 531-536, doi:10.1023/a:1022890119847 (2003).

114 Iraqui, I., Vissers, S., Cartiaux, M. & Urrestarazu, A. Characterisation of Saccharomyces cerevisiae ARO8 and ARO9 genes encoding aromatic aminotransferases I and II reveals a new aminotransferase subfamily. *Mol Gen Genet* **257**, 238-248 (1998).

115 Kang, Z., Zhang, C., Du, G. & Chen, J. Metabolic Engineering of Escherichia coli for Production of 2-phenylethanol from Renewable Glucose. *Applied Biochemistry and Biotechnology* **172**, 2012-2021, doi:10.1007/s12010-013-0659-3 (2014).

116 Thompson, B., Machas, M. & Nielsen, D. R. Engineering and comparison of non-natural pathways for microbial phenol production. *Biotechnology and Bioengineering* **113**, 1745-1754, doi:10.1002/bit.25942 (2016).

117 McKenna, R. & Nielsen, D. R. Styrene biosynthesis from glucose by engineered E. coli. *Metabolic Engineering* **13**, 544-554, doi:http://dx.doi.org/10.1016/j.ymben.2011.06.005 (2011).

118 McKenna, R., Pugh, S., Thompson, B. & Nielsen, D. R. Microbial production of the aromatic building-blocks (S)-styrene oxide and (R)-1,2-phenylethanediol from renewable resources. *Biotechnology Journal* **8**, 1465-1475, doi:10.1002/biot.201300035 (2013).

119 O'Leary, N. D., O'Connor, K. E. & Dobson, A. D. W. Biochemistry, genetics and physiology of microbial styrene degradation. *FEMS Microbiology Reviews* **26**, 403-417, doi:10.1111/j.1574-6976.2002.tb00622.x (2002).

120 Tribe, D. E. (US Patent 4,681,852, 1987).

121 Datsenko, K. A. & Wanner, B. L. One-step inactivation of chromosomal genes in Escherichia coli K-12 using PCR products. *Proc Natl Acad Sci U S A* **97**, 6640-6645 (2000).

122 Flamholz, A., Noor, E., Bar-Even, A. & Milo, R. eQuilibrator—the biochemical thermodynamics calculator. *Nucleic Acids Research* **40**, D770-D775, doi:10.1093/nar/gkr874 (2012).

123 Varma, A., Boesch, B. W. & Palsson, B. O. Biochemical production capabilities of escherichia coli. *Biotechnology and Bioengineering* **42**, 59-73, doi:10.1002/bit.260420109 (1993).

124 Rodriguez, G. M. & Atsumi, S. Toward aldehyde and alkane production by removing aldehyde reductase activity in Escherichia coli. *Metabolic Engineering* **25**, 227-237, doi:10.1016/j.ymben.2014.07.012 (2014).

125 Panke, S., Witholt, B., Schmid, A. & Wubbolts, M. G. Towards a Biocatalyst for (S)-Styrene Oxide Production: Characterization of the Styrene Degradation Pathway of Pseudomonas sp. Strain VLB120. *Appl Environ Microbiol* **64**, 2032-2043 (1998).

126 Warhurst, A. M. & Fewson, C. A. Microbial metabolism and biotransformations of styrene. *Journal of Applied Bacteriology* **77**, 597-606, doi:10.1111/j.1365-2672.1994.tb02807.x (1994).

127 O'Connor, K., Buckley, C. M., Hartmans, S. & Dobson, A. D. Possible regulatory role for nonaromatic carbon sources in styrene degradation by Pseudomonas putida CA-3. *Appl Environ Microbiol* **61**, 544-548 (1995).

128 Parrott, S., Jones, S. & Cooper, R. A. 2-Phenylethylamine catabolism by Escherichia coli K12. *J Gen Microbiol* **133**, 347-351, doi:10.1099/00221287-133-2-347 (1987).

129 Noda, S., Shirai, T., Oyama, S. & Kondo, A. Metabolic design of a platform Escherichia coli strain producing various chorismate derivatives. *Metab Eng* **33**, 119-129, doi:10.1016/j.ymben.2015.11.007 (2016).

130 Gosset, G. Improvement of Escherichia coli production strains by modification of the phosphoenolpyruvate:sugar phosphotransferase system. *Microbial Cell Factories* **4**, 14, doi:10.1186/1475-2859-4-14 (2005).

131 Liu, S. P. *et al.* A systems level engineered E. coli capable of efficiently producing L-phenylalanine. *Process Biochemistry* **49**, 751-757, doi:https://doi.org/10.1016/j.procbio.2014.01.001 (2014).

132 Cunningham, D. S. *et al.* Pyruvate kinase-deficient Escherichia coli exhibits increased plasmid copy number and cyclic AMP levels. *J Bacteriol* **191**, 3041-3049, doi:10.1128/JB.01422-08 (2009).

133 Ho, K. K. & Weiner, H. Isolation and Characterization of an Aldehyde Dehydrogenase Encoded by the aldB Gene of Escherichia coli. *Journal of Bacteriology* **187**, 1067-1073, doi:10.1128/jb.187.3.1067-1073.2005 (2005).

134 Veit, A., Polen, T. & Wendisch, V. F. Global gene expression analysis of glucose overflow metabolism in Escherichia coli and reduction of aerobic acetate formation. *Appl Microbiol Biotechnol* **74**, 406-421, doi:10.1007/s00253-006-0680-3 (2007).

135 Kneen, M. M. *et al.* Characterization of a thiamin diphosphate-dependent phenylpyruvate decarboxylase from Saccharomyces cerevisiae. *FEBS Journal* **278**, 1842-1853, doi:10.1111/j.1742-4658.2011.08103.x (2011).

136 Gelfand, D. H. & Steinberg, R. A. Escherichia coli mutants deficient in the aspartate and aromatic amino acid aminotransferases. *Journal of Bacteriology* **130**, 429-440 (1977).

137 De Mey, M., De Maeseneire, S., Soetaert, W. & Vandamme, E. Minimizing acetate formation in E. coli fermentations. *J Ind Microbiol Biotechnol* **34**, 689-700, doi:10.1007/s10295-007-0244-2 (2007).

138 Sikkema, J., de Bont, J. A. & Poolman, B. Interactions of cyclic hydrocarbons with biological membranes. *J Biol Chem* **269**, 8022-8028 (1994).

139 Tan, Z., Yoon, J. M., Nielsen, D. R., Shanks, J. V. & Jarboe, L. R. Membrane engineering via trans unsaturated fatty acids production improves Escherichia coli robustness and production of biorenewables. *Metabolic Engineering* **35**, 105-113, doi:http://dx.doi.org/10.1016/j.ymben.2016.02.004 (2016).

140 Sendovski, M., Nir, N. & Fishman, A. Bioproduction of 2-Phenylethanol in a Biphasic Ionic Liquid Aqueous System. *Journal of Agricultural and Food Chemistry* **58**, 2260-2265, doi:10.1021/jf903879x (2010).

141 Etschmann, M. M. W., Sell, D. & Schrader, J. Production of 2-phenylethanol and 2-phenylethylacetate from L-phenylalanine by coupling whole-cell biocatalysis with organophilic pervaporation. *Biotechnology and Bioengineering* **92**, 624-634, doi:10.1002/bit.20655 (2005).

142 Achmon, Y., Goldshtein, J., Margel, S. & Fishman, A. Hydrophobic microspheres for in situ removal of 2-phenylethanol from yeast fermentation. *Journal of Microencapsulation* **28**, 628-638, doi:10.3109/02652048.2011.599443 (2011).

143 Achmon, Y., Ben-Barak Zelas, Z. & Fishman, A. Cloning Rosa hybrid phenylacetaldehyde synthase for the production of 2-phenylethanol in a whole cell Escherichia coli system. *Appl Microbiol Biotechnol* **98**, 3603-3611, doi:10.1007/s00253-013-5269-z (2014).

144 Kumar, R., Singh, S. & Singh, O. V. Bioconversion of lignocellulosic biomass: biochemical and molecular perspectives. *J Ind Microbiol Biotechnol* **35**, 377-391, doi:10.1007/s10295-008-0327-8 (2008).

145 Alvira, P., Tomás-Pejó, E., Ballesteros, M. & Negro, M. J. Pretreatment technologies for an efficient bioethanol production process based on enzymatic hydrolysis: A review. *Bioresour Technol* **101**, 4851-4861, doi:10.1016/j.biortech.2009.11.093 (2010).

146 Saha, B. C. Hemicellulose bioconversion. *J Ind Microbiol Biotechnol* **30**, 279-291, doi:10.1007/s10295-003-0049-x (2003).

147 Görke, B. & Stülke, J. Carbon catabolite repression in bacteria: many ways to make the most out of nutrients. *Nat Rev Microbiol* **6**, 613-624, doi:10.1038/nrmicro1932 (2008).

148 Beall, D. S., Ohta, K. & Ingram, L. O. Parametric studies of ethanol production form xylose and other sugars by recombinant Escherichia coli. *Biotechnol Bioeng* **38**, 296-303, doi:10.1002/bit.260380311 (1991).

149 Kim, J. H., Block, D. E. & Mills, D. A. Simultaneous consumption of pentose and hexose sugars: an optimal microbial phenotype for efficient fermentation of lignocellulosic biomass. *Appl Microbiol Biotechnol* **88**, 1077-1085, doi:10.1007/s00253-010-2839-1 (2010).

150 Eiteman, M. A., Lee, S. A. & Altman, E. A co-fermentation strategy to consume sugar mixtures effectively. *J Biol Eng* **2**, 3, doi:10.1186/1754-1611-2-3 (2008).

151 Zhang, H., Pereira, B., Li, Z. & Stephanopoulos, G. Engineering Escherichia coli coculture systems for the production of biochemical products. *Proc Natl Acad Sci U S A* **112**, 8266-8271, doi:10.1073/pnas.1506781112 (2015).

152 Li, F. F., Zhao, Y., Li, B. Z., Qiao, J. J. & Zhao, G. R. Engineering Escherichia coli for production of 4-hydroxymandelic acid using glucose-xylose mixture. *Microb Cell Fact* **15**, 90, doi:10.1186/s12934-016-0489-4 (2016).

153 Yao, Y. F., Wang, C. S., Qiao, J. & Zhao, G. R. Metabolic engineering of Escherichia coli for production of salvianic acid A via an artificial biosynthetic pathway. *Metab Eng* **19**, 79-87, doi:10.1016/j.ymben.2013.06.001 (2013).

154 Sievert, C. *et al.* Experimental evolution reveals an effective avenue to release catabolite repression via mutations in XylR. *Proc Natl Acad Sci U S A* **114**, 7349-7354, doi:10.1073/pnas.1700345114 (2017).

155 Song, S. & Park, C. Organization and regulation of the D-xylose operons in Escherichia coli K-12: XylR acts as a transcriptional activator. *J Bacteriol* **179**, 7025-7032, doi:10.1128/jb.179.22.7025-7032.1997 (1997).

156 Flores, A. D., Ayla, E. Z., Nielsen, D. R. & Wang, X. Engineering a Synthetic, Catabolically Orthogonal Coculture System for Enhanced Conversion of Lignocellulose-Derived Sugars to Ethanol. *ACS Synth Biol* **8**, 1089-1099, doi:10.1021/acssynbio.9b00007 (2019).

157 Jensen, S. I., Lennen, R. M., Herrgård, M. J. & Nielsen, A. T. Seven gene deletions in seven days: Fast generation of Escherichia coli strains tolerant to acetate and osmotic stress. *Sci Rep* **5**, 17874, doi:10.1038/srep17874 (2015).

158 Li, X. T., Thomason, L. C., Sawitzke, J. A., Costantino, N. & Court, D. L. Positive and negative selection using the tetA-sacB cassette: recombineering and P1 transduction in Escherichia coli. *Nucleic Acids Res* **41**, e204, doi:10.1093/nar/gkt1075 (2013).

159 Jantama, K. *et al.* Eliminating side products and increasing succinate yields in engineered strains of Escherichia coli C. *Biotechnol Bioeng* **101**, 881-893, doi:10.1002/bit.22005 (2008).

160 Mohamed, E. T. *et al.* Generation of an *E. coli* platform strain for improved sucrose utilization using adaptive laboratory evolution. *Microbial Cell Factories* **18** (2019).

161 Gonzalez, J. E., Long, C. P. & Antoniewicz, M. R. Comprehensive analysis of glucose and xylose metabolism in Escherichia coli under aerobic and anaerobic conditions by. *Metab Eng* **39**, 9-18, doi:10.1016/j.ymben.2016.11.003 (2017).

162 Shiloach, J. & Fass, R. Growing E. coli to high cell density--a historical perspective on method development. *Biotechnol Adv* **23**, 345-357, doi:10.1016/j.biotechadv.2005.04.004 (2005).

163 Eiteman, M. A. & Altman, E. Overcoming acetate in Escherichia coli recombinant protein fermentations. *Trends Biotechnol* **24**, 530-536, doi:10.1016/j.tibtech.2006.09.001 (2006).

164 Lawford, H. G. & Rousseau, J. D. Effects of pH and acetic acid on glucose and xylose metabolism by a genetically engineered ethanologenic Escherichia coli. *Appl Biochem Biotechnol* **39-40**, 301-322 (1993).

165 Ahn, J. O. *et al.* Exploring the effects of carbon sources on the metabolic capacity for shikimic acid production in Escherichia coli using in silico metabolic predictions. *J Microbiol Biotechnol* **18**, 1773-1784 (2008).

166 Sprenger, G. A. Genetics of pentose-phosphate pathway enzymes of Escherichia coli K-12. *Arch Microbiol* **164**, 324-330 (1995).

167 Peekhaus, N. & Conway, T. What's for dinner?: Entner-Doudoroff metabolism in Escherichia coli. *J Bacteriol* **180**, 3495-3502 (1998).

168 Bettenbrock, K. *et al.* Correlation between growth rates, EIIACrr phosphorylation, and intracellular cyclic AMP levels in Escherichia coli K-12. *J Bacteriol* **189**, 6891-6900, doi:10.1128/JB.00819-07 (2007).

169 Matsumoto, T., Tanaka, T. & Kondo, A. Engineering metabolic pathways in E*scherichia coli* for constructing a “microbial chassis” for biochemical production. *Bioresource Technology* **245**, 1362-1368 (2017).

170 Machas, M. *et al.* Emerging tools, enabling technologies, and future opportunities for the bioproduction of aromatic chemicals. *Journal of Chemical Technology & Biotechnology* **94** (2018).

171 Yoon, S. H. *et al.* Enhanced vanillin production from recombinant E. coli using NTG mutagenesis and adsorbent resin. *Biotechnol Prog* **23**, 1143-1148, doi:10.1021/bp070153r (2007).

172 Li, W., Xie, D. & Frost, J. W. Benzene-free synthesis of catechol: interfacing microbial and chemical catalysis. *J Am Chem Soc* **127**, 2874-2882, doi:10.1021/ja045148n (2005).

173 Scott, C. C. & Finnerty, W. R. Characterization of intracytoplasmic hydrocarbon inclusions from the hydrocarbon-oxidizing Acinetobacter species HO1-N. *J Bacteriol* **127**, 481-489 (1976).

174 Sikkema, J., de Bont, J. A. & Poolman, B. Mechanisms of membrane toxicity of hydrocarbons. *Microbiol Rev* **59**, 201-222 (1995).

175 Jarboe, L. R. *et al.* Metabolic engineering for production of biorenewable fuels and chemicals: contributions of synthetic biology. *J Biomed Biotechnol* **2010**, 761042, doi:10.1155/2010/761042 (2010).

176 Antunes-Madeira, M. C. & Madeira, V. M. Membrane fluidity as affected by the insecticide lindane. *Biochim Biophys Acta* **982**, 161-166 (1989).

177 Lennen, R. M., Politz, M. G., Kruziki, M. A. & Pfleger, B. F. Identification of transport proteins involved in free fatty acid efflux in Escherichia coli. *J Bacteriol* **195**, 135-144, doi:10.1128/JB.01477-12 (2013).

178 Lennen, R. M. & Pfleger, B. F. Modulating membrane composition alters free fatty acid tolerance in Escherichia coli. *PloS one* **8**, e54031, doi:10.1371/journal.pone.0054031 (2013).

179 Brynildsen, M. P. & Liao, J. C. An integrated network approach identifies the isobutanol response network of Escherichia coli. *Mol Syst Biol* **5**, 277, doi:10.1038/msb.2009.34 (2009).

180 Arnold, C. N., McElhanon, J., Lee, A., Leonhart, R. & Siegele, D. A. Global analysis of Escherichia coli gene expression during the acetate-induced acid tolerance response. *J Bacteriol* **183**, 2178-2186, doi:10.1128/JB.183.7.2178-2186.2001 (2001).

181 Rau, M. H., Calero, P., Lennen, R. M., Long, K. S. & Nielsen, A. T. Genome-wide Escherichia coli stress response and improved tolerance towards industrially relevant chemicals. *Microb Cell Fact* **15**, 176, doi:10.1186/s12934-016-0577-5 (2016).

182 Horinouchi, T. *et al.* Transcriptome analysis of parallel-evolved Escherichia coli strains under ethanol stress. *BMC Genomics* **11**, 579, doi:10.1186/1471-2164-11-579 (2010).

183 Lennen, R. M. *et al.* Membrane stresses induced by overproduction of free fatty acids in Escherichia coli. *Appl Environ Microbiol* **77**, 8114-8128, doi:10.1128/AEM.05421-11 (2011).

184 Pomposiello, P. J., Bennik, M. H. & Demple, B. Genome-wide transcriptional profiling of the Escherichia coli responses to superoxide stress and sodium salicylate. *J Bacteriol* **183**, 3890-3902, doi:10.1128/JB.183.13.3890-3902.2001 (2001).

185 Visvalingam, J., Hernandez-Doria, J. D. & Holley, R. A. Examination of the genome-wide transcriptional response of Escherichia coli O157:H7 to cinnamaldehyde exposure. *Appl Environ Microbiol* **79**, 942-950, doi:10.1128/AEM.02767-12 (2013).

186 Zheng, M. *et al.* DNA microarray-mediated transcriptional profiling of the Escherichia coli response to hydrogen peroxide. *J Bacteriol* **183**, 4562-4570, doi:10.1128/JB.183.15.4562-4570.2001 (2001).

187 Erickson, K. E., Winkler, J. D., Nguyen, D. T., Gill, R. T. & Chatterjee, A. The Tolerome: A Database of Transcriptome-Level Contributions to Diverse Escherichia coli Resistance and Tolerance Phenotypes. *ACS Synth Biol* **6**, 2302-2315, doi:10.1021/acssynbio.7b00235 (2017).

188 Yung, P. Y. *et al.* Global transcriptomic responses of Escherichia coli K-12 to volatile organic compounds. *Sci Rep* **6**, 19899, doi:10.1038/srep19899 (2016).

189 Van Dyk, T. K., Templeton, L. J., Cantera, K. A., Sharpe, P. L. & Sariaslani, F. S. Characterization of the Escherichia coli AaeAB efflux pump: a metabolic relief valve? *J Bacteriol* **186**, 7196-7204, doi:10.1128/JB.186.21.7196-7204.2004 (2004).

190 Lin, S. *et al.* Microarray analysis of the transcriptome of the E*scherichia coli* (E*. coli)* regulated by cinnamaldehyde (CMA). **28**, 500-515, doi:10.1080/09540105.2017.1300875 (2017).

191 Jin, D. *et al.* A Transcriptomic Analysis of Saccharomyces cerevisiae Under the Stress of 2-Phenylethanol. *Curr Microbiol* **75**, 1068-1076, doi:10.1007/s00284-018-1488-y (2018).

192 Lian, J. *et al.* Production of biorenewable styrene: utilization of biomass-derived sugars and insights into toxicity. *J Ind Microbiol Biotechnol* **43**, 595-604, doi:10.1007/s10295-016-1734-x (2016).

193 Subhash, S. & Kanduri, C. GeneSCF: a real-time based functional enrichment tool with support for multiple organisms. *BMC Bioinformatics* **17**, 365, doi:10.1186/s12859-016-1250-z (2016).

194 Xie, C. *et al.* KOBAS 2.0: a web server for annotation and identification of enriched pathways and diseases. *Nucleic Acids Res* **39**, W316-322, doi:10.1093/nar/gkr483 (2011).

195 Ai, C. & Kong, L. CGPS: A machine learning-based approach integrating multiple gene set analysis tools for better prioritization of biologically relevant pathways. *J Genet Genomics* **45**, 489-504, doi:10.1016/j.jgg.2018.08.002 (2018).

196 Oliveros, J. C. (2007-2015). Venny. An interactive tool for comparing lists with Venn's diagrams. https://bioinfogp.cnb.csic.es/tools/venny/index.html.

197 Janion, C. Inducible SOS response system of DNA repair and mutagenesis in Escherichia coli. *Int J Biol Sci* **4**, 338-344 (2008).

198 Lou, Z. *et al.* p-Coumaric acid kills bacteria through dual damage mechanisms. *Food Control* **25**, 550-554 (2012).

199 Dörr, T., Lewis, K. & Vulić, M. SOS response induces persistence to fluoroquinolones in Escherichia coli. *PLoS Genet* **5**, e1000760, doi:10.1371/journal.pgen.1000760 (2009).

200 Finkel, S. E. Long-term survival during stationary phase: evolution and the GASP phenotype. *Nat Rev Microbiol* **4**, 113-120, doi:10.1038/nrmicro1340 (2006).

201 Fonville, N. C., Bates, D., Hastings, P. J., Hanawalt, P. C. & Rosenberg, S. M. Role of RecA and the SOS response in thymineless death in Escherichia coli. *PLoS Genet* **6**, e1000865, doi:10.1371/journal.pgen.1000865 (2010).

202 Du, S. & Lutkenhaus, J. Assembly and activation of the Escherichia coli divisome. *Mol Microbiol* **105**, 177-187, doi:10.1111/mmi.13696 (2017).

203 Vicente, M., Gomez, M. J. & Ayala, J. A. Regulation of transcription of cell division genes in the Escherichia coli dcw cluster. *Cell Mol Life Sci* **54**, 317-324, doi:10.1007/s000180050158 (1998).

204 Gray, A. N. *et al.* Coordination of peptidoglycan synthesis and outer membrane constriction during Escherichia coli cell division. *Elife* **4**, doi:10.7554/eLife.07118 (2015).

205 Egan, A. J. F. Bacterial outer membrane constriction. *Mol Microbiol* **107**, 676-687, doi:10.1111/mmi.13908 (2018).

206 King, T., Lucchini, S., Hinton, J. C. & Gobius, K. Transcriptomic analysis of Escherichia coli O157:H7 and K-12 cultures exposed to inorganic and organic acids in stationary phase reveals acidulant- and strain-specific acid tolerance responses. *Appl Environ Microbiol* **76**, 6514-6528, doi:10.1128/AEM.02392-09 (2010).

207 Moreau, P. L. Diversion of the metabolic flux from pyruvate dehydrogenase to pyruvate oxidase decreases oxidative stress during glucose metabolism in nongrowing Escherichia coli cells incubated under aerobic, phosphate starvation conditions. *J Bacteriol* **186**, 7364-7368, doi:10.1128/JB.186.21.7364-7368.2004 (2004).

208 Randall, L. P. & Woodward, M. J. The multiple antibiotic resistance (mar) locus and its significance. *Res Vet Sci* **72**, 87-93, doi:10.1053/rvsc.2001.0537 (2002).

209 Alekshun, M. N. & Levy, S. B. The mar regulon: multiple resistance to antibiotics and other toxic chemicals. *Trends Microbiol* **7**, 410-413 (1999).

210 Barbosa, T. M. & Levy, S. B. Differential expression of over 60 chromosomal genes in Escherichia coli by constitutive expression of MarA. *J Bacteriol* **182**, 3467-3474 (2000).

211 Garcia-Bernardo, J. & Dunlop, M. J. Tunable stochastic pulsing in the Escherichia coli multiple antibiotic resistance network from interlinked positive and negative feedback loops. *PLoS Comput Biol* **9**, e1003229, doi:10.1371/journal.pcbi.1003229 (2013).

212 Martin, R. G., Bartlett, E. S., Rosner, J. L. & Wall, M. E. Activation of the Escherichia coli marA/soxS/rob regulon in response to transcriptional activator concentration. *J Mol Biol* **380**, 278-284, doi:10.1016/j.jmb.2008.05.015 (2008).

213 Nachin, L., Nannmark, U. & Nyström, T. Differential roles of the universal stress proteins of Escherichia coli in oxidative stress resistance, adhesion, and motility. *J Bacteriol* **187**, 6265-6272, doi:10.1128/JB.187.18.6265-6272.2005 (2005).

214 VanBogelen, R. A., Acton, M. A. & Neidhardt, F. C. Induction of the heat shock regulon does not produce thermotolerance in Escherichia coli. *Genes Dev* **1**, 525-531 (1987).

215 Rutherford, B. J. *et al.* Functional genomic study of exogenous n-butanol stress in Escherichia coli. *Appl Environ Microbiol* **76**, 1935-1945, doi:10.1128/AEM.02323-09 (2010).

216 Kitagawa, M., Miyakawa, M., Matsumura, Y. & Tsuchido, T. Escherichia coli small heat shock proteins, IbpA and IbpB, protect enzymes from inactivation by heat and oxidants. *Eur J Biochem* **269**, 2907-2917 (2002).

217 Kuczyńska-Wiśnik, D. *et al.* The Escherichia coli small heat-shock proteins IbpA and IbpB prevent the aggregation of endogenous proteins denatured in vivo during extreme heat shock. *Microbiology* **148**, 1757-1765, doi:10.1099/00221287-148-6-1757 (2002).

218 Kitagawa, M., Matsumura, Y. & Tsuchido, T. Small heat shock proteins, IbpA and IbpB, are involved in resistances to heat and superoxide stresses in Escherichia coli. *FEMS Microbiol Lett* **184**, 165-171, doi:10.1111/j.1574-6968.2000.tb09009.x (2000).

219 Han, X. *et al.* Escherichia coli genes that reduce the lethal effects of stress. *BMC Microbiol* **10**, 35, doi:10.1186/1471-2180-10-35 (2010).

220 Sargentini, N. J., Gularte, N. P. & Hudman, D. A. Screen for genes involved in radiation survival of Escherichia coli and construction of a reference database. *Mutat Res* **793-794**, 1-14, doi:10.1016/j.mrfmmm.2016.10.001 (2016).

221 Reyes, L. H., Almario, M. P. & Kao, K. C. Genomic library screens for genes involved in n-butanol tolerance in Escherichia coli. *PLoS One* **6**, e17678, doi:10.1371/journal.pone.0017678 (2011).

222 Rowley, G., Spector, M., Kormanec, J. & Roberts, M. Pushing the envelope: extracytoplasmic stress responses in bacterial pathogens. *Nat Rev Microbiol* **4**, 383-394, doi:10.1038/nrmicro1394 (2006).

223 Bury-Moné, S. *et al.* Global analysis of extracytoplasmic stress signaling in Escherichia coli. *PLoS Genet* **5**, e1000651, doi:10.1371/journal.pgen.1000651 (2009).

224 Flores-Kim, J. & Darwin, A. J. The Phage Shock Protein Response. *Annu Rev Microbiol* **70**, 83-101, doi:10.1146/annurev-micro-102215-095359 (2016).

225 Manganelli, R. & Gennaro, M. L. Protecting from Envelope Stress: Variations on the Phage-Shock-Protein Theme. *Trends Microbiol* **25**, 205-216, doi:10.1016/j.tim.2016.10.001 (2017).

226 Darwin, A. J. The phage-shock-protein response. *Mol Microbiol* **57**, 621-628, doi:10.1111/j.1365-2958.2005.04694.x (2005).

227 Ades, S. E., Grigorova, I. L. & Gross, C. A. Regulation of the alternative sigma factor sigma(E) during initiation, adaptation, and shutoff of the extracytoplasmic heat shock response in Escherichia coli. *J Bacteriol* **185**, 2512-2519 (2003).

228 Mecsas, J., Rouviere, P. E., Erickson, J. W., Donohue, T. J. & Gross, C. A. The activity of sigma E, an Escherichia coli heat-inducible sigma-factor, is modulated by expression of outer membrane proteins. *Genes Dev* **7**, 2618-2628 (1993).

229 Bianchi, A. A. & Baneyx, F. Hyperosmotic shock induces the sigma32 and sigmaE stress regulons of Escherichia coli. *Mol Microbiol* **34**, 1029-1038 (1999).

230 Wang, Q. P. & Kaguni, J. M. A novel sigma factor is involved in expression of the rpoH gene of Escherichia coli. *J Bacteriol* **171**, 4248-4253, doi:10.1128/jb.171.8.4248-4253.1989 (1989).

231 Gibson, J. L. *et al.* The sigma(E) stress response is required for stress-induced mutation and amplification in Escherichia coli. *Mol Microbiol* **77**, 415-430, doi:10.1111/j.1365-2958.2010.07213.x (2010).

232 Mitchell, A. M. & Silhavy, T. J. Envelope stress responses: balancing damage repair and toxicity. *Nat Rev Microbiol* **17**, 417-428, doi:10.1038/s41579-019-0199-0 (2019).

233 Sandoval, N. R. & Papoutsakis, E. T. Engineering membrane and cell-wall programs for tolerance to toxic chemicals: Beyond solo genes. *Curr Opin Microbiol* **33**, 56-66, doi:10.1016/j.mib.2016.06.005 (2016).

234 Tan, Z., Yoon, J. M., Nielsen, D. R., Shanks, J. V. & Jarboe, L. R. Membrane engineering via trans unsaturated fatty acids production improves Escherichia coli robustness and production of biorenewables. *Metabolic engineering* **35**, 105-113, doi:10.1016/j.ymben.2016.02.004 (2016).

235 Junker, F. & Ramos, J. L. Involvement of the cis/trans isomerase Cti in solvent resistance of Pseudomonas putida DOT-T1E. *J Bacteriol* **181**, 5693-5700 (1999).

236 Bui le, M. *et al.* Improved n-butanol tolerance in Escherichia coli by controlling membrane related functions. *J Biotechnol* **204**, 33-44, doi:10.1016/j.jbiotec.2015.03.025 (2015).

237 Tan, Z. *et al.* Engineering Escherichia coli membrane phospholipid head distribution improves tolerance and production of biorenewables. *Metab Eng* **44**, 1-12, doi:10.1016/j.ymben.2017.08.006 (2017).

238 Heipieper, H. J., Meinhardt, F. & Segura, A. The cis-trans isomerase of unsaturated fatty acids in Pseudomonas and Vibrio: biochemistry, molecular biology and physiological function of a unique stress adaptive mechanism. *FEMS Microbiol Lett* **229**, 1-7 (2003).

239 Surmann, K., Ćudić, E., Hammer, E. & Hunke, S. Molecular and proteome analyses highlight the importance of the Cpx envelope stress system for acid stress and cell wall stability in Escherichia coli. *Microbiologyopen* **5**, 582-596, doi:10.1002/mbo3.353 (2016).

240 Braun, V. & Wolff, H. Attachment of lipoprotein to murein (peptidoglycan) of Escherichia coli in the presence and absence of penicillin FL 1060. *J Bacteriol* **123**, 888-897 (1975).

241 Braun, V. & Rehn, K. Chemical characterization, spatial distribution and function of a lipoprotein (murein-lipoprotein) of the E. coli cell wall. The specific effect of trypsin on the membrane structure. *Eur J Biochem* **10**, 426-438 (1969).

242 Ni, Y., Reye, J. & Chen, R. R. lpp deletion as a permeabilization method. *Biotechnol Bioeng* **97**, 1347-1356, doi:10.1002/bit.21375 (2007).

243 Sherkhanov, S., Korman, T. P. & Bowie, J. U. Improving the tolerance of Escherichia coli to medium-chain fatty acid production. *Metab Eng* **25**, 1-7, doi:10.1016/j.ymben.2014.06.003 (2014).

244 Glebes, T. Y. *et al.* Genome-wide mapping of furfural tolerance genes in Escherichia coli. *PloS one* **9**, e87540, doi:10.1371/journal.pone.0087540 (2014).

245 Wang, L. C., Morgan, L. K., Godakumbura, P., Kenney, L. J. & Anand, G. S. The inner membrane histidine kinase EnvZ senses osmolality via helix-coil transitions in the cytoplasm. *EMBO J* **31**, 2648-2659, doi:10.1038/emboj.2012.99 (2012).

246 Guillier, M. & Gottesman, S. Remodelling of the Escherichia coli outer membrane by two small regulatory RNAs. *Mol Microbiol* **59**, 231-247, doi:10.1111/j.1365-2958.2005.04929.x (2006).

247 Pratt, L. A., Hsing, W., Gibson, K. E. & Silhavy, T. J. From acids to osmZ: multiple factors influence synthesis of the OmpF and OmpC porins in Escherichia coli. *Mol Microbiol* **20**, 911-917 (1996).

248 Rau, M. H., Bojanovič, K., Nielsen, A. T. & Long, K. S. Differential expression of small RNAs under chemical stress and fed-batch fermentation in E. coli. *BMC Genomics* **16**, 1051, doi:10.1186/s12864-015-2231-8 (2015).

249 Nikaido, H. Outer membrane barrier as a mechanism of antimicrobial resistance. *Antimicrob Agents Chemother* **33**, 1831-1836, doi:10.1128/aac.33.11.1831 (1989).

250 Pichler, H. & Emmerstorfer-Augustin, A. Modification of membrane lipid compositions in single-celled organisms - From basics to applications. *Methods* **147**, 50-65, doi:10.1016/j.ymeth.2018.06.009 (2018).

251 Asako, H., Kobayashi, K. & Aono, R. Organic solvent tolerance of Escherichia coli is independent of OmpF levels in the membrane. *Appl Environ Microbiol* **65**, 294-296 (1999).

252 Aono, R. & Kobayashi, H. Cell surface properties of organic solvent-tolerant mutants of Escherichia coli K-12. *Appl Environ Microbiol* **63**, 3637-3642 (1997).

253 Tan, Z., Black, W., Yoon, J. M., Shanks, J. V. & Jarboe, L. R. Improving Escherichia coli membrane integrity and fatty acid production by expression tuning of FadL and OmpF. *Microb Cell Fact* **16**, 38, doi:10.1186/s12934-017-0650-8 (2017).

254 Egler, M., Grosse, C., Grass, G. & Nies, D. H. Role of the extracytoplasmic function protein family sigma factor RpoE in metal resistance of Escherichia coli. *J Bacteriol* **187**, 2297-2307, doi:10.1128/JB.187.7.2297-2307.2005 (2005).

255 Zhang, X. S., García-Contreras, R. & Wood, T. K. YcfR (BhsA) influences Escherichia coli biofilm formation through stress response and surface hydrophobicity. *J Bacteriol* **189**, 3051-3062, doi:10.1128/JB.01832-06 (2007).

256 Chen, Y. *et al.* Lessons in Membrane Engineering for Octanoic Acid Production from Environmental Escherichia coli Isolates. *Appl Environ Microbiol* **84**, doi:10.1128/AEM.01285-18 (2018).

257 Dunlop, M. J. *et al.* Engineering microbial biofuel tolerance and export using efflux pumps. *Molecular systems biology* **7**, 487 (2011).

258 Mingardon, F. *et al.* Improving olefin tolerance and production in E. coli using native and evolved AcrB. *Biotechnol Bioeng* **112**, 879-888, doi:10.1002/bit.25511 (2015).

259 Basak, S., Song, H. & Jiang, R. Error-prone PCR of global transcription factor cyclic AMP receptor protein for enhanced organic solvent (toluene) tolerance. *Process Biochemistry* **47**, 2152-2158 (2012).

260 Anes, J., McCusker, M. P., Fanning, S. & Martins, M. The ins and outs of RND efflux pumps in Escherichia coli. *Front Microbiol* **6**, 587, doi:10.3389/fmicb.2015.00587 (2015).

261 Amaral, L., Fanning, S. & Pagès, J. M. Efflux pumps of gram-negative bacteria: genetic responses to stress and the modulation of their activity by pH, inhibitors, and phenothiazines. *Adv Enzymol Relat Areas Mol Biol* **77**, 61-108 (2011).

262 Molina-Santiago, C., Udaondo, Z., Gómez-Lozano, M., Molin, S. & Ramos, J. L. Global transcriptional response of solvent-sensitive and solvent-tolerant Pseudomonas putida strains exposed to toluene. *Environ Microbiol* **19**, 645-658, doi:10.1111/1462-2920.13585 (2017).

263 Hobbs, E. C., Yin, X., Paul, B. J., Astarita, J. L. & Storz, G. Conserved small protein associates with the multidrug efflux pump AcrB and differentially affects antibiotic resistance. *Proc Natl Acad Sci U S A* **109**, 16696-16701, doi:10.1073/pnas.1210093109 (2012).

264 Calhoun, L. N. & Kwon, Y. M. Structure, function and regulation of the DNA-binding protein Dps and its role in acid and oxidative stress resistance in Escherichia coli: a review. *J Appl Microbiol* **110**, 375-386, doi:10.1111/j.1365-2672.2010.04890.x (2011).

265 Singh, S. K., Parveen, S., SaiSree, L. & Reddy, M. Regulated proteolysis of a cross-link-specific peptidoglycan hydrolase contributes to bacterial morphogenesis. *Proc Natl Acad Sci U S A* **112**, 10956-10961, doi:10.1073/pnas.1507760112 (2015).

266 Singh, S. K., SaiSree, L., Amrutha, R. N. & Reddy, M. Three redundant murein endopeptidases catalyse an essential cleavage step in peptidoglycan synthesis of Escherichia coli K12. *Mol Microbiol* **86**, 1036-1051, doi:10.1111/mmi.12058 (2012).

267 Spratt, B. G., Zhou, J., Taylor, M. & Merrick, M. J. Monofunctional biosynthetic peptidoglycan transglycosylases. *Mol Microbiol* **19**, 639-640 (1996).

268 Derouaux, A. *et al.* The monofunctional glycosyltransferase of Escherichia coli localizes to the cell division site and interacts with penicillin-binding protein 3, FtsW, and FtsN. *J Bacteriol* **190**, 1831-1834, doi:10.1128/JB.01377-07 (2008).

269 Gill, R. T., Valdes, J. J. & Bentley, W. E. A comparative study of global stress gene regulation in response to overexpression of recombinant proteins in Escherichia coli. *Metab Eng* **2**, 178-189, doi:10.1006/mben.2000.0148 (2000).

270 Gill, R. T., DeLisa, M. P., Shiloach, M., Holoman, T. R. & Bentley, W. E. OmpT expression and activity increase in response to recombinant chloramphenicol acetyltransferase overexpression and heat shock in E. coli. *J Mol Microbiol Biotechnol* **2**, 283-289 (2000).

271 Alper, H., Moxley, J., Nevoigt, E., Fink, G. R. & Stephanopoulos, G. Engineering yeast transcription machinery for improved ethanol tolerance and production. *Science (New York, N.Y* **314**, 1565-1568, doi:10.1126/science.1131969 (2006).

272 Lam, F. H., Ghaderi, A., Fink, G. R. & Stephanopoulos, G. Biofuels. Engineering alcohol tolerance in yeast. *Science* **346**, 71-75, doi:10.1126/science.1257859 (2014).

273 Foo, J. L. *et al.* Improving microbial biogasoline production in Escherichia coli using tolerance engineering. *MBio* **5**, e01932, doi:10.1128/mBio.01932-14 (2014).

274 Foo, J. L. & Leong, S. S. Directed evolution of an E. coli inner membrane transporter for improved efflux of biofuel molecules. *Biotechnol Biofuels* **6**, 81, doi:10.1186/1754-6834-6-81 (2013).

275 Jones, C. M., Hernandez Lozada, N. J. & Pfleger, B. F. Efflux systems in bacteria and their metabolic engineering applications. *Appl Microbiol Biotechnol* **99**, 9381-9393, doi:10.1007/s00253-015-6963-9 (2015).

276 Mukhopadhyay, A. Tolerance engineering in bacteria for the production of advanced biofuels and chemicals. *Trends Microbiol* **23**, 498-508, doi:10.1016/j.tim.2015.04.008 (2015).

277 Moore, J. P. *et al.* Inverted Regulation of Multidrug Efflux Pumps, Acid Resistance and Porins in Benzoate-Evolved. *Appl Environ Microbiol*, doi:10.1128/AEM.00966-19 (2019).

278 Rojas, A. *et al.* Three efflux pumps are required to provide efficient tolerance to toluene in Pseudomonas putida DOT-T1E. *J Bacteriol* **183**, 3967-3973, doi:10.1128/JB.183.13.3967-3973.2001 (2001).

279 Ramos, J. L., Duque, E., Godoy, P. & Segura, A. Efflux pumps involved in toluene tolerance in Pseudomonas putida DOT-T1E. *J Bacteriol* **180**, 3323-3329 (1998).

280 García, V. *et al.* Functional analysis of new transporters involved in stress tolerance in Pseudomonas putida DOT-T1E. *Environ Microbiol Rep* **2**, 389-395, doi:10.1111/j.1758-2229.2009.00093.x (2010).

281 Segura, A. *et al.* Fatty acid biosynthesis is involved in solvent tolerance in Pseudomonas putida DOT-T1E. *Environ Microbiol* **6**, 416-423 (2004).

282 Zhang, R., Cao, Y., Liu, W., Xian, M. & Liu, H. Improving phloroglucinol tolerance and production in Escherichia coli by GroESL overexpression. *Microb Cell Fact* **16**, 227, doi:10.1186/s12934-017-0839-x (2017).

283 Konovalova, A., Schwalm, J. A. & Silhavy, T. J. A Suppressor Mutation That Creates a Faster and More Robust σE Envelope Stress Response. *J Bacteriol* **198**, 2345-2351, doi:10.1128/JB.00340-16 (2016).

284 Zaslaver, A. *et al.* A comprehensive library of fluorescent transcriptional reporters for Escherichia coli. *Nat Methods* **3**, 623-628, doi:10.1038/nmeth895 (2006).

285 Pavel, H., Forsman, M. & Shingler, V. An aromatic effector specificity mutant of the transcriptional regulator DmpR overcomes the growth constraints of Pseudomonas sp. strain CF600 on para-substituted methylphenols. *J Bacteriol* **176**, 7550-7557 (1994).

286 Reyes, L. H., Almario, M. P., Winkler, J., Orozco, M. M. & Kao, K. C. Visualizing evolution in real time to determine the molecular mechanisms of n-butanol tolerance in Escherichia coli. *Metab Eng* **14**, 579-590, doi:10.1016/j.ymben.2012.05.002 (2012).

287 LaCroix, R. A., Palsson, B. O. & Feist, A. M. A Model for Designing Adaptive Laboratory Evolution Experiments. *Appl Environ Microbiol* **83**, doi:10.1128/AEM.03115-16 (2017).

288 Kildegaard, K. R. *et al.* Evolution reveals a glutathione-dependent mechanism of 3-hydroxypropionic acid tolerance. *Metab Eng* **26**, 57-66, doi:10.1016/j.ymben.2014.09.004 (2014).

289 Dragosits, M. & Mattanovich, D. Adaptive laboratory evolution -- principles and applications for biotechnology. *Microb Cell Fact* **12**, 64, doi:10.1186/1475-2859-12-64 (2013).

290 Rasila, T. S., Pajunen, M. I. & Savilahti, H. Critical evaluation of random mutagenesis by error-prone polymerase chain reaction protocols, Escherichia coli mutator strain, and hydroxylamine treatment. *Anal Biochem* **388**, 71-80, doi:10.1016/j.ab.2009.02.008 (2009).

291 Emond, S. *et al.* A novel random mutagenesis approach using human mutagenic DNA polymerases to generate enzyme variant libraries. *Protein Eng Des Sel* **21**, 267-274, doi:10.1093/protein/gzn004 (2008).

292 Zaccolo, M., Williams, D. M., Brown, D. M. & Gherardi, E. An approach to random mutagenesis of DNA using mixtures of triphosphate derivatives of nucleoside analogues. *J Mol Biol* **255**, 589-603, doi:10.1006/jmbi.1996.0049 (1996).

293 Halperin, S. O. *et al.* CRISPR-guided DNA polymerases enable diversification of all nucleotides in a tunable window. *Nature* **560**, 248-252, doi:10.1038/s41586-018-0384-8 (2018).

294 Sadanand, S. EvolvR-ing to targeted mutagenesis. *Nat Biotechnol* **36**, 819, doi:10.1038/nbt.4247 (2018).

295 Quan, J. & Tian, J. Circular polymerase extension cloning of complex gene libraries and pathways. *PLoS One* **4**, e6441, doi:10.1371/journal.pone.0006441 (2009).

296 Consortium, U. UniProt: a worldwide hub of protein knowledge. *Nucleic Acids Res* **47**, D506-D515, doi:10.1093/nar/gky1049 (2019).

297 Hemm, M. R., Paul, B. J., Schneider, T. D., Storz, G. & Rudd, K. E. Small membrane proteins found by comparative genomics and ribosome binding site models. *Mol Microbiol* **70**, 1487-1501, doi:10.1111/j.1365-2958.2008.06495.x (2008).

298 Tsukagoshi, N. & Aono, R. Entry into and release of solvents by Escherichia coli in an organic-aqueous two-liquid-phase system and substrate specificity of the AcrAB-TolC solvent-extruding pump. *J Bacteriol* **182**, 4803-4810 (2000).

299 Törnroth-Horsefield, S. *et al.* Crystal structure of AcrB in complex with a single transmembrane subunit reveals another twist. *Structure* **15**, 1663-1673, doi:10.1016/j.str.2007.09.023 (2007).

300 Poblete-Castro, I., Becker, J., Dohnt, K., dos Santos, V. M. & Wittmann, C. Industrial biotechnology of Pseudomonas putida and related species. *Appl Microbiol Biotechnol* **93**, 2279-2290, doi:10.1007/s00253-012-3928-0 (2012).

301 Rojo, F. Traits allowing resistance to organic solvents in Pseudomonas. *Environ Microbiol* **19**, 417-419, doi:10.1111/1462-2920.13631 (2017).

302 Weber, F. J., Ooijkaas, L. P., Schemen, R. M., Hartmans, S. & de Bont, J. A. Adaptation of Pseudomonas putida S12 to high concentrations of styrene and other organic solvents. *Appl Environ Microbiol* **59**, 3502-3504 (1993).

303 Nikel, P. I. & de Lorenzo, V. Pseudomonas putida as a functional chassis for industrial biocatalysis: From native biochemistry to trans-metabolism. *Metab Eng* **50**, 142-155, doi:10.1016/j.ymben.2018.05.005 (2018).

304 Cebolla, A., Guzmán, C. & de Lorenzo, V. Nondisruptive detection of activity of catabolic promoters of Pseudomonas putida with an antigenic surface reporter system. *Appl Environ Microbiol* **62**, 214-220 (1996).

305 Hoffmann, J. & Altenbuchner, J. Functional Characterization of the Mannitol Promoter of Pseudomonas fluorescens DSM 50106 and Its Application for a Mannitol-Inducible Expression System for Pseudomonas putida KT2440. *PLoS One* **10**, e0133248, doi:10.1371/journal.pone.0133248 (2015).

306 Graf, N. & Altenbuchner, J. Genetic engineering of Pseudomonas putida KT2440 for rapid and high-yield production of vanillin from ferulic acid. *Appl Microbiol Biotechnol* **98**, 137-149, doi:10.1007/s00253-013-5303-1 (2014).

307 Herrero, M., de Lorenzo, V., Ensley, B. & Timmis, K. N. A T7 RNA polymerase-based system for the construction of Pseudomonas strains with phenotypes dependent on TOL-meta pathway effectors. *Gene* **134**, 103-106 (1993).

308 Molina-Santiago, C. *et al.* Pseudomonas putida as a platform for the synthesis of aromatic compounds. *Microbiology-Sgm* **162**, 1535-1543, doi:10.1099/mic.0.000333 (2016).

309 Martínez-García, E. & de Lorenzo, V. Engineering multiple genomic deletions in Gram-negative bacteria: analysis of the multi-resistant antibiotic profile of Pseudomonas putida KT2440. *Environ Microbiol* **13**, 2702-2716, doi:10.1111/j.1462-2920.2011.02538.x (2011).

310 Martínez-García, E. & de Lorenzo, V. Transposon-based and plasmid-based genetic tools for editing genomes of gram-negative bacteria. *Methods Mol Biol* **813**, 267-283, doi:10.1007/978-1-61779-412-4_16 (2012).

311 Domröse, A. *et al.* Rapid generation of recombinant. *Synth Syst Biotechnol* **2**, 310-319, doi:10.1016/j.synbio.2017.11.001 (2017).

312 Aparicio, T., de Lorenzo, V. & Martínez-García, E. CRISPR/Cas9-Based Counterselection Boosts Recombineering Efficiency in Pseudomonas putida. *Biotechnol J* **13**, e1700161, doi:10.1002/biot.201700161 (2018).

313 Tan, S. Z., Reisch, C. R. & Prather, K. L. J. A Robust CRISPR Interference Gene Repression System in Pseudomonas. *J Bacteriol* **200**, doi:10.1128/JB.00575-17 (2018).

314 Kim, S. K. *et al.* CRISPR interference-mediated gene regulation in Pseudomonas putida KT2440. *Microb Biotechnol*, doi:10.1111/1751-7915.13382 (2019).

315 Lauritsen, I., Porse, A., Sommer, M. O. A. & Nørholm, M. H. H. A versatile one-step CRISPR-Cas9 based approach to plasmid-curing. *Microb Cell Fact* **16**, 135, doi:10.1186/s12934-017-0748-z (2017).

316 Martínez-García, E. & de Lorenzo, V. Pseudomonas putida in the quest of programmable chemistry. *Curr Opin Biotechnol* **59**, 111-121, doi:10.1016/j.copbio.2019.03.012 (2019).

317 Yu, S., Plan, M. R., Winter, G. & Krömer, J. O. Metabolic Engineering of. *Front Bioeng Biotechnol* **4**, 90, doi:10.3389/fbioe.2016.00090 (2016).

318 Verhoef, S., Wierckx, N., Westerhof, R. G., de Winde, J. H. & Ruijssenaars, H. J. Bioproduction of p-hydroxystyrene from glucose by the solvent-tolerant bacterium Pseudomonas putida S12 in a two-phase water-decanol fermentation. *Appl Environ Microbiol* **75**, 931-936 (2009).

319 Ramos, J. L., Duque, E., Huertas, M. J. & Haïdour, A. Isolation and expansion of the catabolic potential of a Pseudomonas putida strain able to grow in the presence of high concentrations of aromatic hydrocarbons. *J Bacteriol* **177**, 3911-3916 (1995).

320 Vongpichayapaiboon, T., Pongsawasdi, P. & Krusong, K. Optimization of large-ring cyclodextrin production from starch by amylomaltase from Corynebacterium glutamicum and effect of organic solvent on product size. *J Appl Microbiol* **120**, 912-920, doi:10.1111/jam.13087 (2016).

321 Liu, C. G. *et al.* Cellulosic ethanol production: Progress, challenges and strategies for solutions. *Biotechnol Adv* **37**, 491-504, doi:10.1016/j.biotechadv.2019.03.002 (2019).

322 Guimarães, P. M., Teixeira, J. A. & Domingues, L. Fermentation of lactose to bio-ethanol by yeasts as part of integrated solutions for the valorisation of cheese whey. *Biotechnol Adv* **28**, 375-384, doi:10.1016/j.biotechadv.2010.02.002 (2010).

323 Sabri, S., Nielsen, L. K. & Vickers, C. E. Molecular control of sucrose utilization in Escherichia coli W, an efficient sucrose-utilizing strain. *Appl Environ Microbiol* **79**, 478-487, doi:10.1128/AEM.02544-12 (2013).

324 Swinnen, S., Ho, P. W., Klein, M. & Nevoigt, E. Genetic determinants for enhanced glycerol growth of Saccharomyces cerevisiae. *Metab Eng* **36**, 68-79, doi:10.1016/j.ymben.2016.03.003 (2016).

325 Kornberg, H. L. Routes for fructose utilization by Escherichia coli. *J Mol Microbiol Biotechnol* **3**, 355-359 (2001).

326 Poblete-Castro, I., Wittmann, C. & Nikel, P. I. Biochemistry, genetics and biotechnology of glycerol utilization in Pseudomonas species. *Microb Biotechnol*, doi:10.1111/1751-7915.13400 (2019).

327 Kenny, S. T. *et al.* Development of a bioprocess to convert PET derived terephthalic acid and biodiesel derived glycerol to medium chain length polyhydroxyalkanoate. *Appl Microbiol Biotechnol* **95**, 623-633, doi:10.1007/s00253-012-4058-4 (2012).

328 Prieto, A. *et al.* A holistic view of polyhydroxyalkanoate metabolism in Pseudomonas putida. *Environ Microbiol* **18**, 341-357, doi:10.1111/1462-2920.12760 (2016).

329 Chen, G. Q. & Jiang, X. R. Engineering microorganisms for improving polyhydroxyalkanoate biosynthesis. *Curr Opin Biotechnol* **53**, 20-25, doi:10.1016/j.copbio.2017.10.008 (2018).

330 Verhoef, S., Ruijssenaars, H. J., de Bont, J. A. & Wery, J. Bioproduction of p-hydroxybenzoate from renewable feedstock by solvent-tolerant Pseudomonas putida S12. *J Biotechnol* **132**, 49-56, doi:10.1016/j.jbiotec.2007.08.031 (2007).

331 Löwe, H., Schmauder, L., Hobmeier, K., Kremling, A. & Pflüger-Grau, K. Metabolic engineering to expand the substrate spectrum of Pseudomonas putida toward sucrose. *Microbiologyopen* **6**, doi:10.1002/mbo3.473 (2017).

332 Bevan, M. W. & Franssen, M. C. Investing in green and white biotech. *Nat Biotechnol* **24**, 765-767, doi:10.1038/nbt0706-765 (2006).

333 Fadel, M., Keera, A. A., Mouafi, F. E. & Kahil, T. High Level Ethanol from Sugar Cane Molasses by a New Thermotolerant Saccharomyces cerevisiae Strain in Industrial Scale. *Biotechnol Res Int* **2013**, 253286, doi:10.1155/2013/253286 (2013).

334 Wittgens, A. *et al.* Growth independent rhamnolipid production from glucose using the non-pathogenic Pseudomonas putida KT2440. *Microb Cell Fact* **10**, 80, doi:10.1186/1475-2859-10-80 (2011).

335 Löwe, H., Sinner, P., Kremling, A. & Pflüger-Grau, K. Engineering sucrose metabolism in Pseudomonas putida highlights the importance of porins. *Microb Biotechnol*, doi:10.1111/1751-7915.13283 (2018).

336 Nikaido, H. Molecular basis of bacterial outer membrane permeability revisited. *Microbiol Mol Biol Rev* **67**, 593-656, doi:10.1128/mmbr.67.4.593-656.2003 (2003).